Role of Spectrin Mutations in Spinocerebellar Ataxia Type 5 (SCA5)

A DISSERTATION
SUBMITTED TO THE FACULTY OF THE GRADUATE SCHOOL
OF THE UNIVERSITY OF MINNESOTA BY

Damaris Nadia Lorenzo Vila

IN PARTIAL FULFILLMENT OF THE REQUIREMENTS FOR THE
DEGREE OF DOCTOR OF PHILOSOPHY

ADVISOR: Laura P. W. Ranum, Ph.D.

August, 2009

AKNOWLEDGEMENTS

I will take this opportunity to recognize a group of people who has been instrumental during my years as a Graduate Student. Specially, I would like to thank my advisor, Dr. Laura P. W. Ranum, for her encouragement and support. I am very grateful to Laura for her faith in me and my work, and for providing me with the tools and guidance to become an independent scientist. I also would like to thank all past and present members of the Ranum lab for both professional and personal relationships. They are extremely cooperative, friendly, and fun to work with. I am specially thankful to Karen Armbrust and Katie Dick for providing the human β-III spectrin clones and for many useful discussions about SCA5. I want to thank Marcy Weatherspoon for her help with the SSCP screen and Sarah Kreykes for her help collecting DNA samples and clinical information from ataxia families.

I am indebted to Dr. Tom Hays for all his enthusiasm and guidance with the fly project and to all the members of the Hays lab for sharing their expertise, time, and resources with me. In particular, I am greatly thankful to Sarah Mische for her help with the initial characterization of the SCA5 flies and Yungui He for his help with cell culture and anything else I needed in the lab. I extend my most special gratitud to Mingang Li for his friendship, for teaching me a great deal of fly genetics, and for his constant help in the fly room and through each experiment.

Lastly, I want to thank my husband Ismael and my son Edgar for their unlimited love and dedication and my dad, sister, family, and friends for their continuous encouragement.

ABSTRACT

Spinocerebellar ataxia type 5 (SCA5) is a dominant neurodegenerative disorder caused by mutations in the *SPBTN2* gene encoding the cytoskeletal protein β-III spectrin. To get insight into the biology of the disease and the normal function of β-III spectrin, and to estimate the frequency of SCA5 mutations among ataxia patients, I used a forward human genetic approach to identify novel *SPTBN2* mutations. Screening of the *SPTBN2* gene in a cohort of families with dominant ataxia of unknown etiology and a large group of ataxia samples identified seventeen novel variants not found in the general population. Putative mutations were identified in the areas comprising the second calponin homology domain, spectrin repeat two to four, and the ninth spectrin repeat of β-III spectrin. To investigate the downstream effects of the American and German SCA5 mutations in neurons, I established a series of transgenic *Drosophila* models that express human β-III-spectrin or fly β-spectrin proteins containing SCA5 mutations. Through genetic and functional analyses I show that expression of mutant spectrin in the eye causes a progressive neurodegenerative phenotype and expression in larval neurons results in posterior paralysis, reduced synaptic terminal growth, and axonal transport deficits. These phenotypes are genetically enhanced by both dynein and dynactin loss-of-function mutations. I have additionally used the SCA5 fly models to conduct modifier screens and identify genes and biological pathways that may contribute to SCA5 pathogenesis. These studies revealed genetic interactors implicated in a wide range of biological functions including intracellular transport, synapse formation and function, protein homeostasis, and transcription regulation.

TABLE OF CONTENTS

LIST OF FIGURES

Chapter 1

Chapter 2

Chapter 3

Chapter 4

LIST OF TABLES

Chapter 1

Chapter 2

Chapter 3

Chapter 4

Chapter 6

ABREVIATIONS

ADCA	autosomal dominant cerebellar ataxia
ARP1	actin related protein 1
ABD	actin binding domain
BAC	bacterial artificial chromosome
bp, kb, Mb	basepairs, kilobases, megabases
BSA	bovine serum albumin
°C	temperature in degrees Celsius
CEPH	Centre d'Etude du Polymorphisme Humain
CH domain	calponin homology domain
CS	conservation score
CSP	cysteine string protein
Da, kDa	daltons, kilodaltons
Df	deficiency
DNA, cDNA	deoxyribonucleic acid, coding DNA
EAAT4	excitatory amino acid transporter 4
ECL	enhanced chemiluminescence
elav	embryonic lethal, abnormal vision
FITC	fluorescein isothiocyanate
GO	gene ontology
gmr	glass multiple reporter
GluRδ2	glutamate receptor delta 2 subunit
HEK 293	human embryonic kidney cell lines

IgA _____immunoglobulin A

IP _____immunoprecipitation

mGluR1α_____ metabotropic glutamate receptor 1 alpha

MRI_____magnetic resonance imaging

MT_____microtubules

NMJ_____neuromuscular junction

μg, mg, g _____micrograms milligrams, grams

μl, mL, L _____microliters, milliliters, liters

μM, mM, M_____micromolar, millimolar, molar

OD_____optical density

PBS _____phosphate buffered saline

PCR_____polymerase chain reaction

PH domain _____pleckstrin homology domain

RIPA _____radioimmunoprecipitation buffer

RNA, mRNA_____ribonucleic acid; messenger ribonucleic acid

RNAi_____RNA interference

rpm _____revolution per minute

RT-PCR_____reverse transcriptase polymerase chain reaction

SCA_____spinocerebellar ataxia

SCA5_____spinocerebellar ataxia type five

SD _____standard deviation

SEM _____scanning electron microscopy

S.E.M. _____standard error of the mean

SR _____spectrin repeat

SSCP _____single strand conformational polymorphism

SH3 domain _____Src-homology 3 domain

*SPTBN2*_____spectrin, beta, nonerythrocytic, 2

SNP _____single nucleotide polymorphism

TIRF _____total internal reflection fluorescence

UAS_____upstream activating sequence

UTR_____untranslated region

CHAPTER 1

INTRODUCTION TO THE SPINOCEREBELLAR ATAXIAS AND SCA5

I. The spinocerebellar ataxias

The autosomal dominant cerebellar ataxias (ADCAs) also known as spinocerebellar ataxias (SCAs) are a clinically and genetically heterogeneous group of neurological diseases that result in loss of movement and motor coordination. Epidemiological studies indicate that the SCAs are rare disorders, with an estimated prevalence of 5-7 cases in 100,000 individuals (van deWarrenburg *et al*., 2002; Craig *et al*., 2004). The frequency of particular SCA subtypes varies in some populations most likely due to the effect of founder mutations (Duenas *et al*., 2006).

The ADCA classification based on clinical symptoms proposed by Harding describes three main groups (Harding, 1982, 1983). ADCA type I patients present with progressive ataxia accompanied by other neurologic features, including ophthalmoplegia, pyramidal and extrapyramidal signs, peripheral neuropathy, and dementia. In addition to the characteristic cerebellar atrophy, degenerative changes are frequently found in other regions of the central and peripheral nervous systems (Duenas *et al.*, 2006). ADCA type II forms can be clinically distinguished by the presence of progressive retinal and macular degeneration, while ADCA type III patients experience symptoms and degeneration typical of a pure cerebellar condition (Duenas *et al*., 2006).

With the increasing number of genetic loci responsible for dominant ataxias that have been documented, a genetic classification of these hereditary disorders has also emerged. At present, 28 distinct genetic forms of spinocerebellar ataxias have been mapped and 16 disease-associated genes identified (Storey *et al*., 2009; Carlson *et al*.,

2009) (Table 1). Nevertheless, known genetic mutations account for only 40%-60% of hereditary ataxias (Grewal *et al*., 1998; Moseley *et al*., 1998; Sasaki *et al*., 2003) and pathogenic mutations remain undefined for an additional group of 12 SCAs that have been mapped to specific loci (Gardner *et al*., 1994; Brkanac *et al*., 2002; Verbeek *et al*., 2002; Vuillaume *et al*., 2002; Chung *et al*., 2003; Dudding *et al*., 2004; Knight *et al*., 2004; Stevanin *et al*., 2004; Verbeek *et al*., 2004; Guo-Yu *et al*., 2005; Cagnoli *et al*., 2006; Storey *et al*. 2009). For 20%-40% of the SCA families disease loci have not been determined (Sasaki *et al*., 2003) suggesting that the number of SCA subtypes will continue to grow.

About 50% of the families affected with known dominant ataxia mutations have CAG repeat expansions, which are translated into large polyglutamine stretches, within the coding region of the associated genes. These diseases include SCA1, 2, 3, 6, 7, 17 and dentatorubral pallidoluysian atrophy (DRPLA) (Duenas *et al*., 2006; Soong and Paulson, 2007). These seven SCA subtypes belong to a category of neurological disorders referred as “polyglutamine diseases”, which also includes Huntington’s disease (HD) and spinal and bulbar muscular atrophy (SBMA) (Imarisio *et al*., 2008; LaSpada *et al*., 1991). For these diseases a protein “gain-of function” mechanism has been proposed. Expanded polyglutamine proteins are prone to misfolding and aggregation. The presence of nuclear and cytoplasmic inclusions containing the polyglutamine aggregates, in addition to molecular chaperones, transcription factors, and components of protein degradation pathways in disease neurons, have been suggested to contribute to neuronal dysfunction and death (Cummings *et al*., 1998; McCampbell *et al*., 2000; William *et al*., 2009)

Pathogenic expansion mutations have also been identified outside of the protein-coding region of the *SCA8, SCA10,* and *SCA12* genes (Holmes *et al*., 1999; Koob *et al*,. 1999; Matsuura *et al*,. 2000). For these three SCA subtypes the most accepted disease hypothesis is an RNA gain-of-function mechanism, similar to the one suggested for myotonic dystrophy type 1 (DM1) and 2 (DM2), fragile X-associated tremor ataxia syndrome (FXTAS), and Huntington's disease-like-2 (HDL2). This model proposes that the expansion mutations when transcribed into long RNA repeats, can sequester RNA-binding proteins and lead to aberrant splicing of mRNA targets that are required for proper nervous system development and maintenance (Osborne and Thornton., 2006; Ranum and Cooper, 2006).

Interestingly, recent observations indicate that SCA8 repeat expansions are bi-directionally expressed to produce two potential pathogenic molecules (Moseley *et al*., 2006). In this case, neurodegeneration is likely to result from CUG expansion transcripts expressed in the CTG direction and/or the toxicity of a polyglutamine expansion protein expressed in the CAG direction (Moseley *et al*., 2006; Ikeda *et al*., 2008).

Similarly, two mechanisms could contribute to the cerebellar degeneration in SCA12 patients: The presence of transcripts containing the CAG repeat supports a gain-of-function RNA mechanism. Additional studies, however, suggest that expanded CAG tracts in the promoter region of the SCA12 gene (*PPP2R2B*), which encodes a brain-specific regulatory subunit of the protein phosphatase PP2A holoenzyme, may increase gene expression, and consequently alter PP2A activity and the pattern of phosphorylation of essential neuronal protein (Holmes *et al*., 2001, 2003).

In addition to repeat expansion mutations, conventional mutations in genes implicated in different cellular pathways have started to emerge as a new cause of ataxia for a large group of SCAs (Table 1). For example, missense mutations in the *voltage-gated potassium channel (KCNC3), protein kinase C gamma (PKCγ), fibroblast growth factor 14 (FGF14)*, *puratrophin-1 (PLEKHG4)*, and *spectrin, non-erythroid beta chain 2* (*SPTBN2*) genes have been reported in SCA13, SCA14, SCA 27, chromosome 16q22 linked SCA, and SCA5 families, respectively (Waters *et al*., 2006; Chen *et al*., 2003; van Swieten *et al*., 2003; Ikeda *et al*., 2006). More recently, mutations in *tau tubulin kinase-2 (TTBK2)* and *inositol 1, 4, 5-triphosphate receptor, type 1 (ITPR1)* genes have been reported to cause SCA11 and SCA15/16, respectively (Houlden *et al*., 2007; van de Leemput *et al*., 2007; Iwaki *et al*., 2008).

II. Spinocerebellar ataxia type 5 (SCA5)

A. Genetics of SCA5

SCA5 is a slowly progressive form of cerebellar ataxia that was first described by Ranum and colleagues in 1994 (Ranum *et al*., 1994) in a 10-generation American family descended from President Abraham Lincoln's paternal grandparents. Linkage studies performed on DNA collected from 248 family members, including 77 affected individuals were used to map the disease locus to the centromeric region of chromosome 11 (Ranum *et al*., 1994).

Two unrelated German and French pedigrees with similar disease presentation also mapped to the SCA5 locus (Stevanin *et al*., 1999; Bürk *et al*., 2004). The SCA5 critical region was refined to a 2.99 Mb interval containing more than 100 genes, that

was shared by the three families (Ikeda *et al*., 2006). In a further attempt to identify the disease-associated gene, DNA from an affected member of the American SCA5 family was used to generate haploid cell lines and a genomic DNA library of BAC clones covering the conserved interval. Shotgun sequencing analysis of three BAC clones spanning a 255 kb region of haplotype conservation common to the American and French kindreds identified a 39-base pair deletion in exon 12 of the *Spectrin, beta, non-erythrocytic 2* gene (*SPTBN2*) which encodes the protein β-III spectrin (Figure 1).

ß-III spectrin, one of the five β-spectrins in human contains two calponin-homology domains at the N-terminal region, followed by 17 tandem spectrin-repeat domains, and a C-terminal pleckstrin-homology domain. The American SCA5 mutation, which results in an in-frame deletion of 13-amino acids (p.E532_M544del) at the beginning of the third spectrin repeat, was found segregating in all 90 affected individuals and 35 presymptomatic carriers (Ikeda *et al*., 2006).

Sequencing of the *SPTBN2* gene in the French pedigree uncovered a 15-base pair deletion in exon 14 in all six affected family members and one presymptomatic carrier (Ikeda *et al*., 2006). In this case, the mutation produces a deletion of 5 amino acids and the in-frame insertion of a tryptophan residue (p.L629_R634delinsW) at the end of the third spectrin repeat (Figure 1).

Similarly, a T>C single base pair substitution in exon 7 of the *SPTBN2* gene (c.758T>C) was found in all 12 affected members of the German SCA family (Ikeda *et al*., 2006). This mutation replaces a highly conserved leucine residue (p.L253P) within the second calponin homology domain (Figure 1).

B. Clinical, anatomical, and neuropathological features of SCA5

SCA5 primarily affects the cerebellum leading to reduced or impaired motor coordination. Disease onset normally occurs during the third or fourth decade of life, but early (10 year) and late onset (68 year) cases have also been described (Ranum *et al*., 1994; Stevanin *et al*., 1999; Schut *et al*., 2000; Burk *et al*., 2004). At early disease stages, the majority of SCA5 patients present with mild disturbance of gait, incoordination of the upper limbs, and slurred speech (Ranum *et al*., 1994; Stevanin *et al*., 1999; Burk *et al*., 2004). Clinical symptoms summarized in Table 2 worsen over time eventually resulting in disability without generally shortening life span (Schut *et al*., 2000). Adult-onset SCA5 patients do not show signs of bulbar paralysis (Ranum *et al*., 1994) which frequently leads to premature death in more severe forms of cerebellar ataxias. In contrast, some juvenile onset SCA5 patients that have been examined show signs of bulbar and pyramidal tract involvement. These patients develop a weakened cough and swallowing difficulties (Ranum *et al*., 1994; Schut *et al*., 2000), which can lead to a decreased ability to combat respiratory infections and recurrent episodes of pneumonia that may shorten their lifespan (Ranum *et al*., 1994).

Based on the slow progression of the symptoms and the areas of the brain that are affected, SCA5 can be clinically categorized as a pure form of cerebellar ataxia. Magnetic resonance imaging (MRI) studies show that degenerative changes largely involve the cerebellum, whereas the cerebral hemispheres, basal ganglia, inferior vermis, tonsils, and brainstem appear spared (Stevanin *et al*., 1999; Schut *et al*., 2000; Liquori *et al*., 2002; Burk *et al*., 2004). In late disease stages some patients show minimal brainstem

atrophy. Within the cerebellum, there is dramatic atrophy of the cortical region with deterioration of the superior hemispheres and anterior vermis (Figure 2).

Pathological analysis has been performed on a brain from an 89-years old affected female from the American SCA5 family (onset of symptoms in late fifties). The cerebellum from this patient was atrophic (88g) and exhibited a marked degeneration of the anterior vermis and the anterior-superior portions of the cerebellar hemispheres, with relative sparing of the tonsillar cortex (Schut *et al*., 2000; Liquori *et al*., 2002). Histological studies showed a significant thinning of the cerebellar molecular layer of the cerebellum with profound loss of Purkinje cells, milder loss of granular neurons, and the presence of numerous empty basket fibers (Schut *et al*., 2000; Liquori *et al*., 2002).

III. The spectrin cytoskeleton

A. Structural components

The spectrin cytoskeleton is a dense two-dimensional protein network lining the inner surface of the plasma membrane that was first identified and characterized in human erythrocytes (Bennett and Baines, 2001). Central to this network are spectrin molecules, which interact with short actin filaments to form junctional complexes that provide the mechanical support and elasticity that red blood cell membranes need to withstand the turbulence of circulation (Bennett and Giligan, 1993; Bennett and Baines, 2001). The association between spectrin and actin is stabilized by cytoskeletal co-factors like protein 4.1 and adducin. Moreover, the spectrin-actin mesh is linked to the plasma membrane of the erythrocytes through adaptor proteins, including ankyrin (Kennedy *et al*. 1991; Bennett and Baines, 2001). Mutations in spectrin, other components of the spectrin

network, and accessory proteins have been associated with different types of hereditary hemolytic anemias in humans and mice (Tse and Lux, 1999; Delaunay, 2007).

The role of the spectrin cytoskeleton in maintaining the structural integrity of cellular membranes extends beyond human erythrocytes. Homologs of spectrin, ankyrin, and their associated partners are present in almost every cell from all metazoan organisms, including humans in which five β-spectrin and two α-spectrin proteins have been identified (Bennett and Baines, 2001).

Each functional spectrin molecule is a tetrameric complex composed of two α- and two β- subunits (Figure 4). Most of each spectrin subunit consists of contiguous and highly conserved 106-amino acids units folded into a triple α-helical structure known as the "spectrin repeat" (Speicher and Marchesi, 1984; Yan *et al*., 1993). However, the basic structural unit of spectrin is a heterodimer resulting from the association between α- and β-spectrin subunits (Bennett and Baines, 2001). Tetramer formation depends on head-to-head association between two α/β spectrin dimers, in which the amino-terminus of α-spectrin subunits interacts with the carboxy-terminus portion of β-spectrin (Bennett and Healy, 2008) (Figure 4).

The actin binding activity of the spectrin molecule resides at the N-terminal segment of the β-spectrin subunits. This region comprises two tandemly arranged calponin homology (CH) domains, similar in sequence and structure to those identified in other actin-binding proteins, including dystrophin, utrophin, α-actinin, and fimbrin (Djinovic Carugo *et al*., 1997; Banuelos *et al*., 1998).

The association between the spectrin cytoskeleton with the cytoplasmic face of the plasma membrane is facilitated by a β-spectrin binding site for the adaptor protein ankyrin that spans the end of the fourteen and most of the fifteenth spectrin repeat (Kennedy *et al*. 1991). Additionally, spectrin binds membrane and cytosolic proteins using different ankyrin-independent mechanisms (summarized in De Matteis and Morrow, 2000). For instance, the spectrin-membrane association can be achieved via a pleckstrin homology (PH) domain located in the C-terminal segment of β-spectrin. Ligands that bind the PH domain of spectrin include anionic phospholipid components of the lipid bilayer as well as membrane proteins (Bennett and Baines, 2001) (Figure 4). The presence of a Src-homology-3 (SH3) domain in the α-spectrin subunits allows specific interaction with membrane associated proteins and the recruitment to membranes of cytosolic proteins and signaling complexes (Bennett and Baines, 2001). In addition, numerous proteins and membrane lipids can directly interact with the spectrin repeats of both α- and β- polypeptides (De Matteis and Morrow, 2000).

B. Functions

The major role of spectrin in providing elasticity and mechanical strength to cellular membranes has been well established in erythrocytes (Lee and Discher, 2001). Similarly, in the nematode *Caenorhabditis elegans*, spectrins appear to be particularly important for conferring elastic strength to the axonal membranes of motor neurons (Hammarlund *et al*., 2007). Worms that lack β-spectrin are uncoordinated and highly sensitive to axonal breakage caused by movement-induced acute strain (Hammarlund *et al*., 2000, 2007).

One of the most comprehensive analyses of the function of the spectrin cytoskeletal network has been conducted in *Drosophila melanogaster,* where each of the single α- and β-spectrin genes are essential for development (Dubreil *et al*., 2000). The fly spectrin/ankyrin skeleton plays a general scaffolding role and contributes to membrane stability and the formation of discrete membrane domains (Pielage *et al*., 2005, 2006, 2008). Specifically, fly β-spectrin null mutants fail to accumulate the Na, K ATPase at the basolateral domain of midgut epithelial cells (Dubreil *et al*., 2000) whereas the ubiquitous loss of α- and/or β-spectrins results in impaired neurotransmission, and disrupts the subcellular localization of numerous synaptic proteins (Featherstone *et al*., 2001). Additional studies in which spectrin is eliminated in particular tissues using RNA interference (RNAi) techniques have demonstrated that fly β-spectrin is necessary for targeting α-spectrin and ankyrin to the synaptic membrane (Das *et al*., 2006; Pielage *et al*., 2006). Moreover, the fly pre-synaptic spectrin mesh is required for synapse growth and stability at the neuromuscular junction (NMJ) (Featherstone *et al.*, 2001; Pielage *et al*., 2005, 2006). In the absence of α- or β-spectrin, cell adhesion molecules like Fasciclin II (Fas II) and Neuroglian (Nrg), that are essential for normal synaptic formation and stability (Schuster *et al*., 1996; Godenschwege *et al.*, 2006), are absent from the site of the synapse (Pielage *et al*., 2005). The loss of synaptic membrane adhesion proteins follows the initial disruption of the microtubule (MT) cytoskeleton at the synaptic membrane, suggesting that spectrin can additionally influence the stability of synaptic MTs and contribute to synapse disassembly (Pielage *et al*., 2005). Similarly, spectrin removal from the postsynaptic membrane decreases the size and enlarges the spacing of synapses. Remarkably, loss of postsynaptic spectrin not only disrupts the organization of

the neuromuscular junction and the clustering of postsynaptic glutamate receptors, but also alters the distribution of presynaptic molecules (Pielage *et al*., 2006).

In vertebrates, the spectrin scaffold also organizes and stabilizes proteins at the membrane in diverse cell types (Bloch and Morrow, 1989; Jenkins and Bennett, 2001; Ango *et al*., 2004; Bennett and Healy, 2008). Recent studies performed in human bronchial epithelial cells suggest that β-II spectrin is not only required for E-cadherin localization at the lateral membrane (Kizhatil *et al*., 2007a) but in conjunction with ankyrin-G assures the delivery of proteins and phospholipids necessary for lateral membrane biogenesis (Kizhatil *et al*., 2007b).

Within the nervous system, spectrin contributes to the clustering of membrane channels, receptors, and cell adhesion molecules within specialized membrane domains. For example, in mice, β-IV spectrin stabilizes voltage-gated sodium channels and L1 cell adhesion molecules (L1-CAM) at the nodes of Ranvier and initial segments of neurons (Komada and Soriano, 2002; Lacas-Gervais *et al*., 2004). Similarly, human β-III spectrin stabilizes the Purkinje cell excitatory amino acid transporter 4 (EAAT4) at the surface of the dendritic plasma membrane (Jackson *et al*., 2001), a function that is disrupted by SCA5 mutant spectrin (Ikeda *et al*., 2006).

Spectrin has also emerged as a participant in the secretory pathway. Evidence for the existence of a spectrin network that associates with intracellular membranes came from the findings that multiple spectrin and ankyrin isoforms associate with organelle membranes, including Golgi, lysosomes, and intracellular vesicles in cerebellar neurons (Malchiodi-Albedi *et al*., 1993; Beck *et al*., 1994; Devarajan *et al*., 1996; Beck *et al*., 1998; Hoock *et al*., 1997; Godi *et al*., 1998; Stankewich *et al*., 1998; Beck, 2005).

Interestingly, the coat-like pattern and behavior of Golgi-specific spectrins suggests a role for these proteins in vesicle sorting and trafficking (Beck, 2005). In support of this proposal, several studies have identified an interaction of Golgi spectrins with both the dynactin complex (Holleran *et al.*, 2001) and intracellular membranes (De Vos *et al*., 2003). The dynactin-mediated association between spectrin and the microtubule network is likely to provide a stable cytoskeletal scaffold that could contribute to the organization of the Golgi apparatus. In addition, spectrin may participate in intracellular transport events via the regulation of microtubule organization and/or as predicted, it could have a more direct role in mediating the interaction between cargo and motor protein complexes (Holleran *et al.*, 2001; Muresan *et al*., 2001; De Vos *et al*. 2003).

IV. Introduction to human β-III spectrin

A. Expression pattern and functional domains

The *SPTBN2* gene encodes a 2,391 amino-acid β-III spectrin protein (Ohara *et al*., 1998) with high homology to four other human β-spectrin proteins (Stankewich *et al*., 1998). Like other conventional β-spectrin proteins, β-III spectrin contains two N-terminal calponin-homology domains capable of binding actin, followed by 17 consecutive spectrin-repeats, and a C-terminal pleckstrin homology domain. Spectrin repeats 15 and 17 bear the ankyrin-binding and the spectrin self-association domain, respectively (Holleran *et al*., 2001).

ß-III spectrin transcripts are broadly expressed in both fetal and adult human tissues, however, the expression levels vary dramatically with the most abundant

expression detected in the brain and moderate levels detected in kidney, pancreas, liver, testis, and the prostate, pituitary, adrenal, and salivary glands (Ohara *et al*., 1998; Holleran *et al*., 2001). Within the brain, β-III is predominantly expressed in the cerebellum (Ohara *et al*., 1998; Ikeda *et al*., 2006) (Figure 3A) where there is prominent staining of Purkinje cells indicated by immunohistochemistry This pattern of protein localization nicely correlates with the dramatic Purkinje cell loss seen in SCA5. Despite the severe degeneration of the cerebellum observed in an SCA5 autopsy case, the few remain Purkinje neurons show positive β-III spectrin immunoreactivity in the cell bodies, dendrites, and axons (Ikeda *et al*., 2006) [Figure 3B and Ikeda (personal communication)].

B. Proposed functional roles for β-III spectrin

ß-III spectrin was initially characterized as a brain spectrin that associates with Golgi based on its cytoplasmic punctate distribution that overlaps the localization of markers of Golgi and vesicle membranes, and its co-fractionation with vesicle and organelle membrane proteins in a sucrose gradient (Stankewich *et al*., 1998). However, the spectrin antibody used to identify the Golgi-localized spectrin was later found to cross-react with the Golgi-associated protein syne-1 (Gough *et al*., 2003). Additional studies now suggest a role for this protein in the intracellular transport of vesicles and organelles. For instance, β-III spectrin co-purifies with subunits of the dynein motor complex and dynactin in vesicle preparations and directly binds the ARP1 subunit of the dynactin complex (Holleran *et al*., 2001). In addition, β-III spectrin is required for linking dynactin, and thereby dynein, to liposomes and axonal vesicle membranes, and for

reconstituting the motility of synaptic vesicles from squid axoplasm (Muresan *et al*., 2001).

These data support a model in which the interaction between β-III spectrin and ARP1 recruits the dynein-dynactin machinery to intracellular vesicle membranes and provides a direct link between the microtubule-based motor complex and its membrane-bounded cargo (Figure 4A). Interestingly, one the binding sites for ARP1 in β-III spectrin is located in the second CH domain, the same region that binds actin and harbors the German SCA5 mutation (L253P) (Ikeda *et al*., 2006). Recently, Karen Armbrust a former Graduate Student in Dr. Laura Ranum's Lab, identified a novel interaction between $p150^{Glued}$, another subunit of dynactin, and a fragment containing repeats two and three of β-III spectrin (Armbrust *et al*., in preparation). Dr Armbrust's studies additionally show that the American SCA5 mutation reduces the strength of the interaction of β-III spectrin with $p150^{Glued}$. It is likely that disrupting the functional association between the spectrin mesh and the microtubule (MT) cytoskeleton, mutant β-III spectrin may influence the intracellular transport and localization of synaptic components, and contribute to neuronal degeneration.

A role for β-III spectrin has also been proposed in the stabilization of membrane proteins and the formation of specialized membrane domains either by direct association with membrane phospholipids and membrane proteins, or through adaptor proteins like ankyrin (Figure 4B). This proposal is supported by several lines of evidence. First, β-III spectrin physically interacts with the Purkinje cell perisynaptic proteins excitatory amino acid transporter 4 (EAAT4), glutamate receptor delta 2 subunit (GluRδ2), and the metabotropic glutamate receptor 1α (mGluR1α) (Hirai and Matsuda, 1999; Jackson *et*

al., 2001; Armbrust *et al*., in preparation). Second, functional studies show that β-III spectrin stabilizes EAAT4 at the plasma membrane and modulates the uptake of glutamate by EAAT4 (Jackson *et al*., 2001). Importantly, TIRF microscopy analysis conducted in HEK 293 cells show that unlike the wild-type protein, SCA5 mutant spectrin fails to stabilize EAAT4 at the surface of the plasma membrane (Ikeda *et al*., 2006). In addition, cell fractionation studies detect differences in the distribution of the synaptosomal proteins EAAT4 and GluRδ2 in protein extracts from a SCA5 autopsy cerebellum (Ikeda *et al*., 2006). Finally, immunofluorescence studies reveal changes in the distribution of EAAT4 and mGluR1α proteins in the Purkinje dendritic spines of an SCA5 mouse model that conditionally express the American SCA5 mutation in cerebellar Purkinje cells (Armbrust *et al*., in preparation). Changes in the localization and activity of EAAT4, GluRδ2, and mGluR1α at the plasma membrane may alter the regulation of glutamate signaling in the cerebellum and contribute to Purkinje cell degeneration in SCA5.

V. Conclusions

SCA5 is a pure form of cerebellar ataxia with slow progression caused by mutations in the *SPTBN2* gene, which encodes the cytoskeletal protein β-III spectrin highly expressed in Purkinje cells. Although it is not yet clear how β-III spectrin mutations cause Purkinje cell death in SCA5 patients, several lines of evidence have led to the proposal that SCA5 pathogenesis results from destabilization of specialized synaptic membrane domains and/or defects in intracellular transport. The identification and further characterization of SCA5 mutations will allow learning about the normal

function of β-III spectrin and discerning specific molecular mechanisms that may contribute to cerebellar degeneration and ataxia.

VI. Overall Aims and Hypotheses

The overall aim of this work is to understand how spectrin mutations cause Purkinje cell death and cerebellar degeneration, and to define basic cell biological functions that are affected as a consequence of these mutations using human genetic and animal model approaches. Three distinct β-III spectrin mutations have been reported to cause SCA5; however, it is likely that additional mutations in *SPTBN2* also lead to ataxia and neurodegeneration. To get insight into the biology of the disease and the normal function of β-III spectrin and to estimate the frequency of SCA5 mutations among ataxia patients, I used a forward human genetic approach to identify novel *SPTBN2* mutations. For that purpose, I screened the SCA5 gene in a large group of families with dominant ataxia of unknown etiology and individual ataxia cases (Chapter 2). To examine the downstream effects of the SCA5 mutations on neuronal function and to specifically test the hypothesis that spectrin mutations cause intracellular transport deficits, I generated the first transgenic *Drosophila* models of SCA5 by overexpressing human β-III-spectrin or fly β-spectrin proteins containing SCA5 mutations (Chapter 3) and used these models to conduct modifier screens in *Drosophila* and identify genes and biological pathways that may contribute to SCA5 pathogenesis (Chapter 4).

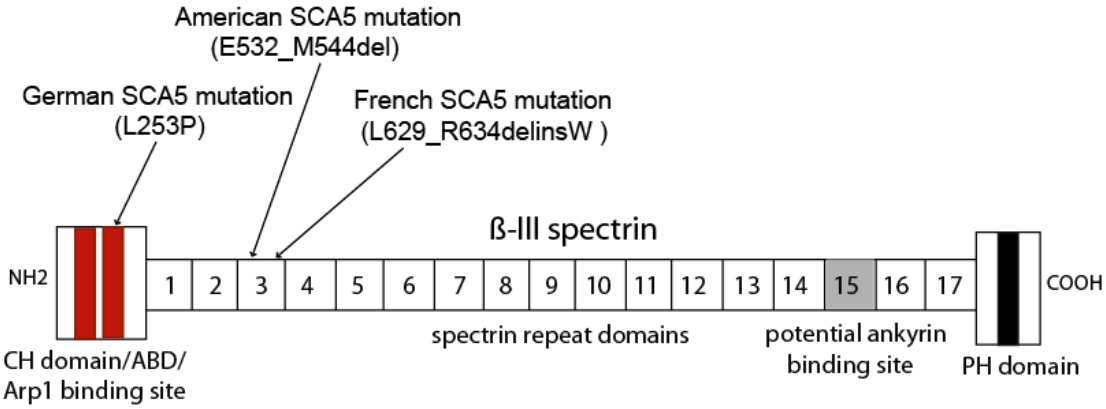

Figure 1. SCA5 mutations. A schematic representation of the functional domains of β-III spectrin is shown along with the position of the three SCA5 mutations. The American SCA5 mutation causes an in-frame deletion of 13 amino acids at the beginning of the third spectrin repeat. The French SCA5 mutation causes an in-frame deletion of 5 amino acids and the insertion of a tryptophan residue at the end of the third spectrin repeat. The German SCA5 mutation replaces an evolutionary conserved leucine residue in the second CH domain. CH: calponin homology domain; ABD: actin binding domain; PH: pleckstrin homology domain.

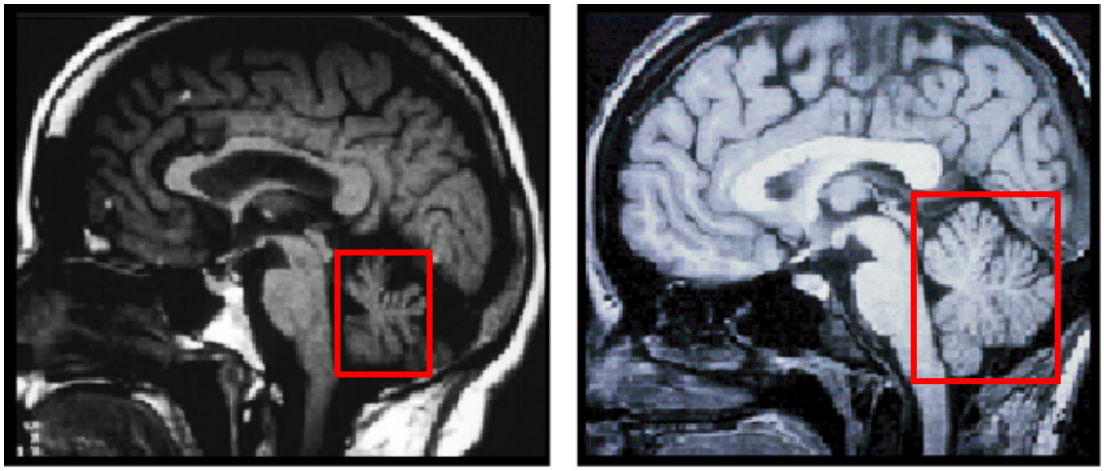

Figure 2. Cerebellar atrophy in SCA5. Sagittal MRI scan from an affected individual at age 64 shows marked cerebellar atrophy with minimal brainstem atrophy, and no evidence of cerebral involvement. There is relative preservation of the posterior hemisphere, posterior vermis, and tonsillar cortex. Modified and reprinted with permission from Liquori *et al*., 2002. Spinocerebellar ataxia type 5. In: M. Manto and M. Pandolfo (Eds.), The Cerebellum and its Disorders. Cambridge University Press©, Cambridge, U.K, pp. 445-450.

A

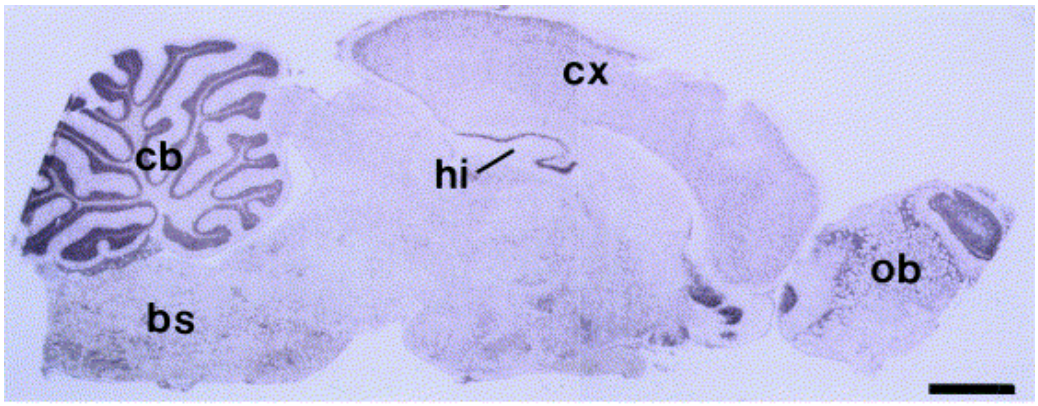

B

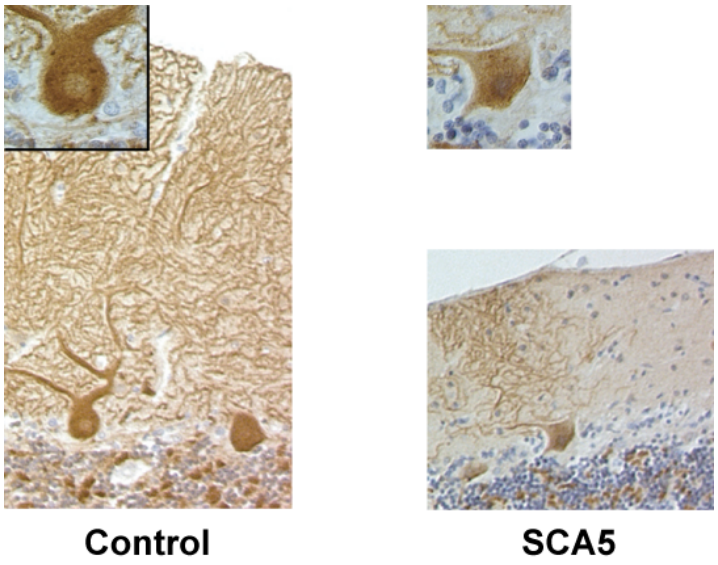

Figure 3. B-III spectrin expression. (A) In situ hybridization analysis of β-III spectrin mRNA in a sagittal section of whole brain shows predominant expression in the cerebellum: ob, olfactory bulb; cx, cerebral cortex; hi, hippocampus; cb, cerebellum; bs, brain stem. Figure and legend are reprinted with permission from Ohara *et al*., 1998, Molecular Brain Research, Vol. 57(2), pp. 181-192. (B) Immunohistochemistry of control and American SCA5 cerebellar tissues. Sections were stained with an antibody raised against the N-terminal portion of β-III spectrin, and visualized at 200X magnification. Enlarged images of the Purkinje cells are also shown (630X). Purkinje cell loss, dendritic atrophy and significant thinning of the molecular layer are seen in SCA5 compared to control. Figure and legend are reprinted with permission from Ikeda *et al*., 2006, *Nature Genetics*, Vol. 38, pp. 184-190.

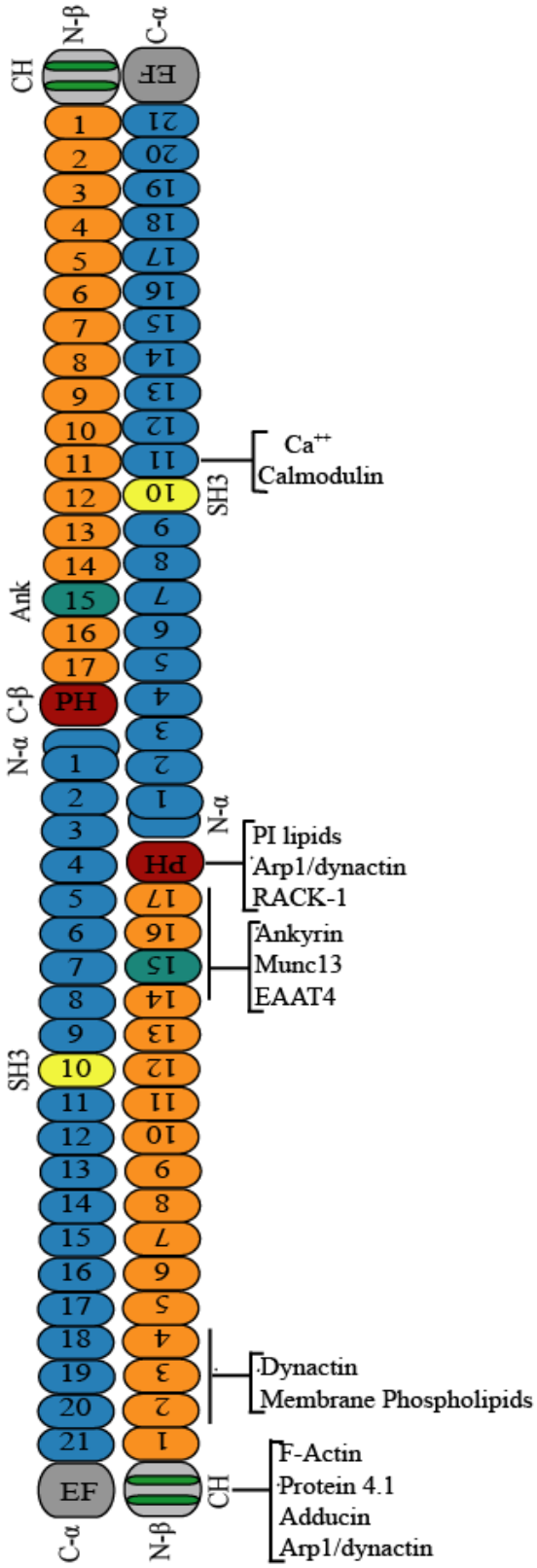
N-β
C-α
CH
EF
SH3
Ca++
Calmodulin
Ank
C-β
N-α
PH
PI lipids
Arp1/dynactin
RACK-1
Ankyrin
Munc13
EAAT4
Dynactin
Membrane Phospholipids
F-Actin
Protein 4.1
Adducin
Arp1/dynactin

Figure 4. The spectrin tetramer. The diagram shows the arrangement of α- and β-spectrins in the spectrin tetramer. The N-terminus of each α-spectrin subunit (blue) associates with the C-terminal portion of β-spectrin (orange) to form a dimer. Tetramer formation depends on the anti-parallel head to head association between two α/β spectrin dimers. Spectrin repeat units are indicated by numbers. Functional domains of α-spectrin include the SH3: Src-homology domain (yellow) and EF: Calcium binding-EF hand domain (gray). Functional domains of β-spectrin include two CH: calponin homology domain (green) and PH: pleckstrin homology domain (red). Examples of ligands known to interact with spectrin are indicated along with their approximate binding site.

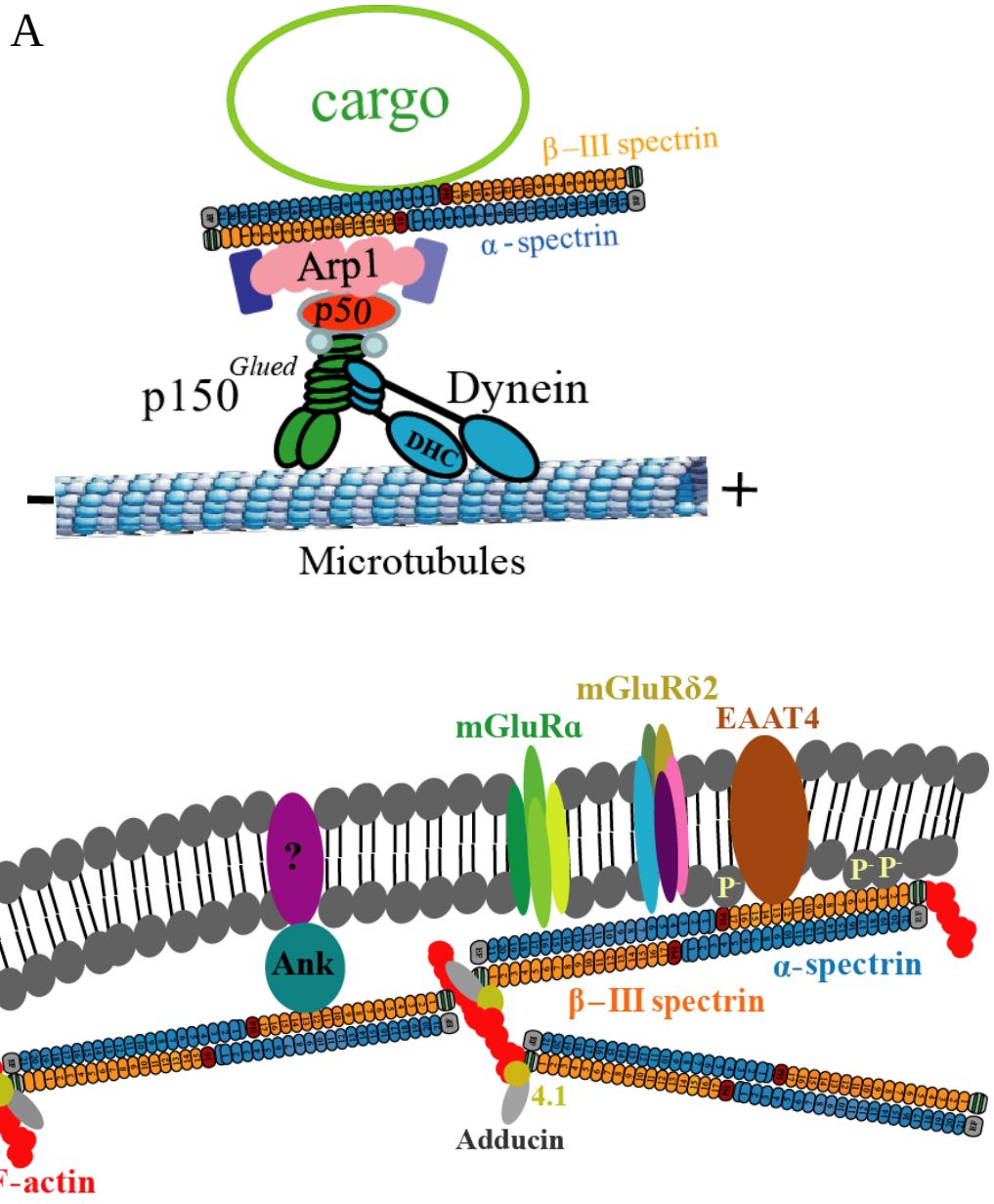

Figure 5. Functions of human β-III spectrin. Schematic diagrams that illustrate the proposed roles of β-III spectrin in: (A) Intracellular transport of vesicles and organelles mediated by the dynein/dynactin transport machinery. (B) Stabilization of membrane proteins and organization of macromolecular complexes in diverse types of specialized membranes domains either by direct association with membrane phospholipids and membrane proteins, or through molecular linkers like ankyrin (Ank).

ADCA TYPE I					*ADCA TYPE III*		
SCA	***Locus***	***Mutation***	***SCA***	***Locus***	***Mutation***	***SCA***	***Locus***	***Mutation***
SCA1	6p23	Coding CAG expansion in *ATXN1*	SCA20	11p11.2 -q12.3	Chromosonal duplication	SCA5	11q13	Mutations in *SPTBN2*
SCA2	12q24	Coding CAG expansion in *ATXN2*	SCA21	7p21- p15	Unknown	SCA6	19p13	Coding CAG expansion in *CACNA1A*
SCA3	14q32	Coding CAG expansion in *ATXN3*	SCA22	1p21-q23	Unknown	SCA11	15q15.2	Mutations in *TTBK2*
SCA4	16q22.1	Unknown	SCA23	20p13-12.2	Unknown	SCA14	19q13	Mutations in *PRKCG*
SCA8	13q21	Coding CAG expansion in *ATXN8* and non-coding CTG expansion in *ATXN8OS*	SCA25	2p21-p13	Unknown	SCA15/16	3p26.2	Mutations in *ITPR1*
SCA10	22q13	Non-coding ATTCT expansion in *ATXN10*	SCA27	13q34	Mutations in *FGF14*	SCA26	19p13.3	Unknown
SCA12	5q32	Non-coding CAG expansion in *PPP2R2B*	SCA28	18p11.2 2-q11.2	Unknown	SCA29	3p26	Unknown
SCA13	19q13.3	Mutations in *KCNC3*	*ADCA TYPE II*			SCA30	4q34.3-q35.1	Unknown
SCA17	6q27	Coding CAG expansion in *TBP*				16q22 linked	16q22.1	Mutations in *PLEKHG4*
SCA18	7q31-q32	Unknown	***SCA***	***Locus***	***Mutation***			
SCA19	1p21-q21	Unknown	SCA7	3p14	Coding CAG expansion in *ATXN7*			

Table 1. Summary of the classification of the autosomal dominant spinocerebellar ataxia loci based on clinical features.

Family	*Age of onset*	*Disease symptoms*	*Neuroimaging results*
American	10-68 years (mean 33 ±13)	Ataxia of trunk, gait and limbs, gaze-evoked nystagmus, dysarthria, loss of vibration sense	Atrophy of the cerebellar vermis and hemispheres, brainstem sparing
French	14-40 years (mean 27±10)	Ataxia of gait and limbs, gaze-evoked nystagmus, increased reflexes, facial myokymia, decreased vibration sense	Atrophy of the cerebellar vermis and hemispheres, spared pons
German	15-50 years (mean 32 ±12)	Ataxia of stance, gait, and limbs, gaze-evoked nystagmus, dysarthria, downbeat nystagmus	Atrophy of the cerebellar vermis and hemispheres, brainstem sparing

Table 2. Clinical features of SCA5. This table summarizes and compares disease features found in affected members of the American, French, and German SCA5 families.

CHAPTER 2

IDENTIFICATION OF NOVEL SCA5 MUTATIONS

I. Introduction

The dominant cerebellar ataxias (SCAs) have long been classified based on clinical symptoms and the areas of the brain, other than the cerebellum, that are affected (Harding, 1982, 1983). However, similar disease features are shared by different SCA subtypes making a specific diagnosis difficult to perform in the absence of other molecular information. Genetic approaches have allowed a more defined ataxia classification. The identification of the causative SCA genes and mutations makes it possible to differentiate these disorders at the molecular level and provides a fraction of ataxia families with accurate diagnosis and genetic counseling options.

As previously described, SCA5 is a pure form of cerebellar ataxia caused by mutations in the *SPTBN2* gene which encodes the cytoskeletal protein β-III spectrin (Ikeda *et al*., 2006). The current disease diagnosis is based on the evaluation of patients for common ataxia symptoms (e.g. loss of coordination, balance, and speech) by a neurologist combined with genetic testing.

Although commercially available screening to date is only being done for regions containing the three initially defined mutations (exons 7, 12, and 14), β-III spectrin is a large protein with seventeen spectrin repeats and various functional domains, all known to play structural and/or functional roles in this protein. Previous studies have demonstrated that the first two spectrin repeats of β-spectrin are critical for the formation of α/β spectrin heterodimers (Ursitti *et al*. 1996). Similarly, individual spectrin repeats,

the two CH domains, the PH domain, and the putative ankyrin binding site have been shown to confer specificity to the interaction of β-spectrins with different binding proteins (Kennedy *et al*. 1991; Sakaguchi *et al*., 1998; Holleran *et al*., 2001; Jackson *et al*., 2001; Leshchyns'ka *et al*., 2003) and membranes (Muresan *et al*., 2001, DeVos *et al*., 2003). Mutations in any of these motifs may impact the structure, binding properties, and overall function of the protein and also may lead to disease.

Consistent with this proposal, numerous studies have reported that different mutations in genes encoding similar proteins can result in variable disease phenotypes. For example, single nucleotide substitutions, small insertions, and deletions in dystrophin can cause Duchenne muscular dystrophy, Becker muscular dystrophy, and X-linked cardiomyopathy (Ortiz-Lopez *et al*., 1997; Hegde et al., 2008).

The identification of additional *SPTBN2* mutations in families and patients with unknown forms of ataxia and the evaluation of their functional impact will contribute to our understanding of the basic biological processes affected in SCA5 and the role of β-III spectrin in disease. Towards this goal, I screened families and individual samples with ataxia of unknown etiology for mutations in *SPTBN2* and identified seventeen putative SCA5 mutations. These findings preliminary estimates the frequency of SCA5 cases within the ataxia community and represent an additional step towards an accurate diagnosis of this genetic condition.

II. Results

To better understand the role of spectrin mutations in ataxia I screened probands from families with dominant ataxias of unknown etiology and a collection of ataxia samples for mutations in the *SPTBN2* gene.

I initially investigated if mutations in the SCA5 gene could be found in affected members of the SCA20 family (Knight *et al*., 2004). The underlying genetic defect in SCA20 has yet to be identified, but the disease locus maps to a portion of the centromeric region of chromosome 11 that includes the SCA5 critical region. Although some of the clinical features of SCA5 and SCA20 differ (Liquori *et al*., 2002; Knight *et al*., 2004), the overlapping localization of both loci raises the possibility that these phenotypic differences result from distinct mutations located within the same gene. To determine whether SCA5 and SCA20 are allelic or genetically distinct diseases I amplified and subsequently sequenced the 37 exons of *SPTBN2*. No changes in the *SPTBN2* sequence were detected, with the exception of a previously reported single-nucleotide polymorphism (SNP) (c.T3173C) and two likely SNPs (c.C657T in exon 6 and c.C5742T in exon 27), neither of which changes the amino acid sequence of the protein and neither of which is located in a position likely to affect splicing. Additionally, no changes were found in 460 bp of genomic DNA upstream of the initiator ATG, covering the entire 5' UTR and an additional 285 bp of the 3' UTR (Lorenzo *et al*., 2006). These data suggest that SCA20 is not caused by a mutation in *SPTBN2* and that SCA20 is a genetically distinct form of SCA.

In support of this result, a duplication of a portion of the SCA20 region (260 kb), that does not include the *SPTBN2* gene, segregates in all affected members of the SCA20

family (Knight *et al*., 2008). Future understanding of the molecular consequences of this duplication will be needed to define the mechanisms of disease.

To identify novel SCA5 mutations, I screened the complete coding sequence plus 50 bp of flanking intron sequence and the 5' and 3' UTRs of *SPTBN2* in probands from 318 dominant ataxia families collected in France and the United States using PCR-single strand conformational polymorphism (SSCP) analysis (Orita *el al*., 1989) combined with direct sequencing. The SSCP methodology relies on the amplification of small DNA fragments that are subsequently denatured and electrophoresed on high resolution, nondenaturing acrylamide gels to promote the refolding and separation of single-stranded nucleic acids segments. Changes of the base composition of a DNA stretch, including single nucleotide substitutions, are likely to alter the secondary structure of the molecule and its electrophoretic mobility.

Therefore, I closely examined the pattern of DNA migration on nondenaturing acrylamide gels and I identified bands with shifted mobility. After reamplifying and sequencing all positive samples, I identified one previously reported SNP (p.R1880H, rs4930388) and a group of novel DNA changes that result in silent and missense mutations throughout the gene. To determine whether these variations are found in the general population, and therefore less likely to be pathogenic, DNA from unrelated controls subjects (*n=800*) was screened. This approach identified three non-reported missense mutations, not found in controls, in three ataxia families collected in France [Figure 6 (red fonts) and Table3]. Clinical and genetic information for these families is summarized in Table 4.

The proband representing family I carries two separate DNA mutations. Cloning

and sequencing of a PCR fragment that harbors the two novel variants revealed that the mutations are on the same haplotype (Figure 7A). The A→G change in exon 17 substitutes a histidine with an arginine in spectrin repeat number nine (H1229R, Figure 6,7B) while the G→A mutation in exon 18 replaces an arginine residue within the linker region between spectrin repeats nine and ten with a glutamine (R1278Q, Figure 6, 7C).

Probands representing families II and III (Figure 7D, E) have the same A→G mutation resulting in a glutamic acid to glycine substitution (E1241G, Figure 6, 7F), which also occurs in the ninth spectrin repeat. DNA was also available for one unaffected member of family II who did not carry a similar mutation (Figure 7D).

Additionally, I describe novel *SPTBN2* mutations and polymorphisms found in a large panel of 6,269 DNA samples sent to Athena Diagnostics for ataxia testing (Figure 6 and Table 3). Most of these DNAs are from patients who have been examined by a neurologist and found to manifest symptoms characteristics of ataxia, but additional clinical and family history information is not available for the majority of these cases.

These DNA samples were screened for mutations in exons 7, 12, and 14 of *SPTBN2*. Sequencing analysis identified the American SCA5 mutation (p.E532_M544del) in five ataxia samples and a group of fourteen putative mutations that I subsequently show are not found in 1,600 control chromosomes screened by PCR-SSCP and sequencing. In addition, non reported SNPs in *SPTBN2* were identified in patients and controls (Table5).

Two of the novel mutations found in the Athena samples (A233G and T251I) occurs in exon 7 of *SPTBN2*, in close proximity to the L253P mutation found in the German SCA5 family. An additional group of five missense changes (R480W, A486T,

Q494D, N508H, and R517W) were identified in exon 12, which encodes the second spectrin repeat, with the A486T being detected in twenty six of these ataxia test samples (Figure 6). The third cluster of mutations was identified in exon 14 of *SPTBN2*. Three of these changes (R634W, R636Q, and L637P) occur within the third spectrin repeat, nearby the French SCA5 mutation (L629_R634delinsW). Additionally, an in frame insertion of eight amino acids (E639_S640insSRRARLQQ) and a single amino acid change (R642W) were identified in the linker region between the third and fourth spectrin repeats, and two additional missense mutations (R658W and L699F) are located in the fourth spectrin repeat (Figure 6).

One of the carriers of the R658W mutation, detected in twenty three ataxia samples but not in controls, is an 8 year old boy. This patient had disease onset between twelve and eighteen months of age and symptoms have gradually worsened to severe loss of coordination, motor weakness, clumsy gait, speech difficulties, and vision abnormalities. MRI analysis performed at age six detected a mild cerebellar cortical atrophy. There is no previous history of ataxia in the family and neither of the unaffected parents carries the mutation. A second individual positive for the R658W mutations is a forty-eight year old male with disease onset at age sixteen. Following a relatively rapid progression of symptoms, he was only able to stand up with the help of railings by age twenty four and became wheelchair bound in his late twenties. This patient also manifests loss of sensory nerve function, muscle weakness, dysarthria, and a mild bilateral hearing loss. DNA was not available from his father but his mother is unaffected and negative for the R658W mutation, and there is no known history of ataxia in the family.

The results from the mutational screen indicate that 0.94% (3/318) of the families

with genetically undefined types of ataxia tested in this study have putative *SPTBN2* mutations. Overall, I found that SCA5 has a prevalence of 0.6% among 820 dominant ataxia pedigrees, including 504 families for which genetic mutations have been already identified, collected at the University of Minnesota and the Hôpital de la Salpêtrière, Similarly, 1.1% (71/6,269) of the ataxia samples from Athena Diagnostics carry known and putative SCA5 mutations not found in the general population.

The majority of new *SPTBN2* variants reported result in single amino acid substitutions. To examine the conservation of the mutation sites across species and to help determine their functional impact, I performed alignments of the protein sequences of ten β-III spectrin orthologues from humans, dog, chimp, rat, mouse, worms, and fly in the regions of the novel *SPTBN2* mutations (Figure 8A). Data provided in Table 3 summarizes the properties of the amino acid side groups, number of carriers, and conservation score (CS: times the mutation site is conserved among homologues) for each of the variants.

First I examined the evolutionary conservation of the sites of the A233G and T251I substitutions identified in the second calponin homology domain of β-III spectrin. Mutations in this region of the protein, including the German SCA5 mutation (L253P), are likely to alter the interaction of spectrin with actin and/or the dynactin complex. The A233 site is conserved in all but one sequence analyzed (CS 9/10) while the T251 position is frequently found replaced by an alanine residue (CS 3/10).

Most of the novel mutations identified in the second spectrin repeat of β-III spectrin, with the exception of the R517W substitution (CS 4/10), replace residues that are highly conserved among β-III spectrin homologues [R480W (CS 10/10), E494D (CS

10/10), A486T (CS 8/10), N508H (CS 8/10)]. In addition, the A486T mutation has been identified in twenty six ataxia samples from Athena Diagnostics but not in controls, which makes it highly likely to be pathogenic.

The R634W (CS 9/10), R636Q (CS 8/10), and L637P (CS 10/10) substitutions clustered in the third spectrin repeat are all highly evolutionary conserved. Furthermore, a similar insertion of a tryptophan at residue 634 has been identified at the end of the French SCA5 mutation (L629_R634delinsW) (Figure 7B). In addition to the five *SPTBN2* mutations mentioned above, all identified in the distal portion of the third spectrin repeat, an in-frame insertion of eight amino acids (E639_S640insSRRARLQQ) and a single residue substitution at a highly conserved position [R642W (CS 7/10)] were also identified in the linker region between spectrin repeats three and four.

In addition, I examined the conservation of two novel changes identified in the fourth spectrin repeat. The R658W mutation (CS 7/10), detected in twenty three ataxia samples and not in controls, replaces an evolutionary conserved arginine residue whereas the site of the L699F mutation is preserved only in a subset of the proteins evaluated (CS 3/10).

I next investigated the functional impact of two putative mutations identified in spectrin repeat nine (H1229R and E1241G) and one in the linker between repeats nine and ten (R1278Q). Two of the novel variations (H1229R and R1278Q) are found on the same haplotype from an ataxia proband (Figure 7A). However, it is unclear whether these mutations segregate with the disease in other affected individuals in this family due to the lack of DNA from additional family members. Based on the amino acid homology, the H1229 (CS 1/10) and E1241 (CS 2/10) residues are poorly conserved with a higher

conservation score found for the R1278 (CS 6/10) position within the linker region.

III. Discussion

Since *SPTBN2* was initially reported as the cause of SCA5 and the three original mutations described no other SCA5 pedigrees or SCA5-associated gene variation has been reported. This study describes a mutational screen of *SPTBN2* and seventeen novel genetic variants identified in probands from families with dominant ataxias of unknown etiology and ataxia samples submitted to Athena Diagnostics for genetic testing.

SCA5 mutations were found at a frequency of 5/1,000 ataxia cases in a combined group of American and French SCA families. Novel *SPTBN2* variants were identified in 0.94% of the families (*n*=318) with undefined dominantly inherited ataxias and in 1.1% of the DNA samples from Athena Diagnostics.

This mutational analysis led to the identification of seventeen putative mutations in the SCA5 gene. Two novel variants were detected in the second calponin homology domain of β-III spectrin. In addition to binding to actin, this region of the protein interacts with the Arp1 subunit of the dynactin complex (Holleran *et al*., 2001). Mutations in this functional domain, including the pathogenic German SCA5 variant, are likely to impair the interaction of β-III spectrin with the actin cytoskeletal network and/or cause deficits in dynein/dynactin mediated intracellular transport.

The majority of the novel variants were identified within the spectrin repeat domains. Mutations affecting the organization and/or stability of the repeat could directly impact the strength of the spectrin tetramer and the interaction with specific proteins. In addition to the reported American and French SCA5 in-frame deletions (Ikeda *et al*.,

2006), twelve additional putative mutations were localized in the region comprising spectrin repeats two to four. Their clustering suggests that this region of β-III spectrin is critical for protein function.

Consistent with this hypothesis, yeast-two hybrid studies performed by Dr. Karen Armbrust, a former Graduate Student in Dr. Ranum's laboratory, identified interactions between proteins from a human brain cDNA library and the second and third repeats of β-III spectrin (Karen Armbrust, personal communication). Analysis of the effects of the novel variants on specific protein-protein interactions that involve human β-III spectrin repeats two to four will be useful to functionally characterize these mutations and to investigate their potential role in disease.

Additionally, two putative mutations were identified in the ninth spectrin repeat of β-III spectrin in dominant families with undefined ataxias. If pathogenic, these variants are predicted to affect the stability of the spectrin molecule and/or protein binding events. Future efforts will focus on the identification of molecules that bind this particular spectrin repeat and the analysis of the effects of mutant spectrin on such interactions.

Additionally, I found separate mutations in linker fragments connecting spectrin repeats three to four and repeats nine to ten. It has been suggested that the secondary α-helical arrangement of the linker regions, which is contiguous with the repeat but not stabilized by the same forces that protect the rest of the structure, determines the stability of folding of the adjacent spectrin repeats (Johnson *et al*., 2007). Significantly, pathogenic mutations in linker regions between spectrin repeats have been shown to cause the unfolding of erythrocyte spectrin tetramers and to directly contribute to various red blood cell disorders (Giorgi *et al*., 2001).

More recent work proposes that linker regions between repeats are critical determinants of both spectrin's stability and poly-functionality (Stabach *et al*., 2009). Specifically, studies suggest that the lack of structural constraints on the linker and the poor homology between linker fragments within a given spectrin, but extremely high conservation of linker sequences at similar positions between different β-spectrins allows development of diverse but unique ligand-binding sites without compromising the structure of the repeat unit (Stabach *et al*., 2009).

The identification of spectrin mutations in SCA5 patients (Ikeda *et al*., 2006) provided the first evidence that pathogenic changes in a cytoskeletal protein can lead to ataxia and neurodegeneration in humans. Nevertheless, multiple studies suggest that other β-spectrin proteins may also contribute to disease. For instance, worms expressing dominant mutations in the *C.elegans* homologue of human β-III spectrin have an uncoordinated phenotype (Park and Horvitz, 1986). Moreover, mice with recessive mutations in the *Spnb4* gene, an orthologue of human β-IV spectrin (*SPTBN4*), develop progressive ataxia with hind limb paralysis, deafness, and tremor (Parkinson *et al*., 2001).

Interestingly, two additional non-erythrocytic human β-spectrins genes (*SPTBN1* and *SPTBN5*) are highly expressed in the brain with the *SPTBN1* locus mapping to the SCA25 critical region (Stevanin *et al*., 2004). It is likely that mutations in these proteins also result in ataxic phenotypes.

In conclusion, this study reports the identification of a novel group of *SPTBN2* mutations in patients with genetically unknown types of ataxia. Although the mechanisms by which β-III spectrin mutations cause cerebellar neurodegeneration are still unclear, these results extend the spectrum of *SPTBN2* mutations likely to contribute to SCA5

pathogenesis. Additional functional studies will clarify the potential role of these mutations in disease and lead to a better understanding of normal spectrin function.

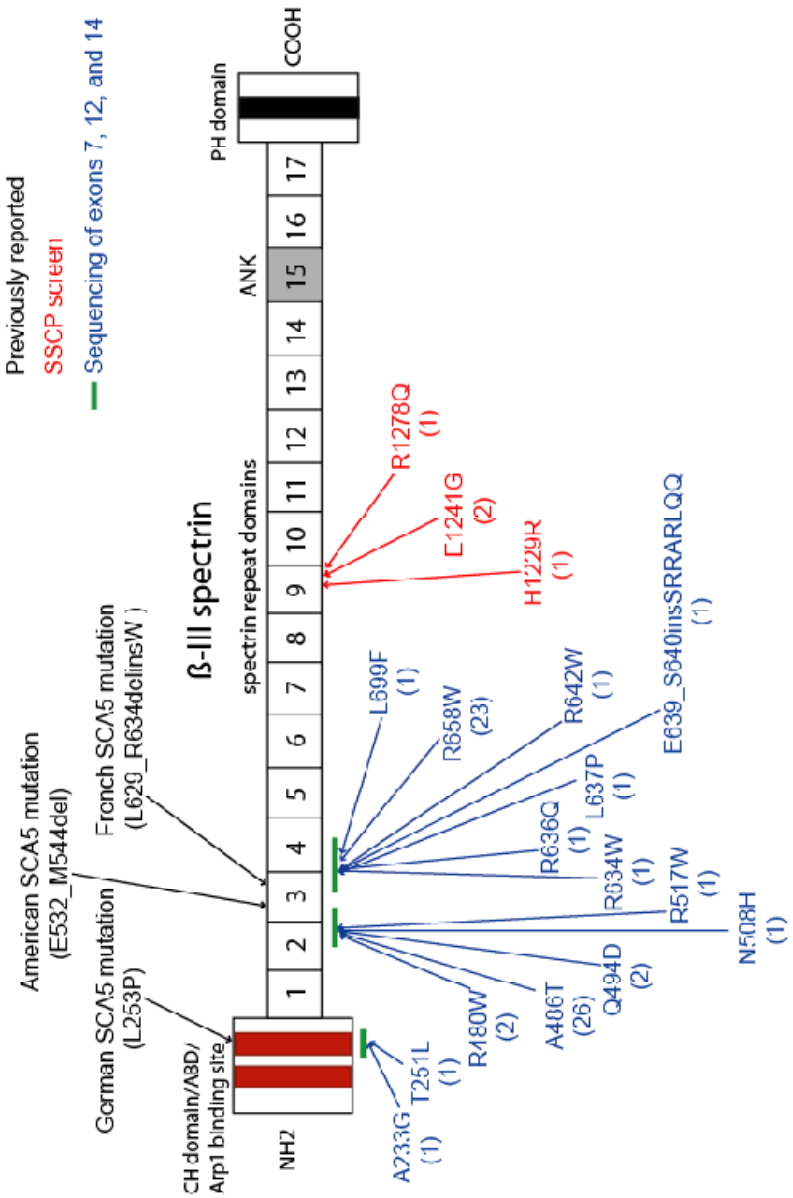

Figure 6. Summary of mutations in the *SPTBN2* gene. A schematic representation of the functional domains of β-III spectrin is shown along with the position of all SCA5 mutations. Previously reported SCA5 mutations are indicated in black. Novel *SPTBN2* mutations identified in this study are indicated below the scheme, with mutations identified through SSCP analysis shown in red and novel variants identified by sequencing analysis shown in blue. Parentheses indicate the number of probands carrying each of the novel amino acid substitutions. CH= calponin homology domain; ABD= actin binding domain; ANK= ankyrin binding site; PH= pleckstrin homology domain.

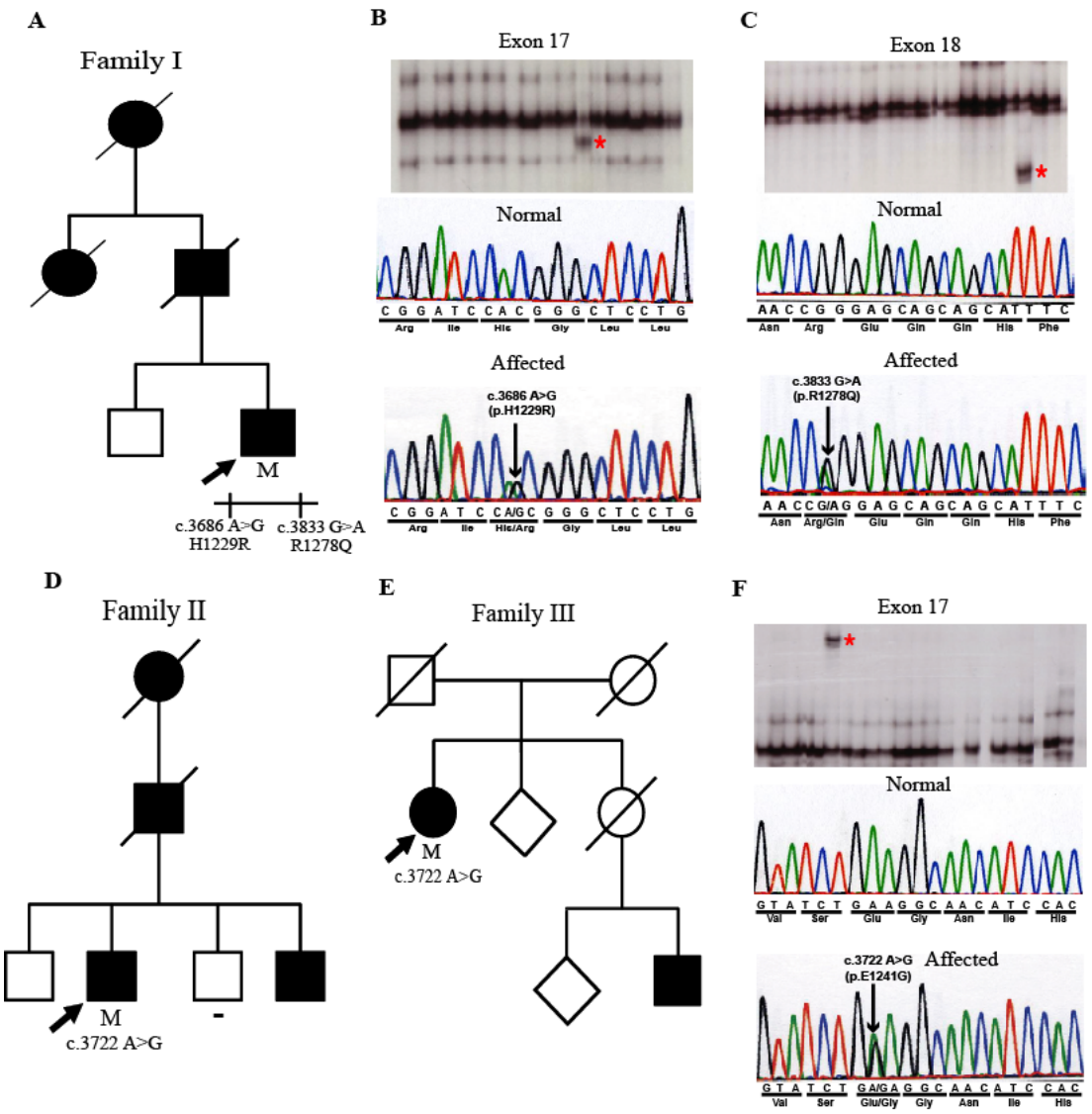

Figure 7. Novel mutations identified in the ninth spectrin repeat of β-III spectrin. Affected pedigrees and mutation analysis are shown. For each coding variation the top panel represents mutation detection by SSCP analysis and asterisks designate DNA bands with shifted mobility. Top electropherograms show *SPTBN2* sequence analysis from an unaffected control and bottom electropherograms correspond to affected individuals carrying novel mutations in *SPTBN2*. (A) The proband representing Family I carries two heterozygous missense mutations in the same chromosome: An H1229R (3686A→G) mutation in exon 17 (B) and a R1278Q (3833G→A) mutation in exon 18 (C). (D-F) Probands from Family II and III carry the same E1241G (3722A→G) mutation in exon 17 of *SPTBN2*. For each pedigree, squares represent males and circles represent females. Black circles/squares indicate clinically affected individuals, arrowheads indicate probands, "M" denotes mutation carriers, and "-" denotes confirmed non carriers of the novel *SPTBN2* mutations.

A

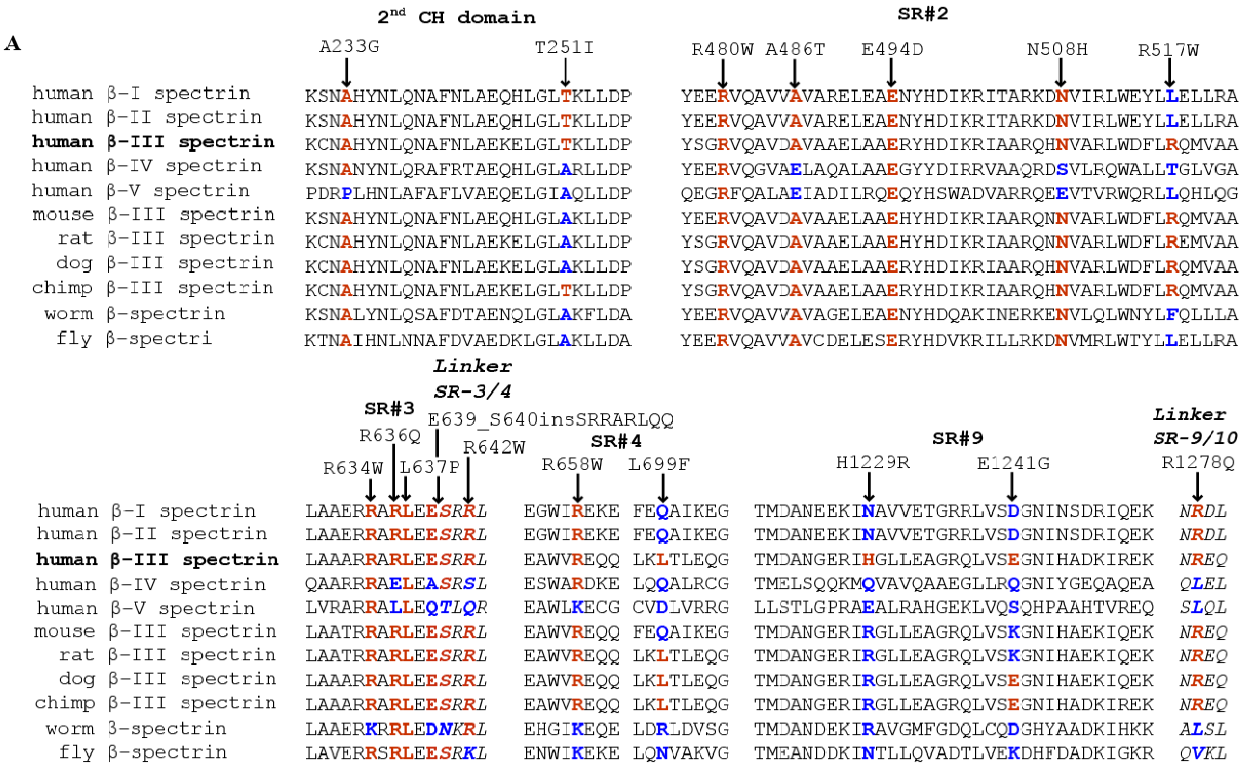
2nd CH domain
SR#2
A233G
T251I
R480W
A486T
E494D
N508H
R517W
human β-I spectrin KSNAHYNLQNAFNLAEQHLGLTKLLDP YEERVQAVVAVARELEAENYHDIKRITARKDNVIRLWEYLLELLRA
human β-II spectrin KSNAHYNLQNAFNLAEQHLGLTKLLDP YEERVQAVVAVARELEAENYHDIKRITARKDNVIRLWEYLLELLRA
human β-III spectrin KCNAHYNLQNAFNLAEKELGLTKLLDP YSGRVQAVDAVAAELAAERYHDIKRIAARQHNVARLWDFLRQMVAA
human β-IV spectrin KSNANYNLQRAFRTAEQHLGLARLLDP YEERVQGVAELAQALAAEGYYDIRRVAAQRDSVLRQWALLTGLVGA
human β-V spectrin PDRPLHNLAFAFLVAEQELGIAQLLDP QEGRFQALAEIADILRQEQYHSWADVARRQEEVTVRWQRLLQHLQG
mouse β-III spectrin KSNAHYNLQNAFNLAEQHLGLAKLLDP YEERVQAVDAVAAELAAEHYHDIKRIAARQNNVARLWDFLRQMVAA
rat β-III spectrin KCNAHYNLQNAFNLAEKELGLAKLLDP YSGRVQAVDAVAAELAAEHYHDIKRIAARQNNVARLWDFLREMVAA
dog β-III spectrin KCNAHYNLQNAFNLAEKELGLAKLLDP YSGRVQAVDAVAAELAAERYHDIKRIAARQHNVARLWDFLRQMVAA
chimp β-III spectrin KCNAHYNLQNAFNLAEKELGLTKLLDP YSGRVQAVDAVAAELAAERYHDIKRIAARQHNVARLWDFLRQMVAA
worm β-spectrin KSNALYNLQSAFDTAENQLGLAKFLDA YEERVQAVVAVAGELEAENYHDQAKINERKENVLQLWNYLFQLLLA
fly β-spectri KTNAIHNLNNAFDVAEDKLGLAKLLDA YEERVQAVVAVCDELESERYHDVKRILLRKDNVMRLWTYLLELLRA
Linker SR-3/4
SR#3
E639_S640insSRRARLQQ
R636Q
R642W
SR#4
R634W
L637P
R658W
L699F
SR#9
H1229R
E1241G
Linker SR-9/10
R1278Q
human β-I spectrin LAAERRARLEESRRL EGWIREKE FEQAIKEG TMDANEEKINAVVETGRRLVSDGNINSDRIQEK NRDL
human β-II spectrin LAAERRARLEESRRL EGWIREKE FEQAIKEG TMDANEEKINAVVETGRRLVSDGNINSDRIQEK NRDL
human β-III spectrin LAAARRARLEESRRL EAWVREQQ LKLTLEQG TMDANGERIHGLLEAGRQLVSEGNIHADKIREK NREQ
human β-IV spectrin QAARRRAELEASRSL ESWARDKE LQQALRCG TMELSQQKMQVAVQAAEGLLRQGNIYGEQAQEA QLEL
human β-V spectrin LVRARRALLEQTLQR EAWLKECG CVDLVRRG LLSTLGPRAEALRAHGEKLVQSQHPAAHTVREQ SLQL
mouse β-III spectrin LAATRRARLEESRRL EAWVREQQ FEQAIKEG TMDANGERIRGLLEAGRQLVSKGNIHAEKIQEK NREQ
rat β-III spectrin LAATRRARLEESRRL EAWVREQQ LKLTLEQG TMDANGERIRGLLEAGRQLVSKGNIHAEKIQEK NREQ
dog β-III spectrin LAAARRARLEESRRL EAWVREQQ LKLTLEQG TMDANGERIRGLLEAGRQLVSEGNIHAEKIQEK NREQ
chimp β-III spectrin LAAARRARLEESRRL EAWVREQQ LKLTLEQG TMDANGERIRGLLEAGRQLVSEGNIHADKIREK NREQ
worm β-spectrin LAAERKRRLEDNKRL EHGIKEQE LDRLDVSG TMDANDEKIRAVGMFGDQLCQDGHYAADKIHKK ALSL
fly β-spectrin LAVERRSRLEESRKL ENWIKEKE LQNVAKVG TMEANDDKINTLLQVADTLVEKDHFDADKIGKR QVKL

B

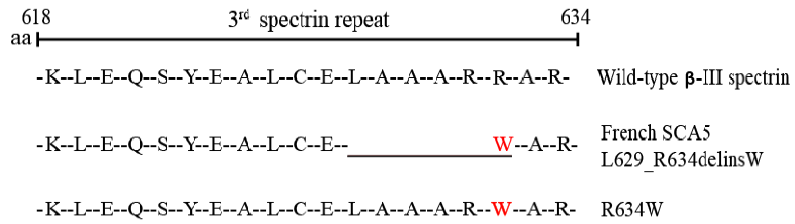
618 aa
3rd spectrin repeat
634
-K--L--E--Q--S--Y--E--A--L--C--E--L--A--A--A--R--R--A--R- Wild-type β-III spectrin
-K--L--E--Q--S--Y--E--A--L--C--E-- W--A--R- French SCA5 L629_R634delinsW
-K--L--E--Q--S--Y--E--A--L--C--E--L--A--A--A--R--W--A--R- R634W

Figure 8. Alignment of amino acid sequences of β-III spectrin homologues in the region containing novel *SPTBN2* mutations (A). Functional domains of human β-III spectrin containing the novel mutations are indicated at the top of the alignment and each mutational site is identified by arrows. Novel substitutions that are evolutionary conserved are shown in red and alternative residues found in other homologues are indicated in blue. (B) Alignment of the protein sequence of β-III spectrin corresponding to the end of the third spectrin repeat illustrates that the R634W variation identified in this study also occurs in the French SCA5 mutation.

Protein change	Amino acid side chain substitution	Carriers (#)	CS
A233G	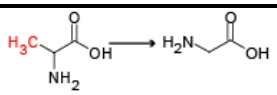	1	9/10
T251I	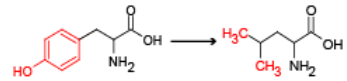	1	3/10
R480W	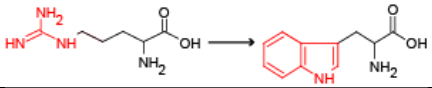	2	10/10
A486T	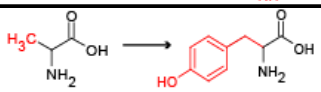	26	8/10
E494D	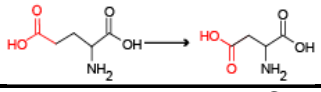	2	10/10
N508H	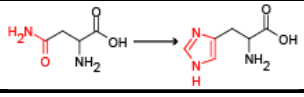	1	8/10
R517W	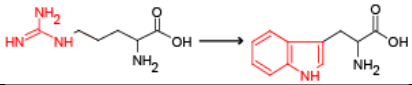	1	4/10
R634W	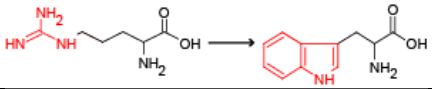	1	9/10
R636Q	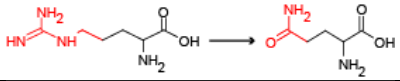	1	8/10
L637P	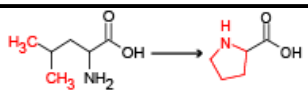	1	10/10
R642W	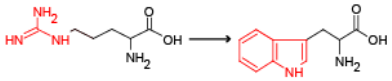	1	7/10
R658W	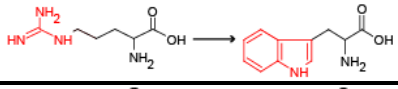	23	7/10
L699F	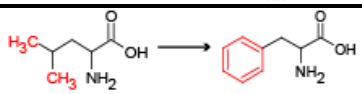	1	3/10
H1229R	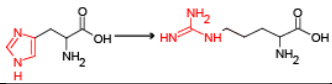	1	0/10
E1241G	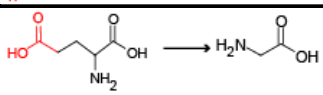	2	2/10
R1278Q	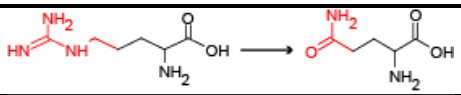	1	6/10

Table 3. Summary of novel *SPTBN2* mutations. The functional significance of each novel variant was analyzed in terms of differences in the properties of the amino acid side chain, number of carriers, and conservation of the mutation site (CS).

Family	Origin	Age of onset	Neurological symptoms	DNA change	Protein change	Domain
I	Moroccan	44y	Cerebellar ataxia and nystagmus	c.3686A>G c.3833G>A	p.H1229R p.R1278Q	SR nine LR between SR 9-10
II	French	38y	Cerebellar ataxia and nystagmus	c.3722A>G	p.E1241G	SR 9
III	Lebanese	60y	Cerebellar ataxia and mild spasticity	c.3722A>G	p.E1241G	SR 9

Table 4. Families with novel *SPTBN2* mutations identified by SSCP analysis. This table summarizes and compares genetic and clinical features found in affected members of the three SCA families with putative mutations in *SPTBN2*. SR: spectrin repeat; LR: linker region between spectrin repeats

Nucleotide change	Protein change	Number of carriers (patients)	Number of carriers (controls)
c.768C>T	p.P256 (none)	3	4
c.1416G>A	p.T472 (none)	13	2
c.1415G>A	p.T472M	1	1
c.1434C>T	p.S478 (none)	6	0
c.1492G>C	p.D498H	2	3
c.1495A>T	p.I499F	1	2
c.1502G>A	p.R501H	1	4
c.1504A>G	p.I502V	3	8
c.1530A>G	p.A510 (none)	1	1
c.1551G>A	p.R517 (none)	1	0
c.1549C>G	p.R517G	0	2
c.1552C>A	p.Q518L	2	25
c.1627C>T	p.L543F	1	19
c.1839G>A	p.S613(none)	2	0
c.1852A>G	p.L618Q	2	5
1881C>T	p.L627(none)	1	0
1885G>A	p.C626 (none)	2	0
1895C>T	p.A632V	1	1
1914G>A	p.E638(none)	1	0
2007G>A	p.T669(none)	1	0
2064C>T	p.G688(none)	2	0
c.5638G>A	p.R1880H	18	34
c.5693C>T	p.A1898 (none)	3	14
IVS11-7G>A	N/A	17	27
IVS11-7G>T	N/A	49	8
IVS11-8C>T	N/A	1	5
IVS6-3 C>T	N/A	2	1

Table 5. Novel SNPs in *SPTBN2* identified in ataxia patients and controls.

CHAPTER 3

ESTABLISHMENT AND MOLECULAR CHARACTERIZATION OF TRANSGENIC SCA5 MODELS IN *DROSOPHILA*

I. Introduction

The pathological features of human neurodegenerative diseases have long been modeled in different organisms ranging from bacteria, yeast, worms, fish, and rodents to primates. The common fruit fly, also known as *Drosophila melanogaster*, has proven to be an excellent organism to unravel basic cellular defects and to identify genes and pathways implicated in human brain disorders, including triplet repeat diseases, Alzheimer's disease, Parkinson disease, and hereditary spastic paraplegia (Bilen and Bonini, 2005). With the accessibility of a complete-sequenced fly genome came the realization of the remarkable conservation of fundamental biological processes between humans and flies (Fortini *et al*., 2000; Reiter *et al*., 2001). The finding that over 60% of human disease-causing genes have close homologues in flies supports the use of *Drosophila* to study the normal roles of these proteins and to manipulate their function to simulate human disease (Hamosh *et al*., 2005). The strength of the fly as a model system also lies in the availability of powerful genetic tools combined with attributes such as a short and well defined life cycle, a large number of progeny, and the presence of a simple and accessible nervous system that is amenable to study at the single cell level.

Drosophila is an attractive system to investigate the molecular mechanisms of SCA5. The fly genome contains one α-spectrin and one canonical β-spectrin genes, each of which is highly expressed at both central and peripheral synapses, and each of which is essential for development (Dubreil *et al*., 2000). The single canonical β-spectrin protein

in flies shares 50% amino acid homology with human β-III spectrin and a conservation of all functional domains, including the regions containing the previously reported American and German SCA5 mutations (Figure 9) and the majority of the novel mutations described in Chapter 2 (Figure 8). Similar to human β-III spectrin, fly β-spectrin has also been implicated in membrane stabilization and intracellular transport functions. Loss or reduced expression of fly β-spectrin in neurons results in severe defects in the formation and stabilization of synaptic junctions (Pielage *et al*., 2005, 2006). Segmental axons from larvae in which expression of β-spectrin has been ubiquitously abolished or conditionally eliminated in neurons show aberrant distribution of synaptic proteins, which accumulate within axonal swellings (Featherstone *et al*., 2001; Pielage *et al*., 2005, 2006). The structural and functional similarities between fly β-spectrin and human β-III spectrin support the use of *Drosophila* to study dominant or dominant negative effects of the SCA5 mutations.

To investigate the molecular basis of SCA5, I used the GAL4/*UAS* expression system (Brand and Perrimon, 1993) to generate transgenic *Drosophila* models that express human β-III-spectrin or fly β-spectrin proteins containing SCA5 mutations. These studies show that expression of the SCA5 mutant spectrin in the eye causes a progressive neurodegenerative phenotype and expression in larval neurons results in posterior paralysis, reduced synaptic terminal growth, and axonal transport deficits. The phenotypes of mutant spectrin flies are genetically enhanced by both dynein and dynactin loss-of-function mutations. These data provide evidence that SCA5 mutant spectrin causes adult-onset neurodegeneration in the fly eye and disrupts intracellular transport processes which are likely to contribute to this progressive neurodegenerative disease.

II. Results

To generate flies that express human β-III-spectrin transgenes, a full-length myc-tagged human *SPTBN2* cDNA, carrying either the wild-type sequence (hSPWT) or mutations found in an American family descended from President Lincoln's paternal grandparents (hSPLN) (Ikeda *et al*., 2006) or the German family mutation (hSPGM) (Ikeda *et al*., 2006) were inserted downstream of the UAS (upstream activating sequence) sites of the *Drosophila* transformation vector pUASp (Rorth, 1998) (Figure 10). These constructs were injected into fly embryos and lines carrying stable integration of the human transgene were established for each genotype.

To begin to study the effects of SCA5 mutations on neurons I first crossed the UAS-*SPTBN2* transgenic flies to the eye-specific glass multiple reporter (*gmr*)-*GAL4* driver line (Freeman *et al*., 1996). This approach allows ectopic expression of the human transgenes in the developing *Drosophila* eye. Expression of human β-III spectrin with the Lincoln family mutation (*gmr*-GAL4/hSPLN) results in a severe rough eye phenotype characterized by disorganized ommatidia and loss of mechanosensory bristles (Figure 11AII) while expression of the German mutant spectrin (*gmr*-GAL4/+; hSPGM/+) causes a milder eye phenotype (Figure 11AIII). In contrast, expression of wild-type human β-III spectrin (*gmr*-GAL4/+; hSPWT/+) causes only a very mild ommatidial phenotype that does not disrupt normal eye development (Figure 11AIV) and is similar to the control driver flies (*gmr*-GAL4/+, Figure 11AI). Protein analysis shows that flies expressing wild-type (*gmr*-GAL4/+; hSPWT/+) and the American mutant spectrin (*gmr*-GAL4/hSPLN) produce comparable levels of transgenic protein, while flies

expressing the German mutant spectrin (*gmr*-GAL4/+; hSPGM/+) have significantly lower β-III spectrin expression (Figure 11C, *P* =0.025, n=4). As expected, the phenotypes are dosage-dependent. Flies carrying two copies of the hSPGM transgene (*gmr*-GAL4/+; hSPGM/hSPGM) express higher levels of β-III spectrin compared to the heterozygous flies (Figure 11B,C) and develop a stronger rough eye phenotype (Figure 11AV).

To determine if the eye phenotypes affect retinal neurons, I performed histological analysis. Sections taken through the eye of 10-day old flies showed a severe disruption of the retinal organization, with thinning of the retina, and loss of retinal neurons in flies expressing the American and German SCA5 mutations (Figure 12A, B, see arrows) compared to flies expressing wild-type β-III spectrin (Figure 12C).

To assess whether the neurodegenerative phenotypes induced by β-III mutations are progressive, I monitored changes in the eye over time. Analysis of flies expressing the SCA5 mutations revealed that the extent of neurodegeneration in the eye became more severe as flies aged. By day 30, eyes from flies expressing the American SCA5 mutation showed dramatic changes in pigmentation and abundant necrotic tissue (Figure 12D-D″). Similarly, heterozygous flies expressing low levels of the German SCA5 mutation developed eye pigmentation abnormalities by day 30 (Figure 12E″) while homozygous flies expressing higher levels of German mutant spectrin showed dramatic changes in eye pigmentation by day two, and patches of severe necrosis by day ten (Figure 12G, G′). In contrast, no changes in external eye morphology or pigmentation were found in control flies expressing wild-type β-III spectrin (Figure 12F-F″). Taken together, these results

demonstrate that expression of human β-III spectrin containing either the American or German mutations causes a progressive, dominant neurodegenerative phenotype.

The basic structural unit of the spectrin network is a dimer formed by direct association between α- and β-spectrin subunits (reviewed in Bennett and Baines, 2001). To begin to understand the molecular basis for the neurodegenerative phenotypes described above, I tested by immunoprecipitation whether human β-III spectrin assembles into the fly α/β spectrin complex. Proteins from flies expressing wild-type human β-III spectrin in the eye were immunoprecipitated with anti-fly α-spectrin antibody and protein blot analysis shows human β-III spectrin and fly α-spectrin interact (Figure 13). These data are consistent with localization studies (not shown) in which human β-III spectrin co-localizes with fly spectrin and indicate that β-III spectrin incorporates into the α/β spectrin complexes in flies.

To help establish that the rough eye phenotypes described above are caused by disruptions in the endogenous fly spectrin pathways, I developed a second set of transgenic flies in which the human SCA5 mutations were incorporated into *Drosophila* cDNA constructs designed to overexpress wild-type (FSPWT) and mutant fly β-spectrin (American mutant: FSPLN; German mutant: FSPGM) (Figure 14). These constructs were injected into fly embryos and lines carrying stable integration of the fly transgene were established for each genotype.

To test the effect of overexpressing endogenous fly β-spectrin transgenes in the *Drosophila* eye, the UAS-Fly ß-Spec transgenic lines were crossed to the *gmr*-GAL4

driver and flies expressing comparable levels of fly β-spectrin were used for further analysis (Figure 15D). Similar to results above, with the human mutant β-III spectrin, strong degenerative eye phenotypes are observed when fly β-spectrin containing either the American or German mutation are expressed (*gmr*-GAL4/+; FSPLN/+ and *gmr*-GAL4/FSPGM, Figure 15B, C). In contrast, animals overexpressing wild-type fly β-spectrin do not develop eye degeneration and only show mild ommatidial disorganization comparable to *gmr*-GAL4/+ control flies (*gmr*-GAL4/FSPWT, Figure 15A). These data suggest that human β-III and fly β-spectrin act in at least some of the same functional pathways when expressed in the fly and supports the use of these model*s* to study dominant or dominant negative effects of the SCA5 mutations.

I further characterized the effects of the SCA5 mutations by expressing the human and fly β-spectrin transgenes in all neurons using the pan-neuronal embryonic lethal, abnormal vision (*elav*)-GAL4 driver and examined synaptogenesis at the neuromuscular junction (NMJ) in third instar larvae. The muscles of the larval body are innervated by bundles of axonal projections known as segmental nerves that originate in the ventral ganglion (Figure 16A). Synaptic boutons appear as swellings on neuronal axons at the sites of contact with the muscle surface. I visualized motor axon terminals on muscle 6/7 by staining with an antibody to the synaptic vesicle-associated cysteine string protein (CSP) and next quantified the number of synaptic boutons as a measure of the growth of synaptic junctions. Quantitative results are reported as relative synapse size (bouton number/NMJ area) to account for differences in bouton number due to variations in muscle size during normal growth and normalized to the *elav*-GAL4 control (Figure 16I).

I observed reduced branching and bouton number in larvae expressing mutant hSPLN, FSPLN, and FSPGM but not the wild-type (hSPWT, FSPWT) transgenes ($P<0.0001$, Figure 16). Although under the same conditions I did not detect differences in bouton counts in larvae expressing the hSPGM transgene (Figure 16D), this result is likely explained by the relatively low expression in this line (Figure 11B).

Proteins required for the formation and maintenance of the synapse are synthesized in the neuronal cell body and actively transported to synaptic terminals in small vesicles. The reduced synaptic growth observed in animals expressing mutant spectrins suggests that intracellular transport deficits contribute to the structural abnormalities at the synapse. To test this hypothesis I examined larvae expressing the American and German SCA5 mutations for the posterior paralysis or "tail-flip" phenotype previously described for mutations that cause aberrant axonal transport (Hurd and Saxton, 1996; Martin *et al*., 1999; Bowman *et al*., 2000; Haghnia *et al*., 2007). Larvae expressing mutant but not wild-type fly β-spectrin in neurons exhibit the tail flip crawling phenotype due to paralysis of the posterior segments of the larval body (Figure 17A-C). Although larvae expressing one copy of the human β-III spectrin transgenes (*elav*-GAL4/+; hSPLN/+ and *elav*-GAL4/+; hSPGM/+) did not develop similar motor defects (Figure 17D), this likely reflects the lower levels of human protein expression compared to fly β-spectrin. Indeed, larvae expressing two copies of the American mutant spectrin transgene (*elav*-GAL4/+; hSPLN/hSPLN) and higher protein levels did exhibit the tail flip phenotype (Figure 17E). Importantly, a single copy of the hSPLN mutant transgene can produce posterior paralysis, if endogenous wild-type β-spectrin gene dosage is reduced (Figure 17F). The

dosage dependence of the hSPLN larval paralysis phenotype suggests that human and fly mutant spectrins inhibit the normal neuronal function of wild-type β-spectrin through a dominant negative mechanism.

To determine if the larval tail paralysis and synaptogenesis phenotypes could be explained by defects in axonal transport, I analyzed the axonal distribution of GFP-tagged synaptic-vesicle membrane protein synaptotagmin (syt-GFP). In larvae expressing wild-type β-spectrin (*elav*-GAL4-syt-GFP/+; FSPWT/+), synaptotagmin was evenly distributed as small puncta (Figure 18A). In contrast, larvae expressing mutant spectrins (*elav*-GAL4-syt-GFP/+; FSPLN/+, *elav*-GAL4-syt-GFP/+; FSPGM/+) showed an accumulation of syt-GFP positive vesicles within axonal aggregates (Figure 18B and C, see arrows). Considering segmental axons have an average diameter of around 0.5 µm (Rusu *et al*., 2007), I next quantified the number of large synaptotagmin accumulations (diameter $\geq$0.7 µm) which are likely to cause axonal swellings, and disrupt the normal trafficking of intracellular cargoes (Gunawardena & Goldstein, 2001). I found a significant difference ($^{***}P<0.0001$) in the frequency of axonal jams in larvae expressing mutant FSPLN and FSPGM transgenes (Figure 18D) compared to wild-type controls. In addition, I show that the distributions of other synaptic vesicle proteins like CSP (Figure 18E), as well as the dynein motor protein (Figure 18F), overlap with sites of synaptotagmin-GFP axonal aggregates.

I also imaged and tracked the dynamic behavior of vesicles in live segmental axons to further determine the effects of the SCA5 mutations on synaptic vesicle transport. In flies overexpressing wild-type β-spectrin, a large number of synaptotagmin-GFP

containing vesicles underwent rapid unidirectional movements (Figure 19A left panel). Kymograph analysis shows that this motion is characterized by long unidirectional runs (diagonal line) interrupted by pauses and/or infrequent short reversals in the direction of vesicle transport (Figure 19BI, II and Movie 1). In contrast, in segmental axons expressing either the American or German SCA5 mutations, the unidirectional bias in vesicle movement was reduced. Synaptotagmin-GFP vesicles exhibited frequent reversals in the direction of transport (zigzag line), traveling for much shorter distances in any one direction (Figure 19A right panel, BIII, IV and Movie 2). In addition, quantitative analysis confirmed that synaptotagmin-GFP vesicles moved significantly slower in mutant compared to wild-type axons (Table 6). The reduced vesicle velocity, versus complete inhibition of vesicle transport, is consistent with a direct affect of the mutant spectrin on transport. Competition by the mutant spectrins may alter the dynamics of motor attachment to vesicular cargo, and/or interfere with the binding of regulatory partners that influence motor activity.

To distinguish whether mutant β-spectrin has an effect on anterograde, retrograde or both types of axonal transport, expression of wild-type or mutant spectrin and the vesicle marker neuronal synaptobrevin-GFP (n-Syb-GFP) was targeted to motor neurons with known microtubule polarity, using the *D42*-GAL4 driver. In control larvae (*D42*-GAL4-n-Syb-GFP/FSPWT) most fluorescent particles were moving in long runs (Movie 3). In contrast, animals expressing the mutant spectrins (*D42*-GAL4-n-Syb-GFP/FSPLN and *D42*-GAL4-n-Syb-GFP; FSPGM) showed numerous stationary n-Syb-GFP particles, some of which were trapped within axonal swellings (Movie 4). Analysis of mean velocity and run length for anterograde and retrograde movements indicate that mutant

spectrin disrupts transport in both directions (Table 7). The GFP-vesicles that retained motility had slower velocities and traveled shorter distances than in controls.

The rough eye and transport phenotypes caused by the mutant spectrins are similar to phenotypes previously described in dynein and dynactin mutants (McGrail *et al*., 1995; Martin *et al*., 1999; Boylan *et al*., 2000). If these phenotypes result from the failure of spectrin to properly engage in retrograde transport, then we would predict that dynein, and/or dynactin mutations, would enhance the mutant spectrin phenotypes. To test this hypothesis, I first crossed flies carrying a hypomorphic dynein heavy chain allele (*DHC64C*$^{6\text{-}10}$) to flies containing a single copy of the hSPLN transgene and scored the resulting progeny for posterior paralysis. In contrast to single mutant animals, which do not show posterior paralysis, larvae expressing both spectrin and dynein mutations (*elav*-GAL4-syt-GFP/+; hSPLN/+; *DHC64C*$^{6\text{-}10}$/+) develop the tail flip (Figure 20AIII) and axonal vesicle accumulation phenotypes (Figure 20BIII). Additionally, double mutant larvae display significant reductions in synapse size at the NMJ compared to single mutant controls and the *elav*-GAL4 control animals (Figure 20C, $^{***}P<0.0001$). A similar genetic interaction occurs between flies expressing the American mutation and the dominant *Gl*^{1} mutation in the p150^{Glued} subunit of dynactin. In progeny carrying the American spectrin transgene in a p150^{Glued} mutant background (*elav*-GAL4-syt-GFP/+; hSPLN/+; *Gl*^{1}/+), but not in control siblings (*elav*-GAL4-syt-GFP/+; hSPLN/+; *Tb*/+; or hSPLN/+; *Gl*^{1}/+) I observe defective axonal transport, larval paralysis, and synaptogenesis deficits (data not shown).

Additionally, I found that dynein and dynactin mutations genetically enhance the

rough eye phenotypes caused by the expression of the SCA5 mutant spectrin. This analysis was facilitated by the generation of recombinant lines that carry both the GAL4 driver and the mutant spectrin transgenes on a single chromosome. The *gmr*-GAL4-hSPLN recombinant chromosome has reduced levels of transgene expression (Figure 20L) and develops a less severe eye phenotype (Figure 20D) which facilitated the detection of genetically enhanced phenotypes. Adult flies with one copy of the American or German mutant spectrin transgenes which are also heterozygous for a hypomorphic mutant dynein allele, $DHC64C^{6\text{-}10}$, exhibit severe eye phenotypes involving disruptions of the ommatidial hexagonal packing and loss of interommatidial bristles (*gmr*-GAL4-hSPLN/+; $DHC64C^{6\text{-}10}$/+ and *gmr*-GAL4-FSPGM/+; $DHC64C^{6\text{-}10}$/+, Figure 20G, H). In contrast, fly strains carrying only the mutant spectrin transgene or the dynein mutation, exhibit only mild or wild-type eye phenotypes (Figure 20D-F). Similarly, the dominant Gl^{1} dynactin mutation, which by itself causes disorganization of the ommatidia (Figure 20I) genetically enhances the phenotypes of flies expressing either the American or German spectrin mutations (*gmr*-GAL4-hSPLN/+; Gl^{1}/+ and *gmr*-GAL4-FSPGM/+; Gl^{1}/+, Figure 20J, K). I excluded the possibility that enhanced phenotypes simply result from alterations in spectrin expression by protein blot (Figure 20M, N). The genetic interactions observed are consistent with the functional intersection of the dynein and spectrin pathways.

III. Discussion

In *Drosophila*, previous work has established that the single α- and β-spectrin genes are essential (Dubreil *et al*., 2000). In contrast, in humans there are four β-spectrin

genes and mutations in one copy of the β-III spectrin gene, which is highly expressed in Purkinje cells, leads to a dominantly inherited form of ataxia (Ikeda *et al*., 2006). I have used ectopic expression of human β-III spectrin and over-expression of endogenous fly β-spectrin to define the basic biological processes affected by the SCA5 mutations and to better understand the mechanisms of neurodegeneration. Consistent with the SCA5 mutations in humans, expression of the β-III mutant proteins in *Drosophila* causes dosage-dependent neuronal phenotypes.

The position of the German mutation in the second calponin homology domain suggests the mutant protein disrupts the normal interactions of the wild-type protein with the actin cytoskeleton and/or the ARP1 subunit of dynactin (Holleran *et al*., 2001). I found that both the German and the American mutations cause intracellular transport deficits that are similar to the phenotypes of mutant Arp1 flies (Haghnia *et al*., 2007). In the case of the American family, the deletion within the third spectrin repeat may result in similar effects on dynactin pathways by disrupting protein-protein interactions that depend on the helical conformation of the spectrin repeats. In support of this proposal Dr. Karen Armbrust in the Ranum laboratory recently conducted a yeast two-hybrid screen and identified a novel interaction between the dynactin subunit $p150^{Glued}$ and spectrin repeats 2 and 3 of β-III spectrin. Additionally, Dr. Armbrust's studies show that the American SCA5 mutation reduces the strength of the interaction of β-III spectrin with $p150^{Glued}$.

The similar phenotypes found in flies expressing the SCA5 mutations in the context of either the human or fly β-spectrin proteins, indicate that some of the binding partners and functional roles of spectrin are conserved between humans and flies. Indeed,

antibodies specific for *Drosophila* α-spectrin can immunoprecipitate human β-III spectrin from protein extracts.

Consistent with possible dominant-negative effects, expression of the SCA5 mutant proteins results in reduced numbers of synaptic boutons at synaptic termini. In *Drosophila*, spectrin function at the synapse has been extensively studied in motor neurons (Featherstone *et al,* 2001; Pielage *et al*., 2005, 2006). Loss of presynaptic spectrin eliminates several essential cell adhesion molecules from synaptic sites and leads to defects in neurotransmission and the disassembly and elimination of synapses at the NMJ (Pielage *et al*., 2005, 2006).

In this study, loss of synapses at the NMJ in SCA5 mutant flies is enhanced in animals heterozygous for dynein-heavy chain and $p150^{Glued}$ mutations. These genetic interactions suggest that spectrin, dynein, and dynactin may interact in a cortical complex that mediates synapse stabilization. Although the protein interactions that mediate synapse stability are not fully understood, one model is that synaptic components at the membrane are stabilized through spectrin and ankyrin linkages to the cytoskeleton (Pielage *et al*., 2006, 2008; Ayalon *et al.*, 2008; Koch *et al*., 2008), and that the establishment of these connections is facilitated by dynein/dynactin recruitment of microtubules (Carminati and Stearns, 1997; Adames and Cooper, 2000; Ligon *et al*. 2001; Schuyler and Pellman, 2001; Dujardin and Vallee, 2002). Consistent with this model, previous studies demonstrate that presynaptic depletion of α- or β-spectrin in flies disrupts the microtubule network underlying the synaptic boutons and precedes the loss of cell adhesion molecules, and the destabilization of synapses (Pielage *et al*., 2006). Additionally, synapse disassembly is also reported following disruption of dynactin

function (Eaton *et al*., 2002).

This investigation provides new evidence that SCA5 mutations cause deficits in transport. I show that expression of mutant spectrin disrupts retrograde and anterograde transport in axons. Velocities and run lengths of vesicles in both directions are significantly reduced and an elevated frequency of reversals is seen. The loss of unidirectional transport may indicate a decreased affinity in the attachment of motors to vesicular cargoes and/or increased competition and switching between oppositely directed motor proteins.

The nature of the axonal aggregates and the extent to which they block the trafficking of organelles is unclear. These aggregates, also detected in *Drosophila* kinesin-1 and dynein mutants, were first thought to originate from accumulation of organelles and/or protein complexes and they could act to physically impede the passage of other moving cargos (Hurd and Saxton, 1996; Martin *et al*., 1999; Bowman *et al*., 2000). More recent work, however, has suggested that the axonal aggregates do not cause a general blockade to organelle transport and that axonal swellings may instead arise through a local autophagy response specifically triggered by the failed transport of mitochondria (Pilling *et al*., 2006). Our own observations indicate that axonal accumulations, or swellings, do not completely block the passage of moving cargoes, since synaptic vesicle proteins (e.g., synaptotagmin, CSP, and synaptobrevin) are transported and localized at synapses. However, the velocities of transport are reduced. In contrast, the velocity and directionality of mitochondrial transport in neurons was apparently unaffected by the mutant spectrins (unpublished results). To that effect, spectrin may not be implicated in the linkage of motors to mitochondria and axonal

swellings produced by the expression of the mutant spectrins are not likely to be triggered by autophagy of trapped mitochondria. Regardless of the mechanism, the accumulation of intracellular cargos in axonal swellings may contribute to the slowly progressive neurodegenerative effects of SCA5.

These results and the fact that dynein and dynactin mutations enhance these phenotypes suggest mutant spectrin perturbs spectrin-dynactin interactions and affects binding of cargo to dynein (Holleran *et al*., 2001). Although I have not directly demonstrated that mutant spectrins compromise dynactin attachment, Arp1 mutants exhibit similar defects, including an increased frequency of synaptic vesicles reversals (Haghnia *et al*., 2007), suggesting that both spectrin and dynactin act together to facilitate cargo-motor protein interactions.

Significantly, mutant spectrins not only disrupt dynein-mediated retrograde transport, but also affect anterograde transport. Most likely this reflects the interdependence between anterograde and retrograde transport that has been reported in multiple systems (Schroer *et al*., 1988; Brady *et al*., 1990; Waterman-Storer *et al*., 1997; Martin *et al*., 1999; Gross *et al.*, 2000, 2002a, b; Pilling *et al*., 2006). Loss of retrograde transport could reduce the recycling of kinesin to the cell body therefore limiting motor protein availability for anterograde transport or may also affect the retrograde transport of factors required for the regulation of anterograde motility. In addition, an increasing number of biochemical and functional analyses suggest dynactin acts as a switch to coordinate plus- and minus-end directed motor activities (Deacon *et al*., 2003; Gross, 2003; Hagnia *et al*., 2007). These results do not exclude the possibility that the SCA5 mutations could affect kinesin-based transport (Hirokawa, 1998; De Matteis and Morrow,

2000; Takeda *et al*., 2000; Paik *et al*., 2004; Hirokawa and Takemura, 2005) even though no direct association between β-spectrin and kinesin-1 has been reported in *Drosophila,* and SCA5 phenotypes are not enhanced by kinesin-1 mutations.

In addition to stabilizing protein domains at the membrane, one hypothesis is that spectrin also mediates the direct association of dynein and dynactin with proteins in membrane-bound cytoplasmic vesicles (Presley *et al.*, 1997; Holleran *et al*., 2001; Muresan *et al*., 2001). Both synapse loss and vesicle transport defects caused by the SCA5 mutations are likely to result from disruptions in the spectrin/dynactin/dynein adapter complex that links both vesicle and synaptic membranes to microtubules. The spectrin adapter network may recruit dynactin and dynein to the plasma membrane, promoting the capture of underlying cortical microtubules, and stabilization of the synaptic membrane. On synaptic vesicles, the spectrin adapter may facilitate the recruitment of the dynactin/dynein motor complex to the membrane, providing for transport of vesicles along the axonal microtubules.

Purkinje cells are among the largest neurons in the human CNS. The decreased efficiency in transport of synaptic components, vesicles, and organelles as well as the compromised stability of specialized neuronal membrane domains may underlie the profound Purkinje cell loss in SCA5 patients.

A

Evolutionary conservation of the American SCA5 mutation (p.E532_M544del)

```
ß-III spectrin   ARRERLLLNLELQKVFQDLLYLMDWMEEMKGRLQSQDLGRHL
fly ß-spectrin   ARRMRLEISLQLQQNFQEMLYILDNMEEIKQLLMTDDYGKHL
                 *** ** :.*:**: **::**::* *** *  * ::* *:**
```

Evolutionary conservation of the German SCA5 mutation (p.L253P)

```
ß-III spectrin   NLQNAFNLAEKELGITKLLDPEDVNVDQPDEKSIITYVATYYH
fly ß-spectrin   NLNNAFDVAEDKLGIAKLLDAEDVFVEHPDEKSIITYVVTYYH
                 **:***::**.:***:****.*** *::**********.****
```

B

Region	AA homology (%)
Entire protein	48
Third spectrin repeat	51
Calponin H domain 1&2	80

Figure 9. Analysis of protein homology between human β-III spectrin and *Drosophila* β-spectrin. (A**)** Alignment of human β-III spectrin and *Drosophila* β-spectrin protein sequences highlighting the homology in the region of the American (underlined region) and German SCA5 mutations. (B) Percent of homology between human β-III spectrin and *Drosophila* β-spectrin at the protein level as well as degree of amino acid conservation in the regions of the SCA5 mutations.

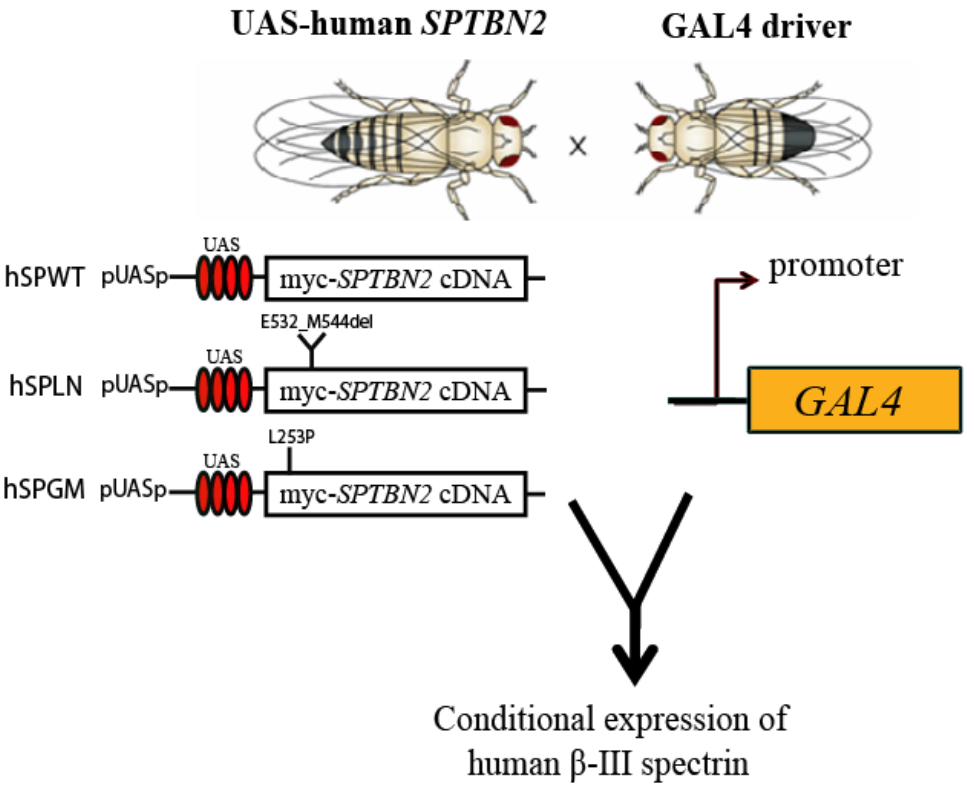

Figure 10. Schematic representation of the constructs generated to conditionally express human β-III spectrin in flies. hSPWT: wild-type, hSPLN: SCA5 American mutation, hSPGM: SCA5 German mutation. The full-length cDNA sequence of human *SPTBN2* gene with an N-terminal myc tag was cloned into pUASp plasmid downstream of the UAS binding sites for the transcription factor GAL4. Crosses to *GAL4* driver lines allow conditional expression of the human transgene.

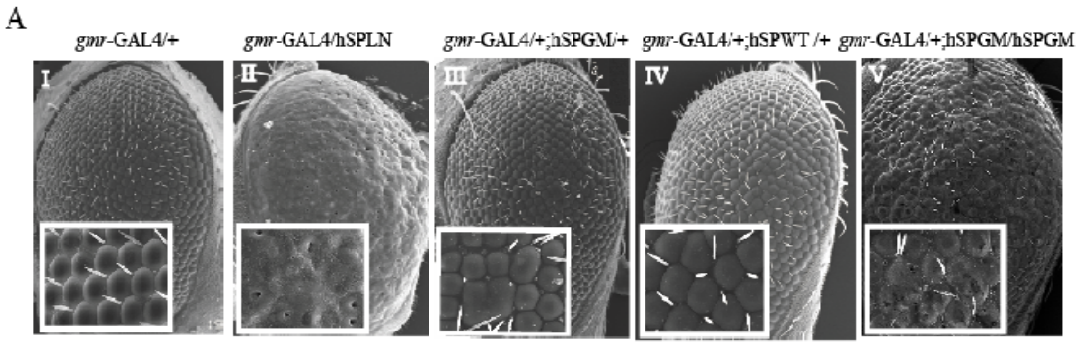
A
gmr-GAL4/+
gmr-GAL4/hSPLN
gmr-GAL4/+;hSPGM/+
gmr-GAL4/+;hSPWT /+
gmr-GAL4/+;hSPGM/hSPGM
I
II
III
IV
V

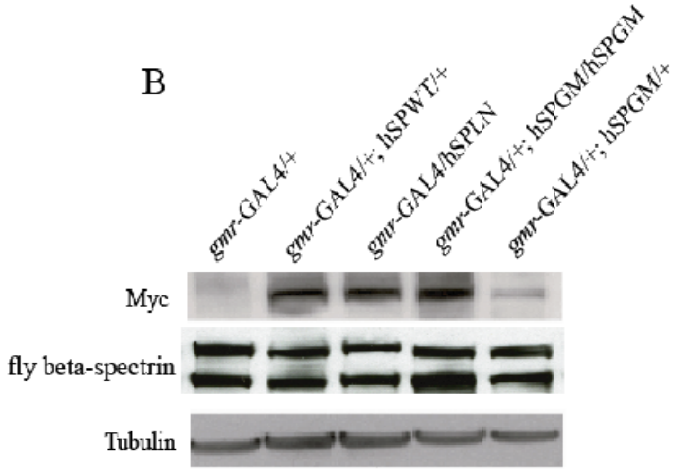
B
gmr-GAL4/+
gmr-GAL4/+; hSPWT/+
gmr-GAL4/hSPLN
gmr-GAL4/+; hSPGM/hSPGM
gmr-GAL4/+; hSPGM/+
Myc
fly beta-spectrin
Tubulin

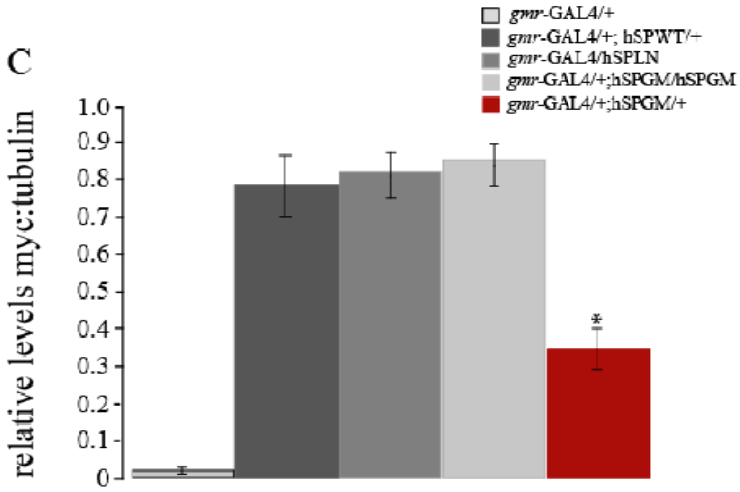
C
gmr-GAL4/+
gmr-GAL4/+; hSPWT/+
gmr-GAL4/hSPLN
gmr-GAL4/+;hSPGM/hSPGM
gmr-GAL4/+;hSPGM/+
relative levels myc:tubulin
1.0
0.9
0.8
0.7
0.6
0.5
0.4
0.3
0.2
0.1
0
*

Figure 11. Expression of mutant β-III spectrin causes a dosage dependent eye phenotype. (A) SEM images of adult fly eyes grown at 25°C. Insets show higher magnification of ommatidial fields. Expression of the mutant hSPLN transgene in the eye results in a fused and disorganized ommatidia missing interommatidial bristles (II). Flies expressing the mutant hSPGM transgene show a mild roughness of the eye (III) with a more severe phenotype in flies expressing two copies of the German SCA5 transgene (V). Flies expressing wild-type β-III spectrin (hSPWT) show only a mild ommatidial phenotype similar to *gmr*-GAL4 control flies (compare IV to I). (B) B-III spectrin expression for the different genotypes was detected using an antibody to the myc epitope with tubulin as a loading control. (C) Bar graph showing mean ratios of myc-tagged spectrin vs. tubulin protein for control (*gmr*-GAL4/+), *gmr*-GAL4/+; hSPWT/+, *gmr*-GAL4/hSPLN; *gmr*-GAL4/+; hSPGM/+), and homozygous *gmr*-GAL4/+; hSPGM/hSPGM flies. Animals expressing one copy of the hSPGM transgene have a significant reduction in β-III spectrin expression (P=0.025, n=4).

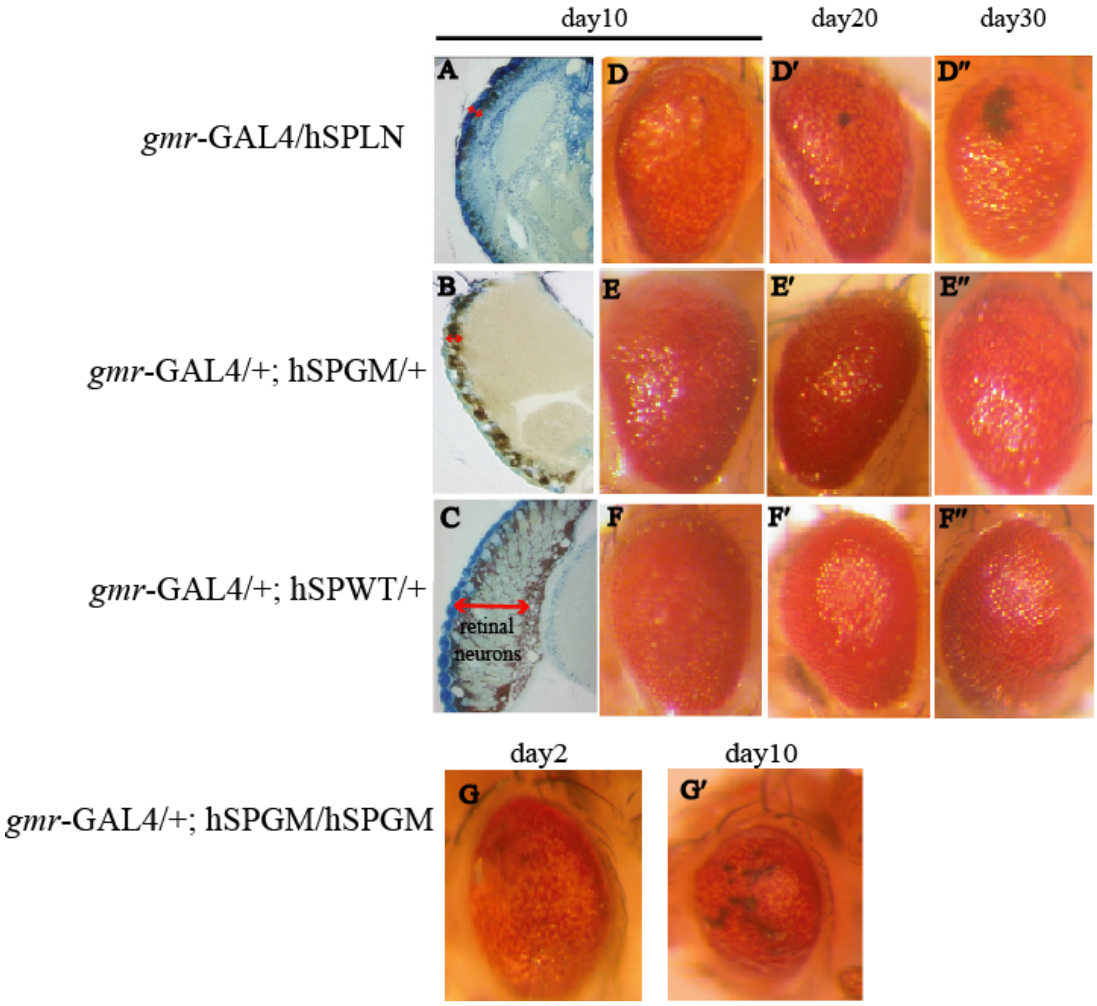

Figure 12. Expression of mutant β-III spectrin causes a progressive neurodegenerative eye phenotype. (A-C) Sections taken through the retina of 10 day old flies show thinning of the retina (arrow) and loss of retinal neurons in flies expressing hSPLN (A) and hSPGM (B) SCA5 transgenes compared to a wild-type control (C). (D-F″) Optical eye images taken at day 10, 20, and 30 illustrate the progression of the eye phenotype. Flies expressing wild-type human β-III spectrin showed no changes in the external eye morphology and pigmentation during the first 30 days of adult life (F-F″). The eye phenotype of flies expressing the hSPLN mutant transgene considerably worsens overtime (D-D″). Flies expressing low levels of the hDPGM mutant spectrin have defects in pigmentation by day 30 (E″). (G,G′) Optical eye images taken at day 2 and 10 correspond to flies expressing two copies of the hSPGM transgene. The severity and progression of the rough eye phenotype worsens with increasing dosage of mutant German β-III spectrin.

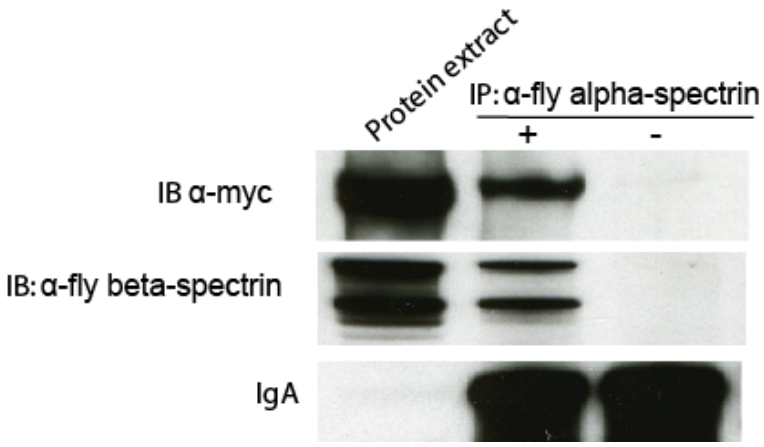

Figure 13. **Human β-III spectrin incorporates into α/β spectrin complexes in *Drosophila*.** Protein extracts from flies expressing the wild-type human β-III spectrin transgene (*gmr*-GAL4/+; hSPWT/+) were subjected to immunoprecipitation using the fly anti- α-spectrin monoclonal antibody 3A9. Precipitated immune complexes were then analyzed by Western blotting assays using either anti-myc or anti-fly β-spectrin antibodies. BSA was used as a control for the IP reaction.

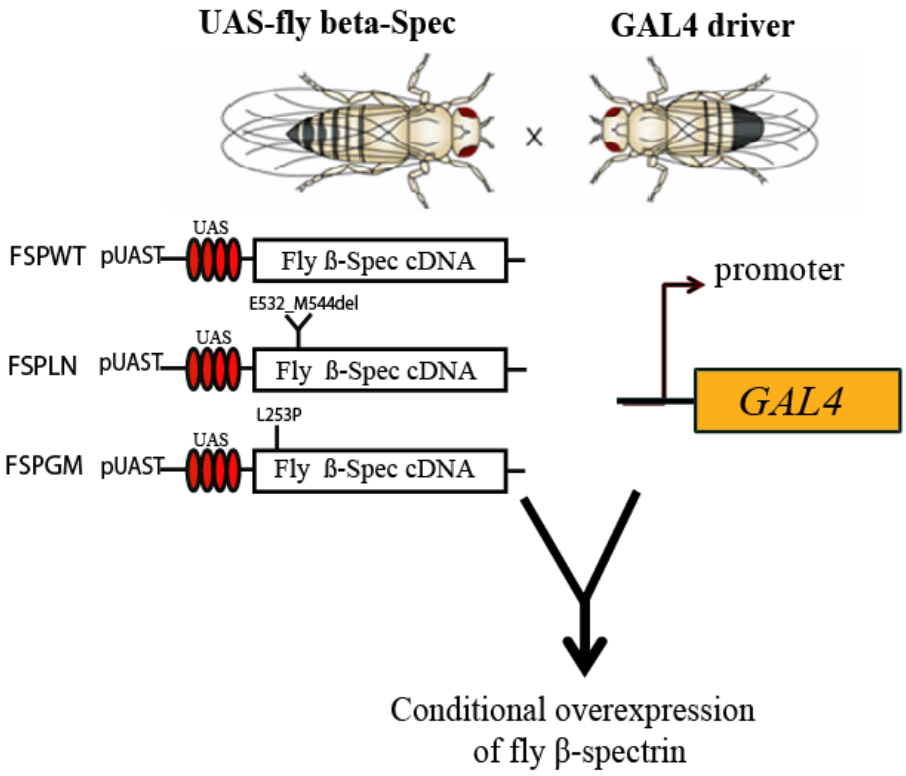

Figure 14. Schematic representation of the constructs generated to conditionally overexpress wild-type and mutant fly β-spectrin in *Drosophila*. FSPWT: wild-type fly β-spectrin, FSPLN: SCA5 American mutation, FSPGM: SCA5 German mutation. The full-length fly β-spectrin cDNA was cloned into pUAST plasmid downstream of the UAS binding sites for the transcription factor GAL4. Crosses to GAL4 driver lines allow conditional overexpression of the fly transgene.

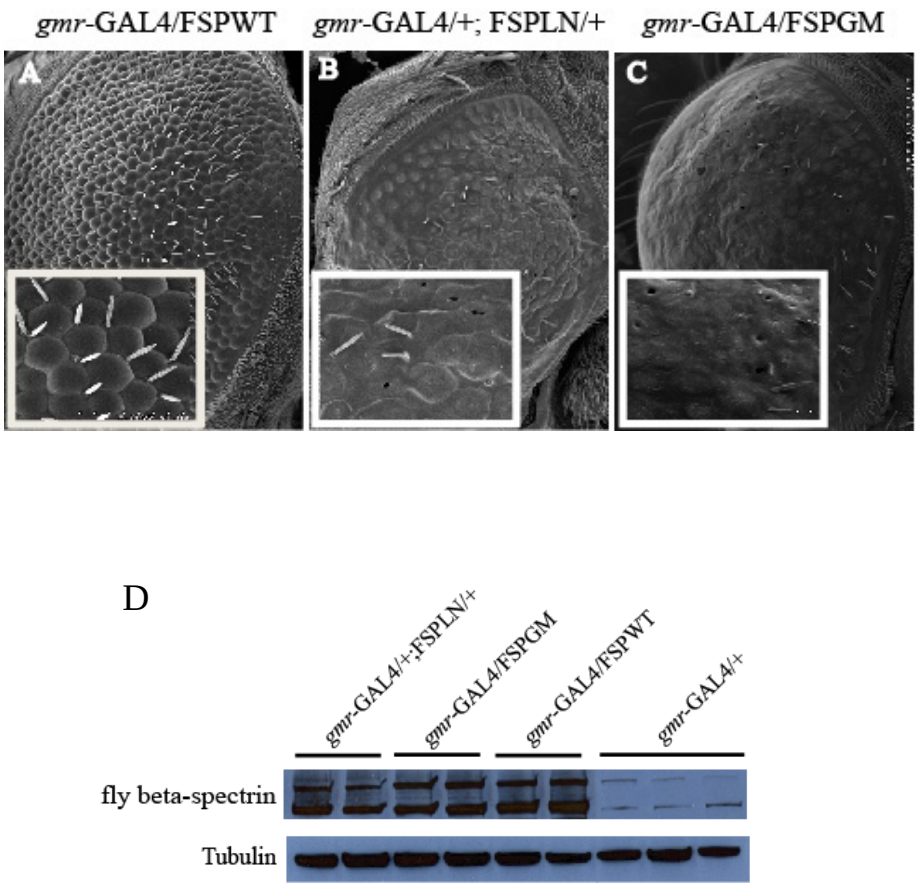

Figure 15. Human β-III spectrin and fly β-spectrin share functional pathways. (A-C) SEM images of adult eyes from flies grown at 25°C. Insets show higher magnification of ommatidia field. Expression of fly β-spectrin carrying either the American (*gmr*-GAL4/+; FSPLN/+, B) or German (*gmr*-GAL4/FSPGM, C) SCA5 mutations in the adult fly eye results in a neurodegenerative eye phenotype. Overexpressing wild-type fly β-spectrin (*gmr*-GAL4/FSPWT, A) results in minor changes in the external morphology of the eye similar to the *gmr*-GAL4 control. (D) Similar expression of fly β-spectrin was detected in transgenic flies from the different genotypes in study when compared to the endogenous levels of the protein detected in the *gmr*-GAL4/+ control line. Tubulin is a loading control.

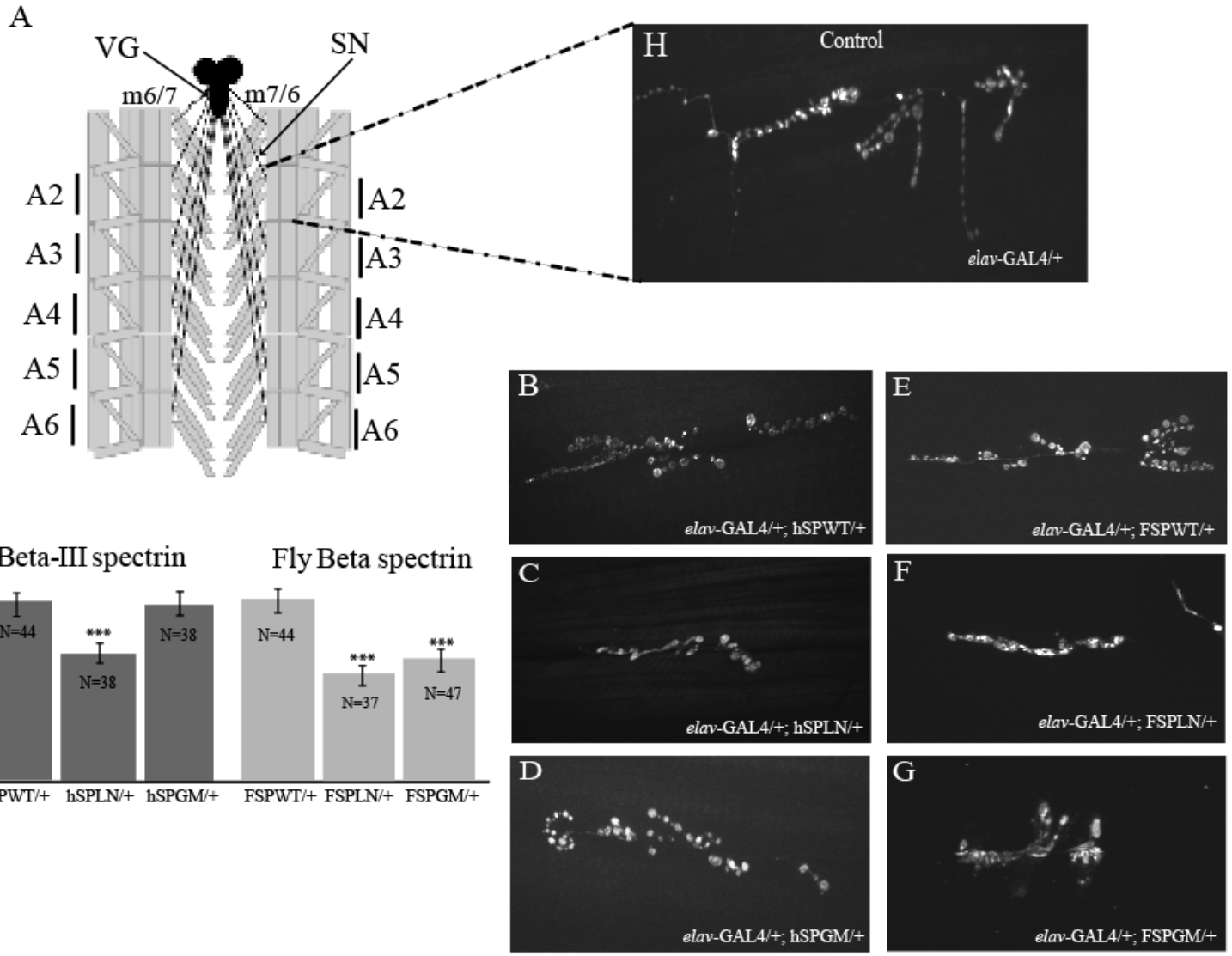
A
VG
SN
m6/7
m7/6
A2
A3
A4
A5
A6
H
Control
elav-GAL4/+
B
elav-GAL4/+; hSPWT/+
E
elav-GAL4/+; FSPWT/+
C
elav-GAL4/+; hSPLN/+
F
elav-GAL4/+; FSPLN/+
D
elav-GAL4/+; hSPGM/+
G
elav-GAL4/+; FSPGM/+
I
Beta-III spectrin
Fly Beta spectrin
Relative synapse size (%)
120
100
80
60
40
20
0
N=40
N=44
N=38
N=38
N=44
N=37
N=47
***
***
***
Control
hSPWT/+
hSPLN/+
hSPGM/+
FSPWT/+
FSPLN/+
FSPGM/+

Figure 16. Spectrin mutations affects synaptic terminal size at the neuromuscular junction. (A**)** Schematic representation of a NMJ preparation from a third instar larvae. The ventral ganglion (VG) constitutes the larval CNS. Axonal projections from motor and sensory neurons bundled together to form segmental nerves (SN) that innervate each abdominal muscle segment (A2-A6). (B-H) Confocal fluorescence images of NMJs on ventral longitudinal muscles 6/7 (m6/7) of larval abdominal segments A2 and A3. Larval synapses were visualized by staining with an antibody to the synaptic vesicle-associated protein CSP. Neuronal expression of the hSPLN, FSPLN, and FSPGM transgenes driven by *elav-GAL4* results in less NMJ expansion, fewer synaptic boutons and branches (C, F, G) when compared to the *elav*-GAL4 control (H). Neuronal expression of hSPWT, hSPGM, or FSPWT transgenes did not affect synapse size (B, D, E). (I) Quantification of bouton number shows a significant reduction in synapse size (number of synaptic boutons per surface area of muscle 6/7) in larvae expressing the hSPLN, FSPLN, and FSPGM mutant transgenes ($^{***}P<0.001$). Numbers are normalized to *elav*-GAL4 (control) in the graph. Data are mean ± S.E.M.

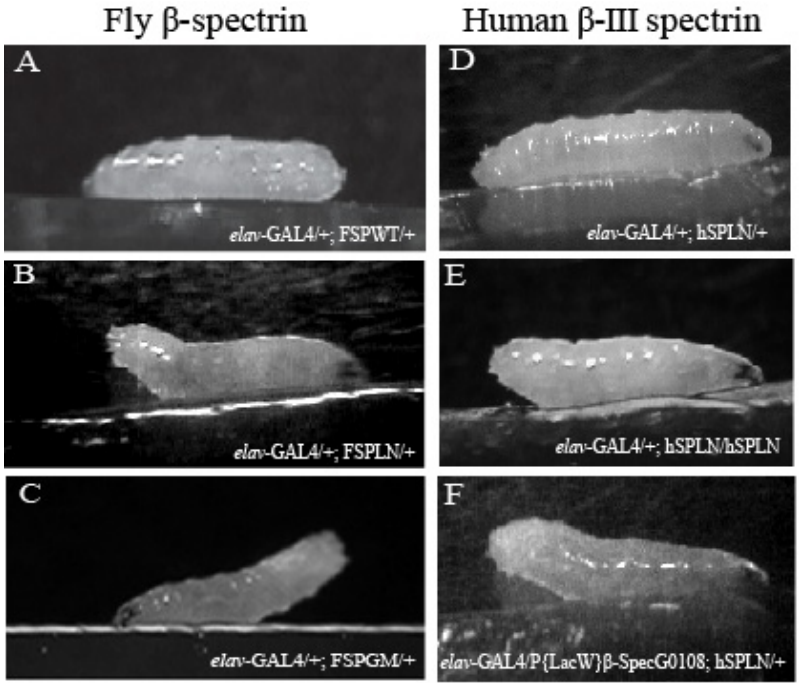

Figure 17. Spectrin mutations cause ventral posterior paralysis of the third intar larvae body. (A) Larvae overexpressing wild-type fly β-spectrin (*elav*-GAL4/+; FSPWT/+) exhibited normal posture when crawling. (B, C) Mutant larvae (*elav*-GAL4/+; FSPLN/+ and *elav*-GAL4/+; FSPGM/+) frequently flipped their tails upward when crawling indicating the development of a posterior paralysis phenotype common to axonal transport mutants in *Drosophila.* (D). Fly expressing low levels of mutant human β-III spectrin (*elav*-GAL4/+; hSPLN/+) exhibited normal posture when crawling. These larvae develop posterior paralysis when expression of the mutant human transgene is increased (E, *elav*-GAL4/+; hSPLN/hSPLN) or expression of endogenous fly β-spectrin is reduced (F, *elav*-GAL4/P{LacW}ß-SpecG0108;hSPLN/+)

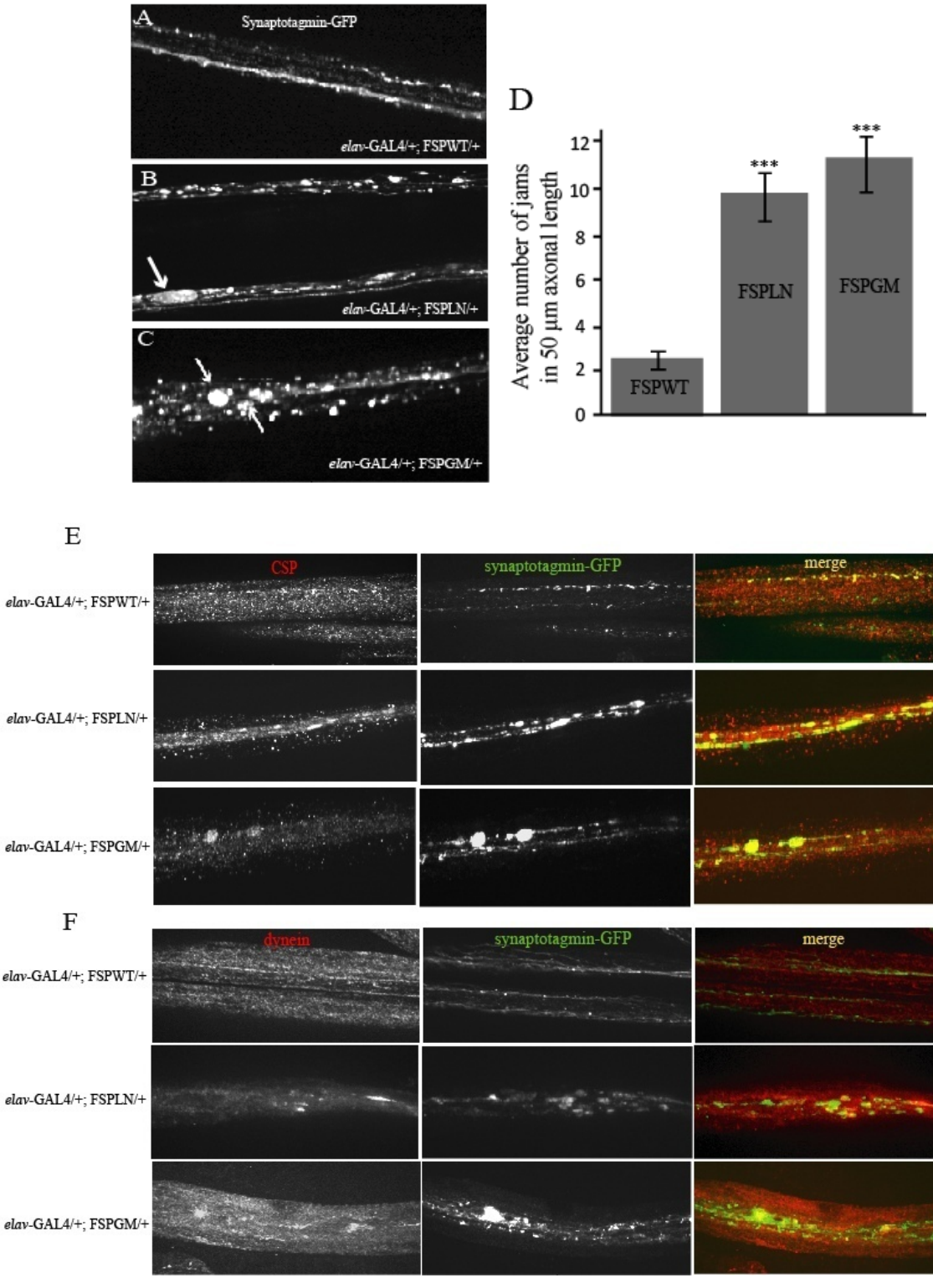
A
Synaptotagmin-GFP
elav-GAL4/+; FSPWT/+
B
elav-GAL4/+; FSPLN/+
C
elav-GAL4/+; FSPGM/+
D
Average number of jams in 50 µm axonal length
0
2
4
6
8
10
12
FSPWT
FSPLN
FSPGM
***
***
E
CSP
synaptotagmin-GFP
merge
elav-GAL4/+; FSPWT/+
elav-GAL4/+; FSPLN/+
elav-GAL4/+; FSPGM/+
F
dynein
synaptotagmin-GFP
merge
elav-GAL4/+; FSPWT/+
elav-GAL4/+; FSPLN/+
elav-GAL4/+; FSPGM/+

Figure 18. Spectrin mutations cause accumulation of synaptic proteins in larval segmental nerves (A-C) Expression of the American and German mutant spectrins cause large synaptotagmin-GFP accumulations (B, C) when compared to the punctuated pattern seen in axons expressing the wild-type protein (A). Large axonal swellings are indicated by arrows. (D) Quantification of the number of synaptotagmin-GFP accumulations in 50 µm of axonal length. At least fifteen segmental nerves were analyzed per genotype. Data represent mean ± S.E.M. Significant differences in the number of axonal jams between wild-type and mutants are denoted by asterisks ($^{***}P<0.001$). (E) Fluorescent images of segmental nerves show the accumulation of the axonal transport cargoes synaptotagmin and CSP within the axonal jams in segmental nerves from mutant but not wild-type fly β-spectrin larvae. (F) Fluorescent images of segmental axons show the accumulation of the motor protein dynein and the synaptic vesicle integral membrane protein synaptotagmin in mutant but not wild-type fly β-spectrin larvae.

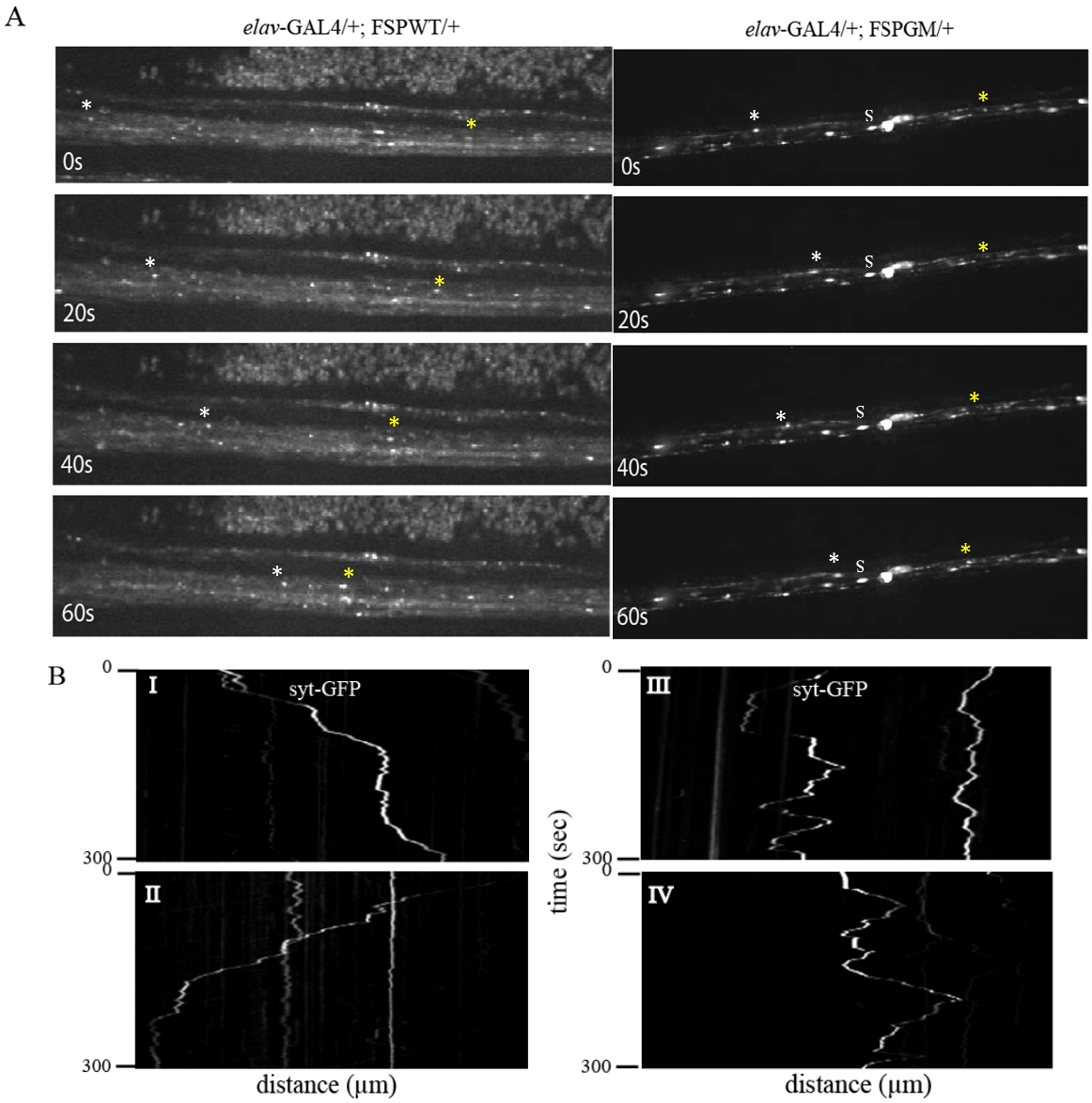

Figure 19. Spectrin mutations disrupt vesicle transport. (A) A series of images from time lapse movies of GFP-synaptotagmin tagged vesicles in the segmental nerves of dissected third instar larvae. The motion of individual organelles in a particular direction is indicated by asterisks (*). A stationary organelle (s) is indicated for reference. (B) Representative kymographs showing the motion of individual synaptotagmin-GFP particles in larval segmental axons as a function of time. Kymographs corresponding to larvae expressing wild-type fly β-spectrin show fluorescent vesicles moving in one defined direction (diagonal lines) and few stationary vesicles appear as vertical lines (I, II). Kymographs from mutant spectrin larvae show stationary GFP-particles, whereas the majority of those moving undergo numerous reversals in the direction of movement (zigzag lines, III, IV)

Figure 20 part I

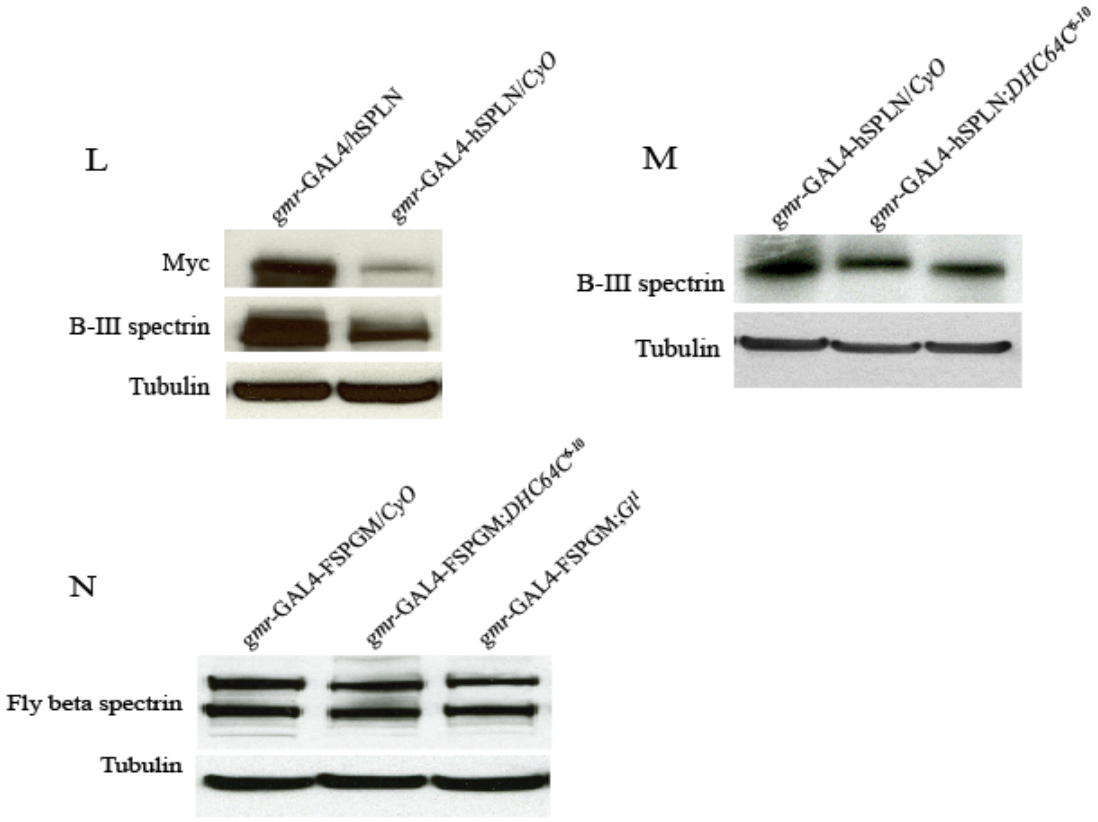

Figure 20 part II

Figure 20. *DHC64C* and *p150^{Glued}* mutant alleles enhance the dominant neurodegenerative phenotypes associated with the SCA5 mutations. Part I. (A) Mutations in human β-III spectrin interact with the cytoplasmic dynein heavy chain *DHC64C$^{6-10}$* mutation to produce posterior paralysis. Larvae shown in AI and AII are heterozygous for the American SCA5 mutation in human β-III spectrin (*elav*-GAL4-syt-GFP/+, hSPLN/+) and the *DHC64C$^{6-10}$* mutant allele, respectively, and exhibit normal locomotion. Double heterozygous animals (*elav*-GAL4-syt-GFP/+, hSPLN/+, *DHC64C$^{6-10}$*/+) developed an abnormal crawling behavior (AIII). (B) Fluorescent images show large synaptotagmin-GFP accumulations within segmental nerves from double heterozygous mutant larvae (BIII, *elav*-GAL4-syt-GFP/+, hSPLN/+, *DHC64C$^{6-10}$*/+). (C) Quantification of bouton number shows significant reduction in synapse size (number of synaptic boutons per surface area of muscle 6/7) in animals expressing the American SCA5 mutation in human β-III spectrin that are also heterozygous for the *DHC64C$^{6-10}$* mutant allele of dynein (*elav*-GAL4-syt-GFP/+, hSPLN/+, *DHC64C$^{6-10}$*/+). Numbers are normalized and compared to *elav*-GAL4 (control) in the graph. Data are mean ± S.E.M, $^{***}P<0.001$.

(D-K) SEM images of *Drosophila* eyes. Recombinant lines expressing the American SCA5 mutation in β-III spectrin (*gmr*-GAL4-hSPLN/*CyO*, 5D*) or the German SCA5 mutation in fly β-spectrin (*gmr*-GAL4-FSPGM/*CyO*, 5E) show disorganization in the arrangement of the ommatidia and bristles of the adult eye. *Note the recombinant *gmr*-GAL4-hSPLN line showed reduced levels of transgene expression and produced a less severe eye degeneration, making it easy to distinguish changes in the phenotype. *DHC64C$^{6-10}$*/+ flies have a wild-type eye (F), but in combination with *gmr*-GAL4-hSPLN or *gmr*-GAL4-FSPGM mutant spectrin alleles produce a more severe eye phenotype than either parent (G, H). Eyes expressing the dominant *Gl^{1}* mutation exhibit a rough eye phenotype, with disordered ommatidia (I). Similarly, the combination of the *Gl^{1}* dynactin mutant allele and *gmr*-GAL4-hSPLN or *gmr*-GAL4-FSPGM mutant spectrins result in a dominant enhancement of the eye degeneration. Eyes from double mutant flies are reduced in size and show a dramatic roughens of the eye surface (J, K).

Part II. (L) Human β-III spectrin expression is reduced in recombinant lines used for genetic interaction analysis. Total proteins from fly heads were subjected to Western-blot analysis using antibody specific to human β-III spectrin, or the myc epitope. Reduced expression of the human transgene is observed in flies carrying the *gmr*-GAL4-hSPLN/*CyO* recombinant chromosome as compared to the original *gmr*-GAL4/ hSPLN line. (M, N). The enhancement of mutant β-spectrin induced neurodegeneration by the *DHC64C$^{6-10}$* and *Gl^{1}* mutant alleles does not result from changes in transgenes expression. Total proteins from fly heads were subjected to Western-blot analysis using an antibody specific to human B-III spectrin (M) or fly β-spectrin (N). Tubulin functions as a loading control.

Genotype	Net velocity (µm/s ± S D)	Number of particles	*P* value
elav-GAL4/+; FSPWT/+	0.75 ± 0.23	89	
elav-GAL4/+; FSPLN/+	0.43 ± 0.2*	88	< 0.0001
elav-GAL4/+; FSPGM/+	0.48 ± 0.15*	86	< 0.0001

Table 6. Analysis of synaptotagmin-GFP vesicles motions in segmental nerves expressing wild-type or mutant β-spectrin driven by *elav*-GAL4. Net velocity was determined by adding all velocities for each tracked GFP particle over the entire time of motion. Data shown represent mean ± SD. Asterisks denote significant differences for mutant relative to wild-type.

Genotype	Anterograde runs					Retrograde run				
	Velocity (µm/s ± SD)	*P* value	Run length (µm ± SD)	*P* value	N	Velocity (µm/s ± SD)	*P* value	Run length (µm ± SD)	*P* value	N
*D4-2*GAL4/+;FSPWT/+	0.78 ± 0.13		9.6 ± 2.5		54	- 0.72 ± 0.15		9.2 ± 3.1		80
D42-GAL4/FSPLN	0.5 ± 0.17*	< 0.0001	6.8 ± 3.1*	< 0.0001	76	-0.55 ± 0.11*	< 0.0001	7.2 ± 2.5*	< 0.0001	97
D42-GAL4/+;FSPGM/+	0.44 ±0.15*	< 0.0001	6.1 ± 2.7*	< 0.0001	81	-0.48 ± 0.18*	< 0.0001	7.4 ± 3.3*	< 0.0001	135

Table 7. Analysis of transport parameters for anterograde and retrograde synaptobrevin-GFP containing vesicles in wild-type and mutant segmental nerves. Average velocity and run length for both anterograde and retrograde moving particles are reduced in mutant β-spectrin larvae in comparison to wild-type. Data shown represent mean ± SD. Asterisks denote statistical significant differences for mutant relative to wild-type.

Movie M1. Motion of GFP-synaptotagmin bearing synaptic vesicles in segmental nerves expressing wild-type fly β-spectrin driven by *elav*-GAL4 (*elav*-GAL4-syt-GFP/+; FSPWT/+). Images were acquired continuously at a rate of one frame every 1 second.

Movie M2. Motion of GFP-synaptotagmin bearing synaptic vesicles in segmental nerves expressing the German SCA5 mutant spectrin (*elav*-GAL4-syt-GFP/+; FSPGM/+). Images were acquired continuously at a rate of one frame every 1 second.

Movie M3. Motion of GFP-n-Synaptobrevin bearing synaptic vesicles in the motor axons of a third intar larvae overexpressing wild-type fly β-spectrin (*D42*-GAL4-n-Syb-GFP/+; FSPWT/+). Images were acquired continuously at a rate of one frame every 1 second.

Movie M4. Motion of GFP-n-Synaptobrevin bearing synaptic vesicles in the motor axons of a third intar larvae expressing the German SCA5 mutant spectrin (*D42*-GAL4-n-Syb-GFP/+; FSPGM/+). Images were acquired continuously at a rate of one frame every 1 second.

CHAPTER 4

Genetic screen for modifiers of SCA5-induced neurodegeneration in *Drosophila*

I. Introduction

One of the main advantages of modeling human disorders in *Drosophila* is the availability of genetic tools that facilitate the unbiased identification of genetic interactors and biological pathways. Large collections of fly mutants allow screening strategies that test the effects that modifying or eliminating expression of genes across the genome have on specific mutation induced phenotypes (Driscoll and Gerstbrein, 2003). Specific modifier screens developed to test genetic interactions caused by loss-of-function mutations include mutant panels generated by chemical and X-ray mutagenesis, chromosomal deletions, lethal P-element insertions, and RNAi. Modifier screens that allow testing the effects of gene overexpression include mutant panels generated by enhancer insertion (EP- enhancer promoter) (Rorth, 1996). I used two strategies, deficiency and P-element-insertions, to screen for genetic modifiers of the SCA5 mutations and briefly describe these strategies below.

Deletion-based genetic screens detect modifications of specific phenotypes that appear in flies that are hemizygous for the interactor gene in a disease or gene specific mutant background. The effect of deleting one copy of numerous genes at a time can be

tested by using libraries of flies with overlapping deletions that span each of the *Drosophila* chromosomes (Ryder *et al*., 2004; Parks *et al*., 2004). A primary screen is usually performed first using a fly collection with relatively large deletions followed by subsequent rounds of screening using smaller deletions, RNAi transgenic lines, P-element insertion lines. Known mutant alleles of candidate genes are then used to further define chromosomal regions containing putative interactors and ultimately identify modifiers.

P-element-based genetic screens are performed using a library of fly lines, each of them carrying a single P-element insertion associated with a known gene (Bellen *et al*., 2004). Screens using lethal P-element insertions are more likely to detect loss-of function modifiers because the insertion of the transposable element into the promoter or into an exon frequently disrupts gene expression (Crowther *et al*., 2008). New types of transposable elements that contain a *GAL4*-UAS element, known as enhancer promoter (EP)-elements, now also allow the isolation of gain-of function modifiers.

To reveal insight into pathways that may modulate SCA5-induced neurodegeneration, I performed two genetic screens in *Drosophila*. These studies revealed genetic modifiers implicated in a wide range of biological functions including intracellular transport, synapse formation and function, protein homeostasis, transcription regulation and energy production.

II. Results

To identify genes and biological pathways implicated in SCA5 pathogenesis, I screened both a *P*-element lethal and a deficiency collection for modifiers of SCA5-induced eye neurodegeneration in *Drosophila*. Both approaches used recombinant lines that carry the *gmr*-GAL4 driver and either the American (*gmr*-GAL4-hSPLN) or German (*gmr*-GAL4-FSPGM) mutant spectrin transgenes on a single chromosome. In these flies, moderate levels of mutant spectrin accumulate in the retina causing mild eye degeneration at 25 °C (Figure 21 A-B, left panels).

I initially examined a collection of 112 third chromosome deficiency stocks known as the Bloomington Deficiency kit (Parks *et al*., 2004). These deficiencies collectively span approximately 93% of the genes on the third chromosome. Flies carrying the SCA5 recombinant chromosomes were crossed to deficiency lines with normal eye morphology, and progeny containing both mutant spectrin transgene and deficiency (*gmr*-GAL4-hSPLN/+; *Df*/+ or *gmr*-GAL4-FSPGM/+; *Df*/+) were scored for changes in eye morphology. Initial results from this screen identified ten regions that modify the rough eye phenotype associated with SCA5 mutant spectrins (Table 9 and Figure 21). Similar analysis using small overlapping deficiencies indicate that four of the regions identified in the primary screen were false positive (Table 10) and confirmed that the genomic region deleted by *Df(3R)T-32* (Table 10) contains genetic modifiers of the SCA5 eye phenotype.

The *Df(3R)T-32* deletion was identified in the primary screen as a strong enhancer of the eye phenotype of flies expressing the German SCA5 transgene (Figure 21B, right

panel). This deficiency spans the chromosomal region 86E2-87C7 and deletes approximately 186 genes. A series of overlapping deficiencies within this region narrowed the potential modifier to the 86E2-87B11genomic region, containing 161 genes (Figure 22). By testing P-element insertions known to disrupt a set of genes within the small 86E13-87B3 region I found that *CG4830*, *lethal (3)04629*, and *svp* genetic loci modified the SCA5 eye phenotype (Figure 22, arrowheads). However, these preliminary studies only tested the effect of P-element insertion in 38 out 161 genes mapped to the 86E2-87B11 candidate region, and additional P-element lines need to be used to screen all known genes in this region.

The *CG4830* gene (FBgn0037996) maps to the cytological location 87B2 and functions in the metabolic processing of fatty acids to result in energy production. The second interactor gene, s*even up* (*svp)* (CG11502, FBgn0003651, location 87B5), acts as a ligand-dependent nuclear receptor as well as a transcription factor. This gene has been broadly implicated in nervous system and embryonic development, organ morphogenesis, and synaptic transmission. The third putative modifier, *lethal (3)04629* (FBgn0010844), has been mapped to the cytological position 86E17-19, but its biological function has not been defined.

While the use of deficiency collections allows relatively rapid screening of the entire genome, the identification of actual modifier loci is often tedious and difficult to perform and the results are not always straightforward. Differences in the genetic background of the deficiencies, including secondary mutations increase the probability of getting false positive results. To avoid these problems, I used an alternative approach and

performed a second screen using lethal *P*-element insertions in which the exact genomic site of the insertion is known for each individual line. Although available collections of lethal P-element insertions do not yet span the entire genome, this methodology usually allows the more efficient identification of genetic interactors.

I screened a subset of 800 available lethal *P*-element insertion stocks spanning the left arm of the second chromosome (2L). Similar to the deficiency screen, the *P*-element lines were individually crossed to flies bearing the SCA5 recombinant chromosomes that allow expressing the American or German SCA5 mutations in the eye, and progeny carrying both the spectrin mutant transgene and *P*-element insertion were examined for changes in eye morphology (Figure 23A). This approach identified 74 genes that enhance SCA5-induced eye degeneration (Table 11). An example of a genetic interaction detected through the screen is shown in Figure 23B.

To verify that specific transposon insertions are responsible for enhancing the SCA5- eye phenotype, I tested whether the eye changes would be reverted after *P*-element excision. In brief, the *P*-element transposable elements were individually mobilized for each of the lines that showed genetic interaction with mutant spectrin transgenes (Table 11) by providing the Δ2-3 transposase source Hop2. Five independent males, in which the *P*-element was precisely excised, were identified for each of the modifier P-element lines by their white eye color, and these revertants were crossed to females carrying mutant spectrin recombinant chromosomes (*gmr*-GAL4-hSPLN/*CyO* or *gmr*-GAL4-FSPGM/*CyO*). I found that all but two of the lines tested (*P*{lacW}*kis*^{k1023} and *P*{lacW}*lilli*^{k05431}) showed reversion of the eye phenotype after P-

element excision. However, because the *kis* and *lilli* loci were identified multiple times in the screen, a similar analysis using additional *P*-element insertions in these two genes (*P*{w[+mC]=lacW}*kis*[k13416] and *P*{PZ}*lilli*^{00632}) was preformed. These additional crosses show eye phenotype reversion after transposon excision and confirm that kis and lilli also genetically interact with the mutant spectrin transgenes, Taken together, reversion analysis proves that *P*-element insertions described in Table 11 cause of the enhancement of the SCA5 eye phenotype.

Genetic interactors identified through the screen were classified into six major categories according to their known biological functions defined by Gene Ontology (GO) terms (Table 11, see Figure 24 for summary of major categories). Consistent with a proposed role for SCA5 mutant spectrin in intracellular transport and synapse stability (Chapter 4) a large group of modifiers fall into two major classes that include components of the transport machinery (Class 1) as well as proteins that are required for synapse formation and function (Class2) (Table 11-I). The classification of the remaining modifiers was based on their role in protein folding and degradation (Class 3), protein synthesis (Class 4), RNA synthesis and processing (Class 5), and miscellaneous functions (Class 6) (Table 11-II and III).

Class I modifiers include the dynactin subunit p25 (*dyn-p25*), the anterograde-directed motor protein nebbish (*Neb*), the kinesin-associated protein milton (*Milt*), and the GTPase dynamin related protein 1 (*Drp1*). Interactors that fall into the class 2 category are either required for neurotransmitter-mediated signaling, including the aspartate/glutamate transporter Eaat2 (*Eaat2*) and the alpha subunit of the acetylcholine

receptor (*AcRα-34E*), or the organization of the cortical actin cytoskeleton in neurons. Within the last cluster are the actin related protein Arc-p20 (*Arc-p20*); capulet (*Capt*), Ced-12 (*Ced-12*), and wing blister (*wb*). An additional group of four genetic interactors, known to be required for both intracellular transport and synapse function, were identified and placed into Class 1/2. This group includes the synaptic vesicle proteins synaptotagmin (*Syt1*) and syntaxin (*Syx5*), the MT-associated protein Jupiter (*Jup*), and the actin and MT-binding protein Cytoplasmic linker protein 190 (*CLIP-190*).

In addition, I identified molecular chaperones and genes involved in proteasomal degradation as modifiers of the SCA5 eye phenotype. Class 3 genes include: the Hsp70/90 organizing protein (*Hop*) member of the Hsp70 family, the Rpn11 (*Rpn11*) constituent of the proteasome, as well as the component of the ubiquitin-mediated protein quality control pathway Cul-2 (*Cul-2*), Nedd8 (*Nedd8*) and guftagu (*gft*).

Other modifiers of SCA5 neurodegeneration directly regulate protein synthesis (Class 4). Among those are ribosomal constituents, including the Ribosomal protein S13 (*RpS13*), Ribosomal protein S27A (*RpS27A*), and Ribosomal protein L30 (*RpL30*); translation initiation [e.g. Eukaryotic initiation factor 4a (*eIF-4a)* and Trip1 (*Trip1*)] and elongation [e.g. Elongation factor 2b (*Ef2b*)] factors. The Class 5 group of modifiers identified in the screen is comprised of RNA synthesis and processing genes, including various transcription factors, chromatin remodeling proteins, nuclear hormone receptors, and the mRNA splicing regulators Heterogeneous nuclear ribonucleoprotein at 27C (*Hrb27C*) and hoi-polloi (*Hoip*) (refer to Table 11-II and III for details). Genes in the last category of interactors (Class 6) are predicted to be involved a variety of molecular

functions ranging from energy production, ion transport to signal transduction and cell division (Table 11-III).

Overall, analysis of the modifiers suggest that, although defects in intracellular transport, synapse stability and function as well as the regulation of protein folding and degradation may directly impact the SCA5-associated phenotypes, abnormal mutant spectrin interaction with the transcriptional and translational machinery, and additional pathways are also likely to contribute to SCA5 pathogenesis.

In a first attempt to characterize modifiers identified in the screen I conducted analysis of larval phase lethality with the goal of identifying homozygous P-element insertion lines, that survive until third intar larvae. Positive lines identified through this strategy can be used to investigate neuronal phenotypes likely to be relevant to SCA5 in the third instar larvae, including synaptogenesis and axonal transport functions. Larval lethality was determined by crossing female flies from lethal P-element stocks that showed genetic interaction with mutant spectrin transgenes to a reciprocal translocation chromosome (*FM6, TM6BTb*) that facilitates the detection of homozygous mutant larvae. Preliminary results indicate that at least seven homozygous P-element lines survive until or past third instar larvae stages (Table 11). Further efforts will initially focus on studying the individual effect of this small group of genetic interactors in neurons and the consequences of their genetic interaction with mutant spectrin transgenes.

III. Discussion

I have performed two unbiased genetic screens in *Drosophila* and identified different chromosome regions and genes that modify the rough eye phenotypes seen in SCA5 mutant flies.

The third chromosome deficiency screen detected ten regions that are likely to contain SCA5 interactors. Four of these regions were excluded by secondary screens and five remaining chromosomal segments will require a more detailed examination. I found that chromosomal fragment 86E2-87B14, which is deleted by *Df(3R)T-32*, contains at least three modifier genes whose activities are implicated in energy production and transcription regulation. Preliminary studies conducted to uncover modifier loci within the 86E2-87B14 region only tested the effect of P-element insertion in 38 out 161 genes mapped to this interval. Candidates of interest yet to be examined include the pan-neuronal transcription factor prosper (*pros*), the mitochondrial ribosomal protein L40 (*mRpL40*), the Proteasome 25kD subunit (*Pros25*), members of the Hsp70 family (*Hsp70Aa* and *Hsp70Ab*), and eight members of the *Drosophila* family of glutathione transferase proteins (*GstD1-3, GstD4-8,* and *GstD10*).

A second genetic screen based on lethal P-element identified 74 interactors within the second chromosome. Modifiers were found to be implicated in intracellular transport, synapse formation and function, protein homeostasis, transcriptional regulation and a range of other biological functions.

My discovery that various components of the transport machinery modify the SCA5 mutant transgenes supports the model that defects in intracellular transport

contribute to Purkinje cell degeneration in SCA5. Interestingly, two different anterograde-based motor proteins (nebbish and Milton) were found to modify the spectrin eye phenotype. This result is consistent with the effects of SCA5 mutant spectrin on the bidirectional motion of synaptic vesicles described in Chapter 3. Future characterization of the interaction between spectrin and anterograde motor proteins in *Drosophila* will allow investigations of the specificity of cargo-motor protein recognition and the role of spectrin in anterograde transport.

In support of a requirement of spectrin for synapse maintenance and function, the P-element screen also identified a group of interactor that are required for the transport of synaptic vesicles to synaptic terminals and synapse formation (e.g. syntaxin and synaptotagmin), or for synaptic transmission (e.g. PgK). Importantly, the glutamate transporter EAAT2 was also identified in the screen suggesting that like in humans mutant spectrin also interacts with proteins that regulate glutamate signaling in flies.

Neurons require precise regulation of the microtubule (MT) and actin cytoskeletons to maintain proper organization and function of synaptic regions. Modifiers that affect the association of spectrin with the MT cytoskeleton or the stability of the MT network (e.g. dynactin subunit p25, CLIP-190, and Jupiter) are likely to impact the intracellular transport of synaptic components and signaling molecules, and the overall

stability and function of synapses.

The spectrin mesh also contributes to the stability of synaptic membranes and the formation of specialized membrane domains through the association with the actin cytoskeleton (Bennett and Baines, 2001). Consistent with a model in which the SCA5 mutations disrupt these functions, numerous interactors identified in the screen are required for proper actin polymerization and the organization of the cortical actin network. One attractive example is the actin-binding protein capulet (*capt*) which is an essential regulator of actin dynamics (Baum and Perrimon, 2001). Genetic and functional studies show that capulet mutants have abnormal aggregates of actin filaments within dendrites. Strikingly, perturbation of capulet function affects both actin dynamics and MT-based functions since capullet genetically interacts with kinesin heavy chain to disrupt the transport of cargo along MT networks in fly dendrites (Medina *et al.*, 2008). It would be interesting to investigate the neuronal phenotypes of flies that express the SCA5 spectrin mutations in a capulet mutant background to better define the contribution of the interaction between the spectrin and actin networks to SCA5 phenotypes.

The third category of interactors suggests protein folding and protein degradation pathways contribute to SCA5 pathogenesis. In support of this idea, recent studies performed in the Ranum lab indicate that the German SCA5 mutation affects the stability and solubility of human β-III spectrin, and causes misfolding and aggregation of the protein (Krueger *et al.*, in preparation). Similarly, results with the American SCA5 mutation show dramatic changes in the intracellular localization of β-III spectrin and accumulation of small protein aggregates in Purkinje cell bodies of SCA5 mutant mice (Armbrust *et al.*, in preparation). In addition, various synaptic components and motor

proteins were found to accumulate in axonal swellings in SCA5 mutant flies (Chapter 3). The accumulation of misfolded proteins in aggregates is a hallmark of Alzheimer's and Parkinson's diseases, amyotrophic lateral sclerosis, and polyglutamine expansion disorders and might represent a point of convergence of different neurodegenerative human disorders including SCA5. It would be interesting to test if overexpression of molecular chaperones suppresses or mitigates the neuronal phenotypes associated with the SCA5 mutations as shown for different *Drosophila* and mammalian models of polyglutamine disorders (Chan *et al*., 2000; Cummings *et al*., 2001; Bilen and Bonini, 2007).

A large group of genes involved in protein synthesis and in the synthesis and processing of RNA were also identified in the screen. These findings underscore the importance of pathways controlling protein homeostasis in SCA5 pathogenesis. Additional investigation is necessary to establish specific molecular mechanisms by which these modifiers modulate SCA5 neurodegeneration. However, it is likely that overall RNA synthesis and processing defects may contribute to disease by disrupting the equilibrium among protein synthesis, folding, and degradation or by directly affecting expression of genes that are required for neuronal homeostasis.

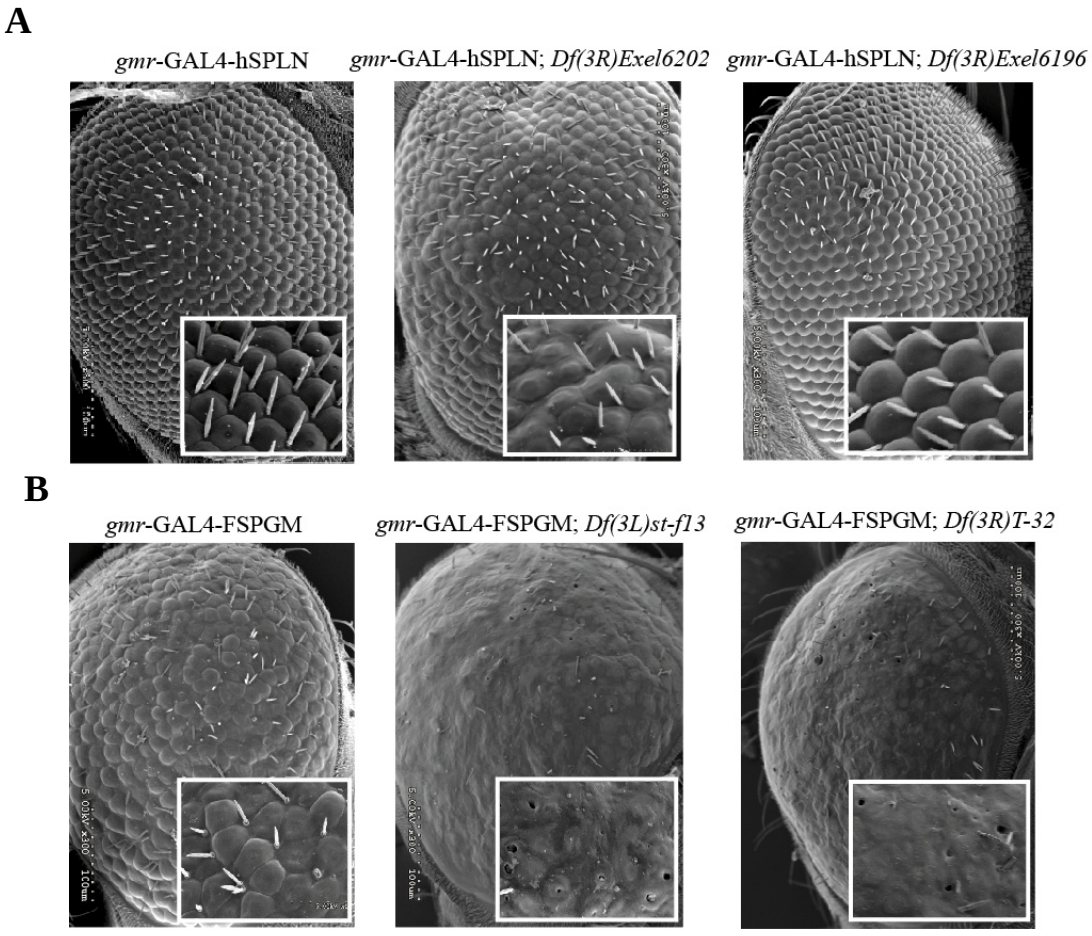

Figure 21. Third chromosome deficiencies modify the dominant neurodegenerative eye associated with the SCA5 mutations. SEM images of eyes from flies expressing mutant spectrin and selected examples of deficiencies that modify the SCA5 rough eye phenotype. (A) From left to right. The SCA5 American recombinant chromosome expresses the American SCA5 mutation in human β-III spectrin in the adult eye and produces a mild eye phenotype. *Df(3R)Excel 6202* genetically interact with the spectrin mutant transgene to produce a more severe eye phenotype while *Df(3R)Excel 6196* slightly suppressed the eye degeneration. (B) From left to right. The SCA5 German recombinant chromosome expresses the German SCA5 mutation in fly β- spectrin in the adult eye and produces a moderate rough eye phenotype that is enhanced by both *Df(3L)st-f13* and *Df(3R)T-32*.

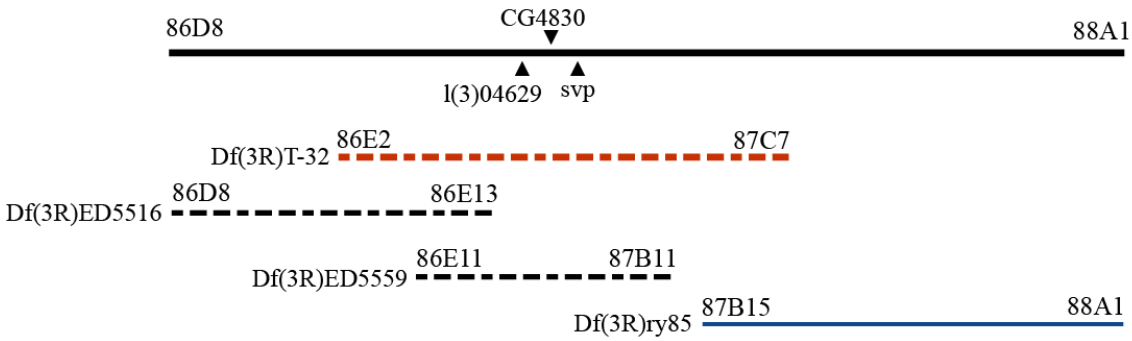

Figure 22. Genomic region of the third chromosome containing putative SCA5 interactors. Df(3R)T-32 (red dashed lines) was identified in a primary screen for modifiers of SCA5 rough eye phenotype. Smaller deletions within this region (Df(3R)ED5516 and Df(3R)ED5559) shown as black dashed lines also enhance the SCA5 eye phenotype. Df(3R)ry85 (solid blue line) does not modify the eye phenotype. Arrowheads indicate the position of three genetic loci that genetically interact with the SCA5 transgenes.

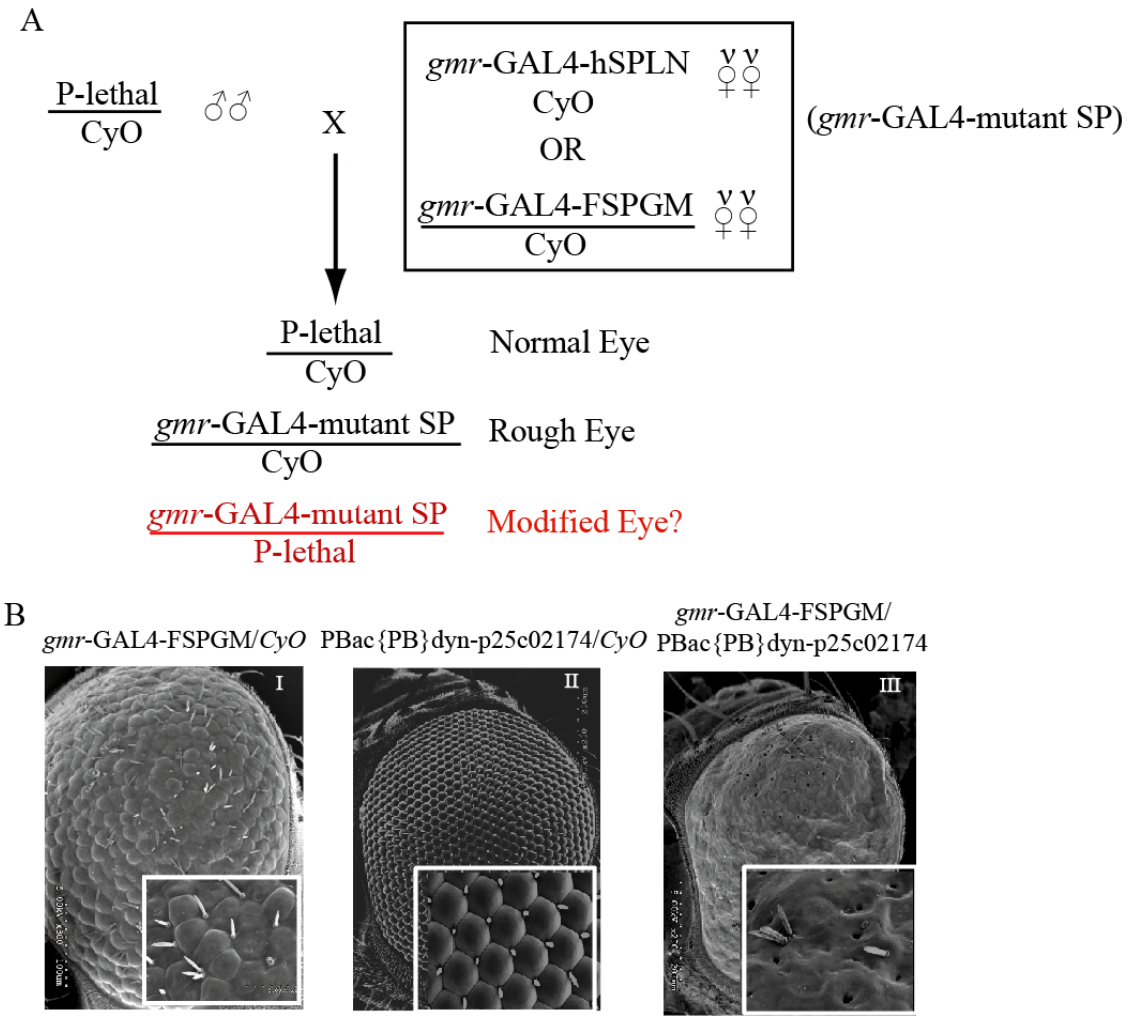

Figure 23. P-element screen identifies modifiers of SCA5-neurodegenerative eye phenotype. (A) Breeding strategy used to screen for genetic interactors. Progeny bearing both a lethal P-element insertion and a mutant spectrin recombinant chromosome (red) are score for changes in the eye phenotype when compared to their siblings of different genotypes. (B) Example of genetic interactor identified in the screen. Flies bearing a lethal P-element insertion in the *dyn-25* gene have a wild-type eye (II), but in combination with the *gmr*-GAL4-FSPGM mutant spectrin allele (I) produce a more severe eye phenotype than either parent (III).

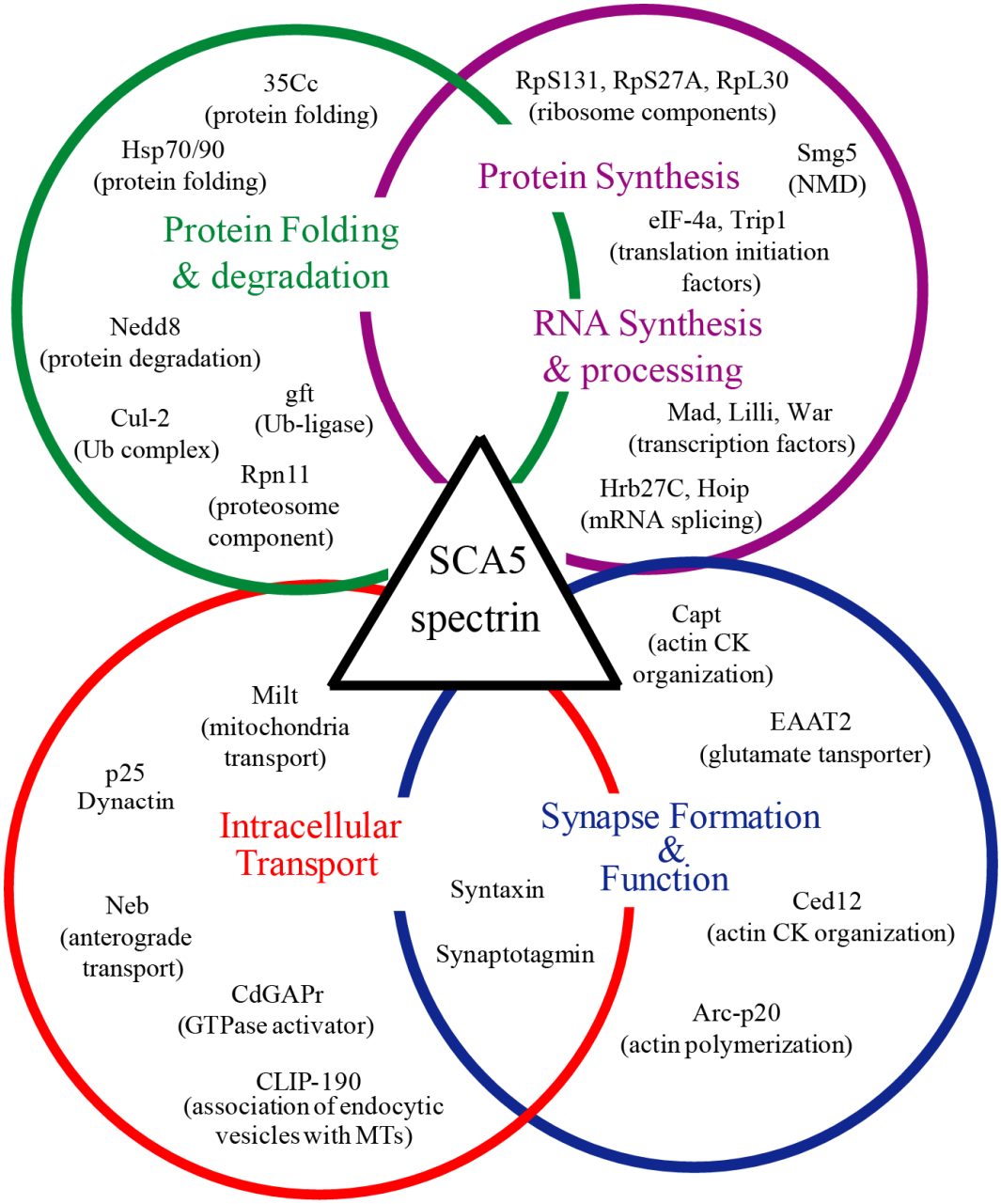

Figure 24. Major categories of modifiers of SCA5-associated neurodegeneration based on functional activities. Examples of genetic interactors identified in the screen are given for each functional class.

Deficiency stock	Deleted segment	Enhancer/ Suppressor	Cross to *gmr*-GAL4-hSPLN	Cross to *gmr*-GAL4-FSPGM
Df(3L)W10	75A6-7;75C1-2	E	+	+
Df(3L)st-f13	72C1--73A4	E	++	++
Df(3R)T-32	86E2-4;87C6-7	E	N	++
Df(3R)Dl-BX12	91F1--92D6	E	+	N
Df(3R)e-R1	93B6--93D4	E	++	++
Df(3L)HR119	63C6--63F7	E	+	N
Df(3L)XDI98	65A2--65E1	E	++	N
Df(3L)HD1	79D3--79F6	E	N	+
Df(3R)Exel6196	95C12--95D8	S	+	N
Df(3R)Exel6202	96D1--96E2	E	++	+

Table 8. Third chromosome deficiencies modify the SCA5 eye phenotype. List of deficiencies isolated as modifiers of the SCA5 rough eye phenotype. Deficiencies are classified as enhancers (E) or suppressors (S). Genetic interactions with either the *gmr*-GAL4-hSPLN or *gmr*-GAL4-FSPGM mutant recombinant chromosomes are listed as none (N), slight interaction (+), or strong interaction (++).

Modifier deficiency from primary screen	Overlapping deficiency	Deleted segment	Modifier effect
Df(3R)T-32 (86E2-4;87C6-7) E++	*Df(3R)ED5516*	86D8--86E13	E++
	Df(3R)ED5559	86E11--87B11	E++
	Df(3R)ry85	87B15--88A1	N
Df(3L)HR119 63C6--63F7 E+	*Df(3L)ED208*	63C1--63F5	N
	Df(3L)GN50	63E2--64B17	N
Df(3L)XDI98 65A2--65E1 E++	*Df(3L)Exel7210*	65A1--65A5	N
	Df(3L)Exel8101/	65A3--65A9	N
Df(3L)st-f13 (72C1--73A4) E++	*Df(3L)ED4606*	72D4--73C4	N
Df(3L)HD1 (79D3--79F6) E+	*Df(3L)ED230*	79C2--80A4	N

Table 9. Secondary screen defines a third chromosome region that modifies the SCA5-associated neurodegenerative eye phenotype. List of overlapping deficiencies used in a secondary screen to define third chromosome regions containing putative modifiers of the SCA5 rough eye phenotype. Genetic interactions with mutant spectrin recombinant chromosomes are listed as none (N), slight enhancement (E+), or strong enhancement (E++).

Class	Gene symbol	Alleles Tested	Human Orthologue	GO term
Class 1: Intracellular Transport	*Neb*	neb^{k05702}	*KIF14*	Plus-end-directed microtubule (MT) motor activity; ATP binding
	dyn-p25	dyn-p25^{c02174}	*DCTN5*	MT-based movement; dynactin complex
	Mhc	Mhc^{k10423}	*MYHC* genes	ATP binding; motor activity;
	Milt	milt^{k04704} milt^{EY14443}	*TRACK1*	Kinesin-associated mitochondrial adaptor activity; axonal transport of mitochondria
	Drp1	Drp1^{KG03815}	*DNML1N*	GTPase activity; intracellular distribution of mitochondria
Class 1/2: Intracellular Transport & Synapse Function	*CLIP-190*	CLIP-190^{KG06490}	*CLIP-170*	Actin binding; endocytic vesicles-MTs association
	Jup	Jupiter^{DG10706}	Unknown	Component of MT cytoskeleton
	Syx5	Syx5^{EP2313} Syx5^{EY07901}	*STX5*	Neurotransmitter secretion; synaptic vesicle-mediated transport and docking
	Syt1	Syt1^{T77}	*SYT-1*	Synaptogenesis; synaptic vesicle transport and endocytosis
Class 2: Synapse Formation & Function	*Capt*	capt^{k01217} capt^{f00786}	*CAP2*	actin filament organization; cytoskeleton organization
	Arc-p20	Arc-p20^{e00819}	*ARPC4*	cortical actin cytoskeleton organization; actin polymerization
	Ced-12	Ced-12^{c06760}	*ELMO1*	Actin filament organization
	wb	wb^{09437}	*LAMA2*	Actin binding, receptor binding, cell adhesion
	Pgk	Pgk^{KG06443}	Unknown	Synaptic transmission, energy production
	Eaat2	Eaat2^{e03003}	*EAAT2*	Aspartate/Glutamate transporter
	AcRα-34E	nAcRα-34E^{f00872}	*CHRNA7*	Neurotransmitter receptor activity
	CG32447	CG32447^{KG04533}	Unknown	Metabotropic glutamate receptor signaling pathway
Class 3: Protein Folding & Degradation	*Hop*	Hop^{k00616}	*TIP1*	Protein folding
	l(2)35Cc	l(2)35Cc^{KG01622}	Unknown	Protein folding
	Cul-2	cul-2^{02074}	*CUL2*	Ub-dependent protein degradation
	Rpn11	Rpn11^{f00386}	*PAD1*	Proteasome constituent
	Nedd8	KG03071	*NEDD8*	Ub-dependent protein degradation;
	gft	gft^{EY11031} gft^{06430}	*CUL3*	Ub-dependent protein degradation; axon and dendrite morphogenesis

Table 10-I. Activities of genetic modifiers of SCA5 neurodegeneration

Class	Gene symbol	Alleles Tested	Human Orthologue	GO term
Class 4: Protein synthesis	*Smg5*	Smg5^{e04233}	*SMG5*	mRNA nonsense- mediated decay
	eIF-4a	eIF-4a^{k07519}	*EIF4A2*	Translation initiation factor activity
	RpS13	RpS13^{k09614}	*RPS13*	Structural constituent of ribosome
	RpS27A	RpS27A^{04820}	*CEP80*	Structural constituent of ribosome
	Rpl30	RpL30^{k00308} RpL30^{k09918} CG31793^{DG05508}	Unknown	Structural constituent of ribosome
	Trip1	Trip1^{KG06360}	*TRIP-1*	Translation initiation factor activity
	Ef2b	Ef2b^{f07154}	*EEF-2*	Translation elongation factor activity
	At-Thr	Aats-thr^{k04203}	*TARS*	Threonine-tRNA ligase activity
	Brat	brat^{k06028}	Unknown	Translation regulator activity
Class 5: RNA synthesis & processing	*Hoip*	hoip^{k07104}	*NHP2L1*	Nuclear mRNA splicing
	Hrb27C	Hrb27C^{k02814} Hrb27C^{EY12571}	*DAZAP1*	Nuclear mRNA splicing,
	Lilli	lilli^{k05431} lilli^{00632}	FMR2P	Transcription factor (TF) activity
	War	BG00946	Unknown	TF activity; brain development, dendrite morphogenesis
	Trf	Trf^{1}	Unknown	TF activity
	Chinmo	chinmo^{k13009}	Unknown	Dendrite morphogenesis, CNS development
	Kis	kis^{k10237} kis^{k13416}	Unknown	ATP-dependent helicase activity
	Kr-h1	Kr-h1^{k04411} Kr-h1^{KG00354}	Unknown	Zinc finger TF
	Mad	Mad^{KG00581} Mad^{k00237}	*SMAD1*	TF activity; TGF-beta receptor signaling pathway
	Crp	crp^{KG08234} crp^{k00809}	TFAP4	TF activity
	Df31	Df31^{k05815}	Unknown	histone binding, regulation of transcription
	Zf30c	zf30C^{k02506}	Unknown	Zinc finger TF; neuron development
	Lid	lid^{k06801} lid^{10424}	*JARID1A*	histone acetyltransferase activity ; zinc finger TF
	Hr39	Hr39^{Scim}	*Unknown*	Nuclear hormone receptor; TF activity
	Tai	tai^{k05809}	*NCOA2*	Ligand-dependent nuclear receptor transcription coactivator activity

Table 10-II. Activities of genetic modifiers of SCA5 neurodegeneration (cont.)

Class	Gene symbol	Alleles Tested	Human Orthologue	GO term
Class 5: RNA synthesis & processing (cont)	*esg*	esg^{k00606}	*SNAI2*	Zinc finger TF; CNS development
	Su(H)	$Su(H)^{M28}$ $Su(H)^{k07904}$	*RBP-J*	TF activity; Notch signaling
	net	net^{f04249}	*ATOH8*	TF activity
	crol	$crol^{k05205}$ $crol^{04418}$ $crol^{11}$	*ZNF84*	TF activity
	gcm	$gcm^{KG01117}$	*GCM2*	TF activity; glial cell and dendrite morphogenesis
	bun	bun^{00255}	Unknown	TF activity
	Salm	$salm^{03602}$	*SALL3*	Zinc finger TF
	Hand	$Hand^{f03901}$	*HAND2*	TF activity
	Tup	tup^{d03613}	*ISL-1*	Zinc finger TF
Class 6: Miscelaneous Functions	*Acon*	$Acon^{k07708}$	*ACO2*	Tricarboxylic acid cycle
	Nhe2	$Nhe2^{KG03334}$	*SLC9A3*	sodium-hydrogen antiporter
	Eno	Eno^{e01615} Eno^{f07543}	*ENO1*	Glycolisis
	cype	$cype^{e03803}$	*COX6C*	Cytochrome-c oxidase activity
	CdGAPr	$CdGAPr^{A248}$ $CdGAPr^{EY09626}$	*SNX26*	GTPase activator activity
	FKBP59	$FKBP59^{k00424}$	*FKBP4*	PNS development; calcium ion transport
	Cyclin E	$CycE^{05206}$	*CCNE 1*	Cell cycle regulation
	Akap200	$Akap200^{k07118a}$	Unknown	Protein kinase A binding
	VhaSFD	$VhaSFD^{G00259}$	*ATP6V1H*	Vacuolar proton-transporting V-type ATPase
	dock	$dock^{k13421}$ $dock^{04723}$	*NCK1*	SH3/SH2 adaptor activity; axonal morphogenesis
	Scim 13	$Scim13^{1}$	Unknown	Female meiosis chromosome segregation
	Scim15	$Scim15^{1}$	Unknown	Female meiosis chromosome segregation
	Dpp	$dpp^{KG04600}$	*BMP2*	TGF beta receptor binding
	oaf	$oaf^{KG03408}$ oaf^{Scim-a}	*OAF*	Female meiosis chromosome segregation
	ex	ex^{k12913}	*FRMD6*	Endocytic recycling
	CG8885	$CG8885^{EY05333}$	*SCO1*	Respiratory chain component
	Glu	glu^{k08819}	*SMC4*	Chromosome segregation

Table 10-III. Activities of genetic modifiers of SCA5 neurodegeneration (cont.)

Class	Gene symbol	Alleles	Human Orthologue	GO term
1	*Eaat2*	$Eaat2^{e03003}$	*EAAT2*	Aspartate/Glutamate transporter
2	*Capt*	$capt^{k01217}$ $capt^{f00786}$	*CAP2*	actin filament organization; cytoskeleton organization
3	*Hop*	Hop^{k00616}	*TIP1*	Protein folding
4	*RpS27A*	$RpS27A^{04820}$	*CEP80*	Structural constituent of ribosome
5	*Hrb27C*	$Hrb27C^{EY12571}$	*DAZAP1*	Regulation of nuclear mRNA splicing
5	*Kis*	kis^{k13416}	Unknown	ATP-dependent helicase activity; chromatin binding
5	*Hr39*	$Hr39^{Scim}$	Unknown	Nuclear hormone receptor

Table 11. Lethal phase analysis of SCA5 genetic interactors. List of genetic interactors for which homozygous P-element insertion alleles survive until or past third instar larvae stages.

CHAPTER 5

CONCLUSIONS AND FUTURE DIRECTIONS

SCA5, a slowly progressive neurodegenerative disorder that results in Purkinje cell loss and cerebellar degeneration, is caused by mutations in the cytoskeletal protein β-III spectrin. Although the molecular mechanisms by which mutant spectrin causes cerebellar dysfunction are still unclear, recent studies suggest that at least two different but not mutually exclusive pathways are likely to contribute to disease. First, β-III spectrin is a scaffolding molecule required for the proper localization of a number of perisynaptic proteins on Purkinje cell dendrites including EAAT4, mGluR1α, and mGluRδ2 (Ikeda *et al*., 2006; Armbrust *et al*., in preparation). Furthermore, proper stabilization of EAAT4 by B-III spectrin is required for glutamate uptake (Jackson *et a*l., 2001). By interfering with the function of the wild-type protein, SCA5 mutant spectrin may deregulate glutamate signaling in the cerebellum and cause Purkinje cell death. It is also possible that mutant spectrin alters the membrane localization and/or stability of other synaptic components and thus causes Purkinje cell synaptic dysfunction. Second, β-III spectrin directly interacts with dynactin and is thought to participate in the intracellular transport of cargos mediated by dynein and dynactin.

I have established the first transgenic *Drosophila* models of SCA5 and provide genetic and functional evidence that mutant spectrin disrupts the axonal transport of synaptic vesicles. Moreover, I have shown that SCA5 mutant flies have severe defects in synapse formation. Taken together, these results suggest a potential mechanism that may contribute to disease: failure in the interaction between β-III spectrin and dynactin can

impair the transport of synaptic components and signaling molecules that are required to build and maintain the synapse.

Mutant β-III spectrin may also affect the organization of the underlying microtubule and actin networks that stabilizes synaptic membranes (Pielage *et al*., 2005). Future analysis of the integrity and stability of the actin and MT cytoskeleton at the synapses in a SCA5 mutant background can be conducted to directly test this prediction. Moreover, it will be important to evaluate the neuronal phenotypes produced as the result of the interaction of mutant spectrin with components of the microtubule cytoskeleton and actin-associated proteins identified in the modifier screen.

The accumulation of intracellular cargo in axonal aggregates seen in flies expressing the American and German SCA5 mutations may contribute to the slowly progressive neurodegenerative effects of SCA5. In support of this proposal, the genetic screen I conducted identified various components of the protein folding and degradation pathways as modifiers of SCA5 neurodegeneration. It will be interesting to investigate the molecular downstream effects that overexpressing molecular chaperones have on the phenotypes of fly and murine models of SCA5.

B-III spectrin is expressed in both axons and dendrites of Purkinje cells and severe degeneration of Purkinje cells dendritic arbors have been observed in SCA5 autopsy cerebellum (Ikeda *et al*., 2006). In addition to their role in axonal transport, dynactin, dynein, and kinesin are all required to localize specific cargo to neuronal dendrites and to ensure proper dendrite development and maintenance (Yang *et al*., 2008; Zheng *et al*., 2008; Satoh *et al*., 2008). It will be important to investigate the effects of the SCA5 mutations on dendritic morphology and dendritic transport. Such studies will not only

compare the role of β-III spectrin in axonal versus dendritic functions and the mechanisms of cargo-motor protein specificity, but will also allow a better understanding of the contribution of intracellular transport deficits to SCA5 pathogenesis.

The identification of a group of novel mutation in *SPTBN2* in ataxia patients described in this work expands the spectrum of mutations likely to cause SCA5. It is imperative to determine the impact of the mutations on protein function to clarify their role in disease. For the initial functional characterization of the mutations a panel of bioassays, with simple and reliable readouts should be implemented. For example, novel mutations would be evaluated for their effect on the intracellular localization of β-III spectrin and the stability of EAAT4 at the plasma membrane using cell culture studies. In addition, a panel of assays for yeast developed by Dr. Karen Armbrust would also be used to assess whether these mutations change the strength of the interaction between β-III spectrin and known binding partners including α-spectrin and the dynactin subunit $p150^{Glued}$. This strategy will provide a more complete functional characterization of these variants and help determine whether their downstream effects converge into similar pathways. Putative mutations that are confirmed to be pathogenic can be further characterized through the establishment of murine and fly models.

Future efforts should be additionally focused on understanding the specific mechanisms by which each of the described SCA5 mutations cause cerebellar degeneration and ataxia. The studies I conducted in flies suggest that the American and German SCA5 mutations affect intracellular transport. Moreover, the genetic screen identified interactors implicated in similar pathways as modifier of the eye phenotype produced by expression of either the American or the German mutant proteins. While

preliminary results indicate that the French SCA5 mutation increases the strength of interaction between spectrin and actin (Armbrust *et al*., in preparation) additional studies, including the development of transgenic flies expressing the French SCA5 transgene, will allow further exploration of the mechanisms of pathogenicity, and will ultimately lead to a better understanding of the disease process.

CHAPTER 6

MATERIALS AND METHODS

I. Identification of novel SCA5 mutations

A. Control individuals and patients with SCAs

This clinical and genetic study was approved by the review boards of all implicated institutions and informed consent was obtained from all participating individuals.

Probands representing 318 autosomal dominant ataxia families collected in France and the United States were screened for mutations in *SPTBN2*. The largest group of patients (n = 263), 86% of French ancestry, were recruited by the Department of Genetics of Hôpital de la Salpêtrière, Paris, France. The diagnosis of SCA was determined clinically by an experienced neurologist using the Harding criteria (Hardin, 1982). All patients had been previously excluded as carriers of the SCA1, SCA2, SCA3, SCA6, SCA7, SCA17, or the Dentatorubral-Pallidoluysian atrophy (DRPLA) mutations.

The second cohort of patients screened (n=55), 62% of Caucasian origin, were recruited at the University of Minnesota, Minneapolis, US. Within this group, all probands had tested negative for the expansion mutations in the SCA1, SCA2, SCA3, SCA6, SCA7, SCA8, SCA10, SCA12, and DRPLA genes and similarly did not have mutations in the coding region of the *PRKCG* gene responsible for SCA14.

Additionally, a large group of DNA samples (n= 6,269) sent to Athena Diagnostics for ataxia testing was screened. These samples had tested negative for mutations known to cause the POLG1, AOA1, AOA2, DRPLA, FRDA, SCA1, 2, 3, 6, 7, 8, 10, 14, and 17 forms of ataxia.

To establish that mutations identified in this study were not common polymorphisms, we screened DNA representing 1,600 control chromosomes for each of the mutations detected. Unrelated control DNA samples were obtained from the Centre d'Etude du Polymorphisme Humain (CEPH) panel and from healthy North Americans (*n*= 500) as well as from an ethnically matched group of unrelated French individuals (*n*= 300).

B. DNA extraction

Genomic DNA was extracted from peripheral blood lymphocytes using the Puregene DNA Isolation Kit (Gentra Systems, Minneapolis, MN) according to the manufacturer's protocol.

C. Mutational analysis of the *SPTBN2* gene in ataxia families and controls

Genomic DNA was used to amplify and screen the thirty seven exons of *SPTBN2* using PCR coupled to single strand conformation polymorphism (SSCP) analysis. To maximize the sensitivity of the screen, primers within introns were designed to amplify both the exons and at least 50 bp of intron sequence flanking each of the exons to screen for both coding and potential intronic mutations that may affect splicing. Since the SSCP procedure is more sensitive for small DNA fragments (less than 350 bp), various sets of DNA primers were used to amplify overlapping PCR fragments covering large exons with a total of 43 primer pairs used to screen the entire gene. Amplification products radiolabeled during PCR with γ-^{33}P were denatured at 95°C in the SSCP stop solution (95% formamide, 10 mM NaOH, bromophenol blue, and xylene cyanol), snap cooled on ice, and run on nondenaturing mutation detection enhancement (MDE) gels (Lonza,

Basel, Switzerland) at 4-6 watts constant power for 14 hours at room temperature. SSCP alleles were visualized by autoradiography. All individuals with PCR fragments showing unusual band migration on the SSCP gels were identified and the corresponding PCR fragments re-amplified and sequenced using forward and reverse primers on an ABI3730XL automated sequencer (Applied Biosystems, Foster City, CA). Primers and conditions used for PCR and sequencing are reported in Table 12. Sequences were compared for similarity with the *SPTBN2* genomic sequence available in the non redundant GenBank (http://www.ncbi.nlm.nih.gov/Genbank) database at the NCBI using the BLASTN program (http://www.ncbi.nlm.nih.gov/blast). Identified mutations were validated by repeat sequencing and further characterized by screening 1,600 unrelated control chromosomes and by analysis of segregation within the family, when DNA from other family members was available.

D. Bioinformatic Analysis

Protein sequence alignments were performed using the Clustal W program (http://www.ebi.ac.uk/clustalw).

II. Establishment and molecular characterization of transgenic SCA5 model in *Drosophila*

A. Fly stocks and genetic analyses

Flies were cultured at 25ºC in a 12 hour light/dark cycle on standard medium. Fly stocks were obtained from the Bloomington *Drosophila* Stock Center unless indicated and are listed in FlyBase (http://www.flybase.org).

To analyze *transgene* expression in the eye, *homozygous* virgins for each genotype were crossed to *gmr*-GAL4/*CyO* males. Progeny lacking curly wings were examined. Neuronal expression was driven with *elav-GAL4*. Briefly, *elav*-GAL4/Y males were mated to homozygous virgins for each genotype. Female larvae were selected for further analysis.

To generate transgenic flies expressing synaptotagmin-GFP (syt-GFP) in all neurons or neuronal synaptobrevin-GFP (n-syb-GFP) in motor neurons, homozygous virgins carrying wild-type or mutant spectrin transgenes were crossed to either *elav*-GAL4-syt-GFP/Y (Gepner et al., 1996)or *D42*-GAL4-n-syb-GFP/TM6B, Tb males. GFP-positive larvae were selected for analyses.

To analyze genetic interaction of spectrin mutations with $DHC64C^{6\text{-}10}$ (Gepner *et al*, 1996) and Gl^{1} (Harte and Kankel, 1982) mutants in the eye, standard meiotic recombination was used to generate second chromosomes carrying both the eye specific *gmr-GAL4* driver and either the hSPLN or the FSPGM transgenes. Recombinant chromosomes were maintained over a balancer chromosome carrying the dominant maker *Curly* (*CyO*). Virgin females from *gmr*-GAL4-hSPLN/*CyO* or *gmr*-GAL4-FSPGM/*CyO* lines were mated to $Dhc64C^{6\text{-}10}$/TM6B, D or $Gl^{1}Sb$/LVM males. Progeny carrying the recombinant chromosomes in either the Gl^{1} or $DHC64C^{6\text{-}10}$ mutant backgrounds were identified by the absence of the dominant curly wing phenotype; the Gl^{1} mutation was identified by the bristle phenotype caused by the dominant *Sb* mutation, whereas adult flies carrying the $DHC64C^{6\text{-}10}$ mutation lacked the curly and *Dichaeted* wing phenotypes.

To generate larvae expressing the American SCA5 mutation in all neurons in a

dynein or dynactin mutant background, homozygous virgin females (hSPLN/hSPLN) were crossed to *elav*-GAL4-syn-GFP/Y; *Dhc64C*$^{6-10}$*/TM6B, Tb* or *elav*-GAL4-syn-GFP/Y; *Gl*^{1}*Sb*/*TM6B*, Tb males. Third instar larvae that carries GFP and lacks the *Tubby* (*Tb*) marker were selected for analysis.

B. Generation of the UASp–*SPTBN2* and UAST-β-Spec transgenic flies

To express human β-III spectrin in *Drosophila*, full-length wild-type and mutant (American SCA5 mutation) 5'-*myc*-β-III spectrin cDNA clones (Ikeda *et al*., 2006) were digested KpnI and XbaI and ligated into the *Drosophila* transformation vector pUASp (Rorth, 1998). For generating the German SCA5 transgene, the L253P mutation was introduced into the wild-type 5'*myc*-tagged β-III spectrin construct (Ikeda *et al*., 2006) using the QuikChange II XL Site-Directed Mutagenesis Kit (Stratagene, La Jolla, CA) and primers German Mut F (5'-GGG ACT TAC CAA GCC GCT GGA TCC CGA AGA C-3') and German Mut R (5'-GTC TTC GGG ATC CAG CGG CTT GGT AAG TCC C-3'). The resulting product was cloned into pUASp as described above. Generated UASp constructs are referred here as hSPWT, hSPLN, and hSPGM respectively.

The construct designed to overexpress wild-type fly β-spectrin (FSPWT) was created by generating separate PCR products. Briefly, a partial cDNA clone (AT24411, *Drosophila* Genomics Resource Center Indiana University, Bloomington, IN; http://dgrc.cgb.indiana.edu/), containing the 5' region of the fly β-spectrin mRNA was used to amplify a KpnI-BamHI PCR fragment using primers Fly ForwKpnI (5'-GAC GGT ACC GCC AAG TGA AGT TCA TCC-3') and Fly RevBamHI (5'-CGT ACT CAT CGA TGT ACT CGT TGC C-3'). The remained 3'cDNA sequence was cloned using the

SuperScript™ III One step RT-PCR system with Platinum® Taq high fidelity (Invitrogen, Carlsbad, CA), total RNA from fly embryos, and the gene specific primers Fly ForBamHI (5'-CAG CCA TGA CGA CGG ACA TTT CG-3') and Fly RevXbaI (5'-AGT CTA GAG CTC TTG CTT ATG GTT GCG-3'). Both PCR products were then subcloned using subsequent KpnI-BamHI and BamHI-XbaI digestions into the corresponding cloning sites of pBluescript SK^+ (Stratagene, La Jolla, CA) to generate the pBluescript SK^+/β-Spec WT clone.

The American SCA5 mutant clone (FSPLN) was generated by a PCR approach using primers Fly American-Δ39bp BglII For (5'-CGT ATA TAA GAT CTC GTT GGA CAA CAT GGA GGA GAT C-3') and Fly American-Δ39bp BsrGI Rev For (5'-ACA TCA GCT TGT ACA GGC TGA GGG CGT-3'). The resulting PCR product, which deleted a 39 bp fragment in the region of homology with the deletion mutation found in the American SCA5 family (Supplemental figure S1BI), was subcloned BglII-BsrGI into the pBluescript SK+/β-Spec WT clone. Both wild-type and the American SCA5 mutant full-length cDNAs were then cloned KpnI-XbaI into the *Drosophila* transformation vector $pUAS_T$ (Brand and Perrimon, 1993).

The German SCA5 mutant clone (FSPGM) was generated by introducing the L253P mutation into the FSPWT clone using the QuikChange II XL Site-Directed Mutagenesis Kit (Stratagene, La Jolla, CA) and primers Fly German Mut For (5'-CCT GGC CAA GCC CCT TGA TGC CGA G-3') and Fly German Mut Rev (5'-GTC TTC GGG ATC CAG CGG CTT GGT AAG TCC C-3').

The integrity of each construct was verified by sequencing. Transgenic flies were generated by standard P-element-mediated germline transformation. Multiple lines of

flies with independent transgene insertion were established for each genotype.

C. Preparation of protein extracts

Adult flies for each genotype in study were frozen in liquid nitrogen before collecting and homogenizing heads in radio immunoprecipitation assay lysis buffer (RIPA, 1X PBS, 1% Nonidet P-40, 0.5% sodium deoxycholate, 0.1% SDS) supplemented with Complete Protease Inhibitor Cocktail Tablets (Roche Applied Sciences, Indianapolis, IN). Protein supernatant was collected after centrifugation at 14,000 rpm for 30 minutes at 4ºC and used for immunoprecipitation and western blot analyses.

D. Western blot analysis

Total proteins from fly heads were separated on 4-12% gradient NuPAGE® gels (Invitrogen, Carlsbad, CA). After electrophoresis, gels were electroblotted overnight onto nitrocellulose membranes and incubated with β-III spectrin (1:250, Santa Cruz Biotechnology, Santa Cruz, CA), tubulin (1:5,000, Sigma, St. Louis, MO), or myc (1:2,000, clone 9E10, Sigma) antibodies. Rabbit polyclonal anti-*Drosophila* β-spectrin antibody (kind gift from D. Branton) was used at a 1:5,000 dilution. Immunoreactive bands were visualized using horseradish peroxidase-conjugated secondary antibodies at 1:5,000 dilutions and the ECL™ western blotting detection system (GE Heathcare, Chalfont St. Giles, UK). The Image J analysis software (National Institutes of Health, Bethesda, MD; http://rsb.info.nih.gov/ij) was used to compare protein expression

E. Immunoprecipitation

Protein extracts from fly heads were pre-cleared by addition of 100 µl of a 1:1 Protein A-Sepharose suspension (GE Healthcare, Chalfont St. Giles, UK). Following incubation on a rotator at 4°C for 2 hours this mix was centrifuged for 5 minute at 5,000 rpm. Supernatant aliquots containing 400 µg of total proteins were subsequently used in immunoprecipitation experiments. In parallel, 40 µl of Protein A Sepharose beads were equilibrated in RIPA buffer supplemented with protease inhibitors and further incubated with either 10 µg of mouse anti- *Drosophila* α-spectrin antibody (clone 3A9, Developmental Studies Hybridoma Bank at University of Iowa) or 50 mg/ml of BSA during 1 hour at 4ºC. The antibody-bead complexes were washed free of unbound antibody and incubated with pre-cleared protein lysates overnight at 4ºC. The Protein A-Sepharose beads were then collected by centrifugation for 2 minutes at 2,500 rpm at 4°C and washed five times with ice cold RIPA buffer. Bound proteins were eluted with 2X SDS sample buffer and subjected to SDS-PAGE and Western blot analysis.

F. Scanning Electron and Optical Microscopy of fly eyes

For scanning electron microscopy (SEM) images, fly heads were dehydrated in 100% ethanol, incubated in hexamethyldisilazane (Sigma, St. Louis, MO), dried overnight under vacuum, and coated with gold-palladium. Images were taken with a Hitachi S-3500N variable pressure scanning electron microscope. For optical images, adult flies eyes were photographed with a Nikon digital camera attached to a Zeiss stereoscope.

G. Eye Histology

For histological analysis of eyes, heads from 10 day old flies were fixed for 30 min in a 2% glutaraldehyde/2% osmium tetroxide mix, washed in PBS, fixed for an additional 3 hours in 2% osmium tetroxide, and dehydrated through a graded ethanol series. Heads were further equilibrated in propylene oxide and embedded in Durcupan ACM resin (Electron Microscopy Science, Hatfield, PA). Vertical semi-thin sections were stained with toluidene blue and photographed with a Leica AS/LMD microscope.

H. Larval motility

The behaviors of larvae were compared under a Zeiss stereoscope. Videos of animals expressing mutant and wild-type β-spectrin transgenes were made using a Nikon camcorder.

I. Immunohistochemistry

For immunostaining of segmental nerves, wandering third instar larvae were dissected in 1X PBS and fixed in 4% formaldehyde for 20 minutes as described before (Hurd and Saxton, 1996). Larval fillets were washed three times in PBT (1X PBS, 0.1% TritonX-100) and for one hour in PBT containing 1% BSA (PBT-BSA) before overnight incubation with primary antibodies at 4ºC. Primary antibodies used were mouse anti-CSP (6D6, 1:250, Developmental Studies Hybridoma Bank at University of Iowa) and mouse anti-dynein heavy chain antibody (P1H4, 1:250, McGrail and Hays, 1997). Alexa-555 and Alexa-488 conjugated secondary antibodies (Molecular Probes, Eugene, OR) were

used at final concentrations of 1:200 at room temperature for two hours. Larval preparations were washed in PBT-BSA and mounted in Vectashield (Vector, Burlingame, CA).

To examine synaptic morphology, third instar larvae was processed and stained as described above but the ventral ganglia, brain, and segmental nerves were removed to facilitate NMJ visualization. Synaptic boutons were detected by anti-CSP staining and muscle surface delimited by Alexa-488 phalloidin (Molecular Probes, Eugene, OR) staining.

Images of neuromuscular preparation were acquired using a Nikon Eclipse TE200 inverted microscope equipped with the PerkinElmer Confocal Imaging System (PerkinElmer Inc, Waltham, MA) and Hamamatsu's Orca-ER digital camera. Synapses morphology and axonal staining were imaged using 2x2 binning with a 40x planapo (NA 1.3) and a 100x planapo (NA 1.4) objective, respectively and 1μm optical sections. Images were processed in Adobe Photoshop CS3 (Adobe Systems Inc., San Jose, CA).

J. Live imaging of GFP-tagged vesicles in larval segmental axons

Motility analyses were done on neuromuscular preparations by live confocal fluorescence microscopy. Briefly, wandering third instar larvae were dissected in Haemolymph-like solution (HL3) (Yanfei *et al*., 2004) carefully removing gut and fat body to expose segmental nerves. GFP-vesicles were imaged with a Nikon Eclipse TE200 inverted microscope equipped with the PerkinElmer confocal imaging system. Images were acquired continuously at a rate of one frame every 1 second for 300 seconds

with 2x2 binning and a 100× oil planapo (NA 1.4) objective.

K. Statistical Analyses

To quantitatively analyzed synaptogenesis, the NMJ at muscles 6 and 7 of abdominal segments 2 and 3 were examined to determine the number of synaptic boutons and muscle size. The relative synapse size was calculated as the total number of synaptic boutons divided by the corresponding muscle surface area. This relative synaptic terminal size was then averaged for each genotype and normalized as a percent of the control driver numbers.

Analysis of syt-GFP accumulations within larval segmental nerves was carried out as follows. Four segmental nerves were selected from the region immediately posterior to the ventral ganglion and GFP accumulations with a diameter of at least 0.7 µm were counted along a 50 µm axonal segment, using the “analyze particle” function of the MetaMorph image analysis software (Molecular Devices, Sunnyvale, CA). In the analyses, each genotype is represented by five larval preparations.

The movement of GFP-tagged synaptic vesicles was manually tracked with MetaMorph’s "track points" function as described before (Mische *et al*., 2007). To define the direction of organelle movement, segmental nerves were oriented with the motor neurons cell bodies toward the left. Vesicle displacements towards the right were considered anterograde or plus-end runs while right to left motion were designated retrograde or minus-end runs. Particles displaying linear movement for four consecutive frames were selected for analysis. Data from GFP-particles tracking were used to calculate net velocity, mean run velocity, run-length, and standard deviation for each

particle using Microsoft Xcel. Net velocity was determined when directionality of motion could not be determined by summing all velocities displayed for one individual particle over the entire movie interval, including forward runs (positive), reverse runs (negative), and pauses. The trajectory of GFP-tagged synaptic vesicles along a portion of the segmental axon was graphed using the "kymograph" function of MetaMorph.

Statistical significance of the difference between mutant and wild-type was determined for each experiment using the Student's t-test on unpaired data. Significance was established when $P < 0.05$.

III. Modifier screen SCA5 model in *Drosophila*

A. Fly stocks

The deficiency and P-element-insertion stocks used in this study were obtained from the Bloomington Drosophila Stock Center at Indiana University (Bloomington, IN) and are listed in FlyBase (http://www.flybase.org). All genetic experiments were conducted at a constant temperature of 25°C.

B. Modifier Screens

A collection of approximately 120 third chromosome deficiencies and 800 second chromosome P-element insertion lines was screened for modifiers of SCA5-neurodegenerative eye phenotype. For the primary screen, male flies from the deficiency or P-element collections were crossed to *gmr*-GAL4-hSPLN/*CyO* and *gmr*-GAL4-FSPGM/*CyO* virgin females. Progeny carrying mutant spectrin transgene and deficiency

(*gmr*-GAL4-hSPLN/+; Df/+ or *gmr*-GAL4-FSPGM/+; Df/+) or mutant spectrin transgene and P-element (*gmr*-GAL4-hSPLN/P-element or *gmr*-GAL4-FSPGM/P-element) were examined under a dissecting microscope for enhancement or suppression of the rough eye phenotype.

C. P-element excision

Lethal P-element insertions were mobilized by using a Δ2-3 transposase source. In brief, male flies from P-element stocks that showed genetic interaction with mutant spectrin transgenes were crossed to females with the *Sco/CyO,H{w+mC=PΔ2-3}Hop2* transposase chromosome. F1 male progeny of the *CyO,P{w+mC=PΔ2-3}Hop2/P*-element genotype were then crossed to w; Sp/*CyO* females and F2 progeny in which the P-element had been excised were identified by their white eye color. Five independent precise excision males for each line analyzed were crossed to females carrying mutant spectrin recombinant chromosomes (*gmr*-GAL4-hSPLN/*CyO* or *gmr*-GAL4-FSPGM/*CyO*) females to test for modification of the eye phenotype.

D. Lethal phase analysis

Larval lethality was determined by crossing female flies from lethal P-element stocks that showed genetic interaction with mutant spectrin transgenes to a reciprocal translocation chromosome (*FM6, TM6B Tb*) that facilitates the detection of homozygous mutant larvae. Larval progeny lacking the Tb marker were closely monitored during five days to determine whether they survive larval development or the exact phase of larval lethality.

Exon	Forward Primer (5'→3')	Reverse Primer (5'→3')	Ta (°C)	$MgCl_2$ (mM)	Product Size (bp)
exon 1	ctgccttcctgcttcacttt	agggaccaccaagccctcca	57	1	194
exon 2	tcactggccacattctcctt	tcatgacgagctgacaaagc	57	1	283
exon 3	ccctgccaactggtgtttag	ggtccccttggacacttttc	54	1	282
exon 4	agtcccgtgccattttgc	cagggcaggaaccacacc	57	1	250
exon 5	acaccaggagttcctgtcca	gtcaccagctcatggttcct	57	1	226
exon 6	gagctcagccctactcacca	tgctccgagtgctattcctt	57	1	249
exon 7	ttggtgtgggtttcctcttc	cactggtccacctcctgtct	54	1	248
exon 8	gatgtcagccttggaggact	ctggcctttatgcctactgc	57	1	249
exon 9	tgtcacgtccctgtcttctg	tccctgaaggctgtgctaat	57	1	295
exon10	cctcgtgggctttaattctg	atgtgtgcaaggcatctgg	54	1	228
exon11	ccaccctgtcccttccacta	cccagttctgaccagcctaa	54	1	244
exon12	ggtccccacacctcctct	accatctgccgcaagaagt	57	1	255
exon 12b	cacggctctgggacttctt	actttgttccctgcaactgg	57	1	265
exon13	gaaaaacgcagccaggttag	gctcttgatgtgctccttcc	54	1	279
exon14a	ggctgggttaaggctctgac	actgggcttggagttcagc	54	1	365
exon 14b	aggctctgaccctctcctgt	gctgtgtgcttgttgagcag	55	1	278
exon 14c	gtggccaagctagagcagag	cacctcccagaggaaacg	57	1	340
exon15	gctgcctcccacaattcac	tccccattgcttcatttttc	54	1	234
exon16a	ggaagaagcttccaaacagg	ggtctgcacctctctcagc	57	1	320
exon16b	aactgactcgagaggcaaatg	gtcgctgtcgtaggaagagg	57	1	360
exon16c	gcccagagcgagtatagcc	cgggtccctactttgctctt	57	1	267
exon17	tggggaaaatgagctgaatg	ccctgggaaccctaattcat	57	1	278
exon18	ggttagccaaagggtcacaa	cggtaccttgtgctggactt	57	1	240
exon19	cccttggaaatgtccctgtt	gtaccatgggggactctgc	57	1	230

Table 12. Primers and PCR conditions used for PCR amplification and sequencing of the *SPTBN2* gene.

Exon	Forward Primer (5'→3')	Reverse Primer (5'→3')	Ta (°C)	$MgCl_2$ (mM)	Product Size (bp)
exon 20	ggctaatttgggcactttga	ccccttttcttctgctgttca	57	1	354
exon 21	gcggaaatgcagagctaaca	ggagatggtcaatgccaaag	54	1	395
exon 22	tgtccccactcccactaatc	aaaaacacgtccaagtctgg	54	1	233
exon 23	ttcagcattttctcttctgtgg	catccagcatcaggtcagg	57	1	350
exon 24	gatgctggatgccactgtc	agcactgaaggctccacatt	57	1	226
exon 25	gaacagaccggaggtcagag	ctgtgggtcctccactcttc	61	2	328
exon 26a	taacatcacggcatggtctg	gcctcgttgagactgtcctt	54	1	248
exon 26b	ggtcaggagcgcgtagatag	ctctaagcctcccccacct	57	1	249
exon 27	cgctctgcctgactctgac	ctgagccctgggattctcac	57	1	295
exon28	agcaggtgatgctgtttctg	atgtgtgcaaggcatctgg	57	1	228
exon29	tcacatcctggtgctaactca	cctactctggaacccacagg	61	3	201
exon30	ccactctgacccaccatctt	aagccagcacaggtcagg	54	1	300
exon 31	ccctcttacacgcaaccttc	ctcctcctacccaggcatc	57	1	238
exon32-33	ttctgtgttgcctttggtca	tccccattgcttcatttttc	57	1	342
exon 34	ggttagggatctcccgtctc	caggctccagagaggctgta	57	1	335
exon 35	aactgactcgagaggcaaatg	gaccactgttccctgttccta	57	1	360
exon 36	tacgctctcaccagcagcta	cgcacacatccagtcttacc	59	2	243
exon37a	cagctcactttctgcctcct	cgtttttctcgctctcggtt	57	1.5	337
exon37b	aaagacggcagagaacgaga	gttacctggctgccaccac	57	1	352
exon37c	gtccctcaccacggtgtggacag	agagaggctgtggtcaggaa	57	1	289

Table 12 (cont.). Primers and PCR conditions used for PCR amplification and sequencing of the *SPTBN2* gene.

REFERENCES

Adames, N.R., and J.A. Cooper. 2000. Microtubule Interactions with the Cell Cortex Causing Nuclear Movements in Saccharomyces cerevisiae. *J. Cell Biol.* 149:863-874.

Ango, F., G. di Cristo, H. Higashiyama, V. Bennett, P. Wu, and Z.J. Huang. 2004. Ankyrin-Based Subcellular Gradient of Neurofascin, an Immunoglobulin Family Protein, Directs GABAergic Innervation at Purkinje Axon Initial Segment. *Cell*. 119:257-272.

Ayalon, G., J.Q. Davis, P.B. Scotland, and V. Bennett. 2008. An Ankyrin-Based Mechanism for Functional Organization of Dystrophin and Dystroglycan. *Cell*. 135:1189-1200.

Bañuelos, S., M. Saraste, and K.D. Carugo. 1998. Structural comparisons of calponin homology domains: implications for actin binding. *Structure*. 6:1419-1431.

Baum, B., and N. Perrimon. 2001. Spatial control of the actin cytoskeleton in Drosophila epithelial cells. *Nature Cell Biology*. 3:883.

Beck, K.A. 2005. Spectrins and the Golgi. *Biochimica et Biophysica Acta (BBA) - Molecular Cell Research*. 1744:374-382.

Beck, K.A., J.A. Buchanan, V. Malhotra, and W.J. Nelson. 1994. Golgi spectrin: identification of an erythroid beta-spectrin homolog associated with the Golgi complex. *J. Cell Biol.* 127:707-723.

Beck, K.A., and W.J. Nelson. 1998. A spectrin membrane skeleton of the Golgi complex. *Biochimica et Biophysica Acta (BBA) - Molecular Cell Research*. 1404:153-160.

Bellen, H.J., R.W. Levis, G. Liao, Y. He, J.W. Carlson, G. Tsang, M. Evans-Holm, P.R. Hiesinger, K.L. Schulze, G.M. Rubin, R.A. Hoskins, and A.C. Spradling. 2004. The BDGP Gene Disruption Project: Single Transposon Insertions Associated With 40% of Drosophila Genes. *Genetics*. 167:761-781.

Bennett, V., and A.J. Baines. 2001. Spectrin and Ankyrin-Based Pathways: Metazoan Inventions for Integrating Cells Into Tissues. *Physiol. Rev.* 81:1353-1392.

Bennett, V., and D.M. Gilligan. 1993. The spectrin-based membrane skeleton and micron-scale organization of the plasma membrane. *Annu Rev Cell Biol*. 9:27-66.

Bennett, V., and J. Healy. 2008. Organizing the fluid membrane bilayer: diseases linked to spectrin and ankyrin. *Trends in Molecular Medicine*. 14:28-36.

Bilen, J., and N.M. Bonini. 2005. DROSOPHILA AS A MODEL FOR HUMAN NEURODEGENERATIVE DISEASE. *Annual Review of Genetics*. 39:153-171.

Bilen, J., and N.M. Bonini. 2007. Genome-Wide Screen for Modifiers of Ataxin-3 Neurodegeneration in Drosophila. *PLoS Genetics*. 3:e177-1964.

Bloch, R.J., and J.S. Morrow. 1989. An unusual beta-spectrin associated with clustered acetylcholine receptors. *J. Cell Biol.* 108:481-493.

Bowman, A.B., A. Kamal, B.W. Ritchings, A.V. Philp, and M. McGrail. 2000. Kinesin-dependent axonal transport is mediated by the sunday driver (SYD) protein. *Cell*. 103:583.

Boylan, K., M. Serr, and T. Hays. 2000. A Molecular Genetic Analysis of the Interaction between the Cytoplasmic Dynein Intermediate Chain and the Glued (Dynactin) Complex. *Mol. Biol. Cell*. 11:3791-3803.

Brady, S.T., K.K. Pfister, and G.S. Bloom. 1990. A monoclonal antibody against kinesin

inhibits both anterograde and retrograde fast axonal transport in squid axoplasm. *Proceedings of the National Academy of Sciences of the United States of America*. 87:1061-1065.

Brand, A.H., and N. Perrimon. 1993. Targeted gene expression as a means of altering cell fates and generating dominant phenotypes. *Development*. 118:401-415.

Brkanac, Z., L. Bylenok, M. Fernandez, M. Matsushita, H. Lipe, J. Wolff, D. Nochlin, W.H. Raskind, and T.D. Bird. 2002. A New Dominant Spinocerebellar Ataxia Linked to Chromosome 19q13.4-qter. *Arch Neurol*. 59:1291-1295.

Burk, K. 2004. Spinocerebellar ataxia type 5: clinical and molecular genetic features of a German kindred. *Neurology*. 62:327-329.

Cagnoli, C., C. Mariotti, F. Taroni, M. Seri, A. Brussino, C. Michielotto, M. Grisoli, D. Di Bella, N. Migone, C. Gellera, S. Di Donato, and A. Brusco. 2006. SCA28, a novel form of autosomal dominant cerebellar ataxia on chromosome 18p11.22-q11.2. *Brain*. 129:235-242.

Carlson, K., J. Andresen, and H. Orr. 2009. Emerging pathogenic pathways in the spinocerebellar ataxias. *Curr Opin Genet Dev*. 19:247-253.

Carminati, J.L., and T. Stearns. 1997. Microtubules Orient the Mitotic Spindle in Yeast through Dynein-dependent Interactions with the Cell Cortex. *J. Cell Biol.* 138:629-641.

Chan, H.Y.E., J.M. Warrick, G.L. Gray-Board, H.L. Paulson, and N.M. Bonini. 2000. Mechanisms of chaperone suppression of polyglutamine disease: selectivity, synergy and modulation of protein solubility in Drosophila. *Hum. Mol. Genet.* 9:2811-2820.

Chen, D.-H., Z. Brkanac, L.M.J. Christophe Verlinde, X.-J. Tan, L. Bylenok, D. Nochlin, M. Matsushita, H. Lipe, J. Wolff, M. Fernandez, P.J. Cimino, D. Thomas Bird, and W.H. Raskind. 2003. Missense Mutations in the Regulatory Domain of PKC[gamma]: A New Mechanism for Dominant Nonepisodic Cerebellar Ataxia. *The American Journal of Human Genetics*. 72:839-849.

Chung, M.-y., Y.-C. Lu, N.-C. Cheng, and B.-W. Soong. 2003. A novel autosomal dominant spinocerebellar ataxia (SCA22) linked to chromosome 1p21-q23. *Brain*. 126:1293-1299.

Craig, K., S.M. Keers, K. Archibald, A. Curtis, and P.F. Chinnery. 2004. Molecular epidemiology of spinocerebellar ataxia type 6. *Annals of Neurology*. 55:752-755.

Crowther, D.C., R. Page, T. Rival, D.S. Chandraratna, and D.A. Lomas. 2008. Using a Drosophila model of Alzheimer's disease. *In* Drosophila: A toolbox for the study of neurodegenerative disease. A. Mudhler and T.A. Newman, editors. Taylor & Francis Group, New York. 57.

Cummings, C.J., M.A. Mancini, B. Antalffy, D.B. DeFranco, H.T. Orr, and H.Y. Zoghbi. 1998. Chaperone suppression of aggregation and altered subcellular proteasome localization imply protein misfolding in SCA1. *Nature Genetics*. 19:148.

Cummings, C.J., Y. Sun, P. Opal, B. Antalffy, R. Mestril, H.T. Orr, W.H. Dillmann, and H.Y. Zoghbi. 2001. Over-expression of inducible HSP70 chaperone suppresses neuropathology and improves motor function in SCA1 mice. *Hum. Mol. Genet.* 10:1511-1518.

Das, A., C. Base, S. Dhulipala, and R.R. Dubreuil. 2006. Spectrin functions upstream of

ankyrin in a spectrin cytoskeleton assembly pathway. *J. Cell Biol.* 175:325-335.
De Matteis, M.A., and J.S. Morrow. 2000. Spectrin tethers and mesh in the biosynthetic pathway. *J Cell Sci*. 113:2331-2343.
De Vos, K.J., J. Sable, K.E. Miller, and M.P. Sheetz. 2003. Expression of Phosphatidylinositol (4,5) Bisphosphate-specific Pleckstrin Homology Domains Alters Direction But Not the Level of Axonal Transport of Mitochondria. *Mol. Biol. Cell*. 14:3636-3649.
Deacon, S.W., A.S. Serpinskaya, P.S. Vaughan, M.L. Fanarraga, I. Vernos, K.T. Vaughan, and V.I. Gelfand. 2003. Dynactin is required for bidirectional organelle transport. *J. Cell Biol.* 160:297-301.
Delaunay, J. 2007. The molecular basis of hereditary red cell membrane disorders. *Blood Reviews*. 21:1-20.
Devarajan, P., P.R. Stabach, A.S. Mann, T. Ardito, M. Kashgarian, and J.S. Morrow. 1996. Identification of a small cytoplasmic ankyrin (AnkG119) in the kidney and muscle that binds beta I sigma spectrin and associates with the Golgi apparatus. *J. Cell Biol.* 133:819-830.
Djinovic Carugo, K., S. Bañuelos, and M. Saraste. 1997. Crystal structure of a calponin homology domain. *Nat Struct Biol*. 3:175-179.
Driscoll, M., and B. Gerstbrein. 2003. Dying for a cause: invertebrate genetics takes on human neurodegeneration. *Nat Rev Genet*. 4:181-194.
Dubreuil, R.R., P. Wang, S. Dahl, J. Lee, and L.S.B. Goldstein. 2000. Drosophila {beta} Spectrin Functions Independently of {alpha} Spectrin to Polarize the Na,K ATPase in Epithelial Cells. *J. Cell Biol.* 149:647-656.
Dudding, T.E., K. Friend, P.W. Schofield, S. Lee, I.A. Wilkinson, and R.I. Richards. 2004. Autosomal dominant congenital non-progressive ataxia overlaps with the SCA15 locus. *Neurology*. 63:2288-2292.
Duenas, A.M., R. Goold, and P. Giunti. 2006. Molecular pathogenesis of spinocerebellar ataxias. *Brain*. 129:1357-1370.
Dujardin, D.L., and R.B. Vallee. 2002. Dynein at the cortex. *Current Opinion in Cell Biology*. 14:44-49.
Eaton, B.A., R.D. Fetter, and G.W. Davis. 2002. Dynactin Is Necessary for Synapse Stabilization. *Neuron*. 34:729-741.
Featherstone, D.E., W.S. Davis, R.R. Dubreuil, and K. Broadie. 2001. Drosophila {alpha}- and {beta}-Spectrin Mutations Disrupt Presynaptic Neurotransmitter Release. *J. Neurosci.* 21:4215-4224.
Fortini, M.E., M.P. Skupski, M.S. Boguski, and I.K. Hariharan. 2000. A Survey of Human Disease Gene Counterparts in the Drosophila Genome. *J. Cell Biol.* 150:23F-30.
Freeman, M. 1996. Reiterative Use of the EGF Receptor Triggers Differentiation of All Cell Types in the Drosophila Eye. *Cell*. 87:651-660.
Gardner, K., K. Alderson, B. Galster, C. Kaplan, M. Leppert, and L. Ptacek. 1994. Autosomal dominant spinocerebellar ataxia: clinical description of a distinct hereditary ataxia and genetic localization to chromosome 16 (SCA4) in a Utah kindred. *Neurology*. 44:A361.
Gepner, J., M.G. Li, S. Ludmann, C. Kortas, K. Boylan, S.J.P. Iyadurai, M. McGrail, and

T.S. Hays. 1996. Cytoplasmic Dynein Function Is Essential in Drosophila melanogaster. *Genetics*. 142:865-878.

Giorgi, M., C.D. Cianci, P.G. Gallagher, and J.S. Morrow. 2001. Spectrin Oligomerization is Cooperatively Coupled to Membrane Assembly: A Linkage Targeted by Many Hereditary Hemolytic Anemias? *Experimental and Molecular Pathology*. 70:215-230.

Godenschwege, T.A., L.V. Kristiansen, S.B. Uthaman, M. Hortsch, and R.K. Murphey. 2006. A Conserved Role for Drosophila Neuroglian and Human L1-CAM in Central-Synapse Formation. *Current Biology*. 16:12-23.

Godi, A., I. Santone, P. Pertile, P. Devarajan, P.R. Stabach, J.S. Morrow, G. Di Tullio, R. Polishchuk, T.C. Petrucci, A. Luini, and M.A. De Matteis. 1998. ADP ribosylation factor regulates spectrin binding to the Golgi complex. *Proceedings of the National Academy of Sciences of the United States of America*. 95:8607-8612.

Gough, L.L., J. Fan, S. Chu, S. Winnick, and K.A. Beck. 2003. Golgi Localization of Syne-1. *Mol. Biol. Cell*. 14:2410-2424.

Grewal, R., E. Tayag, K. Figueroa, A. Durazo, C. Nunez, and S. Pulst. 1998. Clinical and genetic analysis of a distinct autosomal dominant spinocerebellar ataxia. *Neurology*. 51:1423-1426.

Gross, S.P. 2003. Dynactin: Coordinating Motors with Opposite Inclinations. *Current Biology*. 13:R320-R322.

Gross, S.P., M.C. Tuma, S.W. Deacon, A.S. Serpinskaya, A.R. Reilein, and V.I. Gelfand. 2002a. Interactions and regulation of molecular motors in Xenopus melanophores. *J. Cell Biol.* 156:855-865.

Gross, S.P., M.A. Welte, S.M. Block, and E.F. Wieschaus. 2000. Dynein-mediated Cargo Transport In Vivo: A Switch Controls Travel Distance. *J. Cell Biol.* 148:945-956.

Gross, S.P., M.A. Welte, S.M. Block, and E.F. Wieschaus. 2002b. Coordination of opposite-polarity microtubule motors. *J. Cell Biol.* 156:715-724.

Gunawardena, S., and L.S.B. Goldstein. 2001. Disruption of Axonal Transport and Neuronal Viability by Amyloid Precursor Protein Mutations in Drosophila. *Neuron*. 32:389-401.

Guo-Yun, Y., J.H. Michael, J.R. Matthew, X. Ting-Dong, and M.G. Christopher. 2005. Spinocerebellar ataxia type 26 maps to chromosome 19p13.3 adjacent to SCA6. *Annals of Neurology*. 57:349-354.

Haghnia, M., V. Cavalli, S.B. Shah, K. Schimmelpfeng, R. Brusch, G. Yang, C. Herrera, A. Pilling, and L.S.B. Goldstein. 2007. Dynactin Is Required for Coordinated Bidirectional Motility, but Not for Dynein Membrane Attachment. *Mol. Biol. Cell*. 18:2081-2089.

Hammarlund, M., W.S. Davis, and E.M. Jorgensen. 2000. Mutations in {beta}-Spectrin Disrupt Axon Outgrowth and Sarcomere Structure. *J. Cell Biol.* 149:931-942.

Hammarlund, M., E.M. Jorgensen, and M.J. Bastiani. 2007. Axons break in animals lacking {beta}-spectrin. *J. Cell Biol.* 176:269-275.

Hamosh, A., A.F. Scott, J.S. Amberger, C.A. Bocchini, and V.A. McKusick. 2005. Online Mendelian Inheritance in Man (OMIM), a knowledgebase of human genes and genetic disorders. *Nucl. Acids Res.* 33:D514-517.

Harding, A. 1983. Clasiffication of the hereditary ataxias and paraplegias. *The Lancet*. 231:1151-1155.

Harding, A.E. 1982. The clinical features and classification of the late onset autosomal dominant cerebellar ataxia: a study of 11 families, including descendants of 'The Drew Family of Walworth'. *Brain*. 105:1-28.

Harte, P.J., and D.R. Kankel. 1982. Genetic analysis of mutations at the Glued locus and interacting loci in Drosophila melanogaster. *Genetics*. 101:477-501.

Hegde, M.R., E.L.H. Chin, J.G. Mulle, D.T. Okou, S.T. Warren, and M.E. Zwick. 2008. Microarray-based mutation detection in the <I>dystrophin</I> gene. *Human Mutation*. 29:1091-1099.

Hirai, H., and S. Matsuda. 1999. Interaction of the C-terminal domain of [delta] glutamate receptor with spectrin in the dendritic spines of cultured Purkinje cells. *Neuroscience Research*. 34:281-287.

Hirokawa, N. 1998. Kinesin and Dynein Superfamily Proteins and the Mechanism of Organelle Transport. *Science*. 279:519-526.

Hirokawa, N., and R. Takemura. 2005. Molecular motors and mechanisms of directional transport in neurons. *Nat. Rev. Neurosci.* 6:201.

Holleran, E.A., L.A. Ligon, M. Tokito, M.C. Stankewich, J.S. Morrow, and E.L.F. Holzbaur. 2001. beta III Spectrin Binds to the Arp1 Subunit of Dynactin. *J. Biol. Chem.* 276:36598-36605.

Holmes, S.E., E.O. Hearn, C.A. Ross, and R.L. Margolis. 2001. SCA12: an unusual mutation leads to an unusual spinocerebellar ataxia. *Brain Research Bulletin*. 56:397-403.

Holmes, S.E., E. O'Hearn, and R.L. Margolis. 2003. Why is SCA12 different from other SCAs? *Cytogenetic & Genome Research*. 100:189-197.

Holmes, S.E., E.E. O'Hearn, M.G. McInnis, D.A. Gorelick-Feldman, J.J. Kleiderlein, C. Callahan, N.G. Kwak, R.G. Ingersoll-Ashworth, M. Sherr, A.J. Sumner, A.H. Sharp, U. Ananth, W.K. Seltzer, M.A. Boss, A.-M. Vieria-Saecker, J.T. Epplen, O. Riess, C.A. Ross, and R.L. Margolis. 1999. Expansion of a novel CAG trinucleotide repeat in the 5' region of PPP2R2B is associated with SCA12. *Nature Genetics*. 23:391.

Hoock, T.C., L.L. Peters, and S.E. Lux. 1997. Isoforms of Ankyrin-3 That Lack the NH2-terminal Repeats Associate with Mouse Macrophage Lysosomes. *J. Cell Biol.* 136:1059-1070.

Houlden, H., J. Johnson, C. Gardner-Thorpe, T. Lashley, D. Hernandez, P. Worth, A.B. Singleton, D.A. Hilton, J. Holton, T. Revesz, M.B. Davis, P. Giunti, and N.W. Wood. 2007. Mutations in TTBK2, encoding a kinase implicated in tau phosphorylation, segregate with spinocerebellar ataxia type 11. *Nature Genetics*. 39:1434-1436.

Hurd, D.D., and W.M. Saxton. 1996. Kinesin Mutations Cause Motor Neuron Disease Phenotypes by Disrupting Fast Axonal Transport in Drosophila. *Genetics*. 144:1075-1085.

Ikeda, Y., R. Daughters, and L. Ranum. 2008. Bidirectional expression of the SCA8 expansion mutation: one mutation, two genes. *Cerebellum*. 7:150-158.

Ikeda, Y., K.A. Dick, M.R. Weatherspoon, D. Gincel, K.R. Armbrust, J.C. Dalton, G.

Stevanin, A. Durr, C. Zuhlke, K. Burk, H.B. Clark, A. Brice, J.D. Rothstein, L.J. Schut, J.W. Day, and L.P. Ranum. 2006. Spectrin mutations cause spinocerebellar ataxia type 5. *Nat Genet*. 38:184-90.

Imarisio, S., J. Carmichael, V. Korolchuk, C. Chen, S. Saiki, C. Rose, G. Krishna, J. Davies, E. Ttofi, B. Underwood, and D. Rubinsztein. 2008. Huntington's disease: from pathology and genetics to potential therapies. *Biochem J*. 412:191-209.

Iwaki, A., Y. Kawano, S. Miura, H. Shibata, D. Matsuse, D. Li, L. Furuya, Y. Ohyagi, T. Taniwaki, J. Kira, and Y. Fukumaki. 2008. Heterozygous deletion of ITPR1, but not SUMF1, in spinocerebellar ataxia type 16. *J Med Genet* 45:32-35.

Jackson, M., W. Song, M.-Y. Liu, L. Jin, M. Dykes-Hoberg, C.-l.G. Lin, W.J. Bowers, H.J. Federoff, P.C. Sternweis, and J.D. Rothstein. 2001. Modulation of the neuronal glutamate transporter EAAT4 by two interacting proteins. *Nature*. 410:89-93.

Jenkins, S.M., and V. Bennett. 2001. Ankyrin-G coordinates assembly of the spectrin-based membrane skeleton, voltage-gated sodium channels, and L1 CAMs at Purkinje neuron initial segments. *J. Cell Biol.* 155:739-746.

Johnson, C.P., M. Gaetani, V. Ortiz, N. Bhasin, S. Harper, P.G. Gallagher, D.W. Speicher, and D.E. Discher. 2007. Pathogenic proline mutation in the linker between spectrin repeats: disease caused by spectrin unfolding. *Blood*. 109:3538-3543.

Kennedy, S.P., S.L. Warren, B.G. Forget, and J.S. Morrow. 1991. Ankyrin binds to the 15th repetitive unit of erythroid and nonerythroid beta-spectrin. *J. Cell Biol.* 115:267-277.

Kizhatil, K., J.Q. Davis, L. Davis, J. Hoffman, B.L.M. Hogan, and V. Bennett. 2007a. Ankyrin-G Is a Molecular Partner of E-cadherin in Epithelial Cells and Early Embryos. *J. Biol. Chem.* 282:26552-26561.

Kizhatil, K., W. Yoon, P.J. Mohler, L.H. Davis, J.A. Hoffman, and V. Bennett. 2007b. Ankyrin-G and beta2-Spectrin Collaborate in Biogenesis of Lateral Membrane of Human Bronchial Epithelial Cells. *J. Biol. Chem.* 282:2029-2037.

Knight, M.A., D. Hernandez, S.J. Diede, H.G. Dauwerse, I. Rafferty, J. van de Leemput, S.M. Forrest, R.J.M. Gardner, E. Storey, G.-J.B. van Ommen, S.J. Tapscott, K.H. Fischbeck, and A.B. Singleton. 2008. A duplication at chromosome 11q12.2-11q12.3 is associated with spinocerebellar ataxia type 20. *Hum. Mol. Genet.* 17:3847-3853.

Knight, M.A., R.J. McKinlay Gardner, M. Bahlo, T. Matsuura, J.A. Dixon, S.M. Forrest, and E. Storey. 2004. Dominantly inherited ataxia and dysphonia with dentate calcification: spinocerebellar ataxia type 20. *Brain*. 127:1172-1181.

Koch, I., H. Schwarz, D. Beuchle, B. Goellner, M. Langegger, and H. Aberle. 2008. Drosophila Ankyrin 2 Is Required for Synaptic Stability. *Neuron*. 58:210-222.

Komada, M., and P. Soriano. 2002. Beta IV-spectrin regulates sodium channel clustering through ankyrin-G at axon initial segments and nodes of Ranvier. *J. Cell Biol.* 156:337-348.

Koob, M.D., M.L. Moseley, L.J. Schut, K.A. Benzow, T.D. Bird, J.W. Day, and L.P.W. Ranum. 1999. An untranslated CTG expansion causes a novel form of spinocerebellar ataxia (SCA8). *Nature Genetics*. 21:379.

La Spada, A., E. Wilson, D. Lubahn, A. Harding, and K. Fischbeck. 1991. Androgen

receptor gene mutations in X-linked spinal and bulbar muscular atrophy. *Nature*. 352:77-79.

Lacas-Gervais, S., J. Guo, N. Strenzke, E. Scarfone, M. Kolpe, M. Jahkel, P. De Camilli, T. Moser, M.N. Rasband, and M. Solimena. 2004. beta IV{Sigma}1 spectrin stabilizes the nodes of Ranvier and axon initial segments. *J. Cell Biol.* 166:983-990.

Lee, J.C.M., and D.E. Discher. 2001. Deformation-Enhanced Fluctuations in the Red Cell Skeleton with Theoretical Relations to Elasticity, Connectivity, and Spectrin Unfolding. *Biophysical Journal*. 81:3178-3192.

Leshchyns'ka, I., V. Sytnyk, J.S. Morrow, and M. Schachner. 2003. Neural cell adhesion molecule (NCAM) association with PKC{beta}2 via {beta}I spectrin is implicated in NCAM-mediated neurite outgrowth. *J. Cell Biol.* 161:625-639.

Ligon, L.A., S. Karki, M. Tokito, and E.L.F. Holzbaur. 2001. Dynein binds to beta-catenin and may tether microtubules at adherens junctions. *Nature Cell Biology*. 3:913.

Liquori, C.L., L.J. Schut, H.B. Clark, J.W. Day, and L.P.W. Ranum. 2002. Spinocerebellar ataxia type 5 (SCA5). *In* The Cerebellum and Its Disorders
M. Pandolfo, editor. Cambridge University Press, Cambridge. 445-450.

Lorenzo, D., S. Forrest, Y. Ikeda, K. Dick, L. Ranum, and M. Knight. 2006. Spinocerebellar ataxia type 20 is genetically distinct from spinocerebellar ataxia type 5. *Neurology*. 67:2084-2085.

Malchiodi-Albedi, F., M. Ceccarini, J.C. Winkelmann, J.S. Morrow, and T.C. Petrucci. 1993. The 270 kDa splice variant of erythrocyte beta-spectrin (beta I sigma 2) segregates in vivo and in vitro to specific domains of cerebellar neurons. *J Cell Sci*. 106:67-78.

Martin, M., S.J. Iyadurai, A. Gassman, J.G. Gindhart, Jr., T.S. Hays, and W.M. Saxton. 1999. Cytoplasmic Dynein, the Dynactin Complex, and Kinesin Are Interdependent and Essential for Fast Axonal Transport. *Mol. Biol. Cell*. 10:3717-3728.

Matsuura, T., T. Yamagata, D.L. Burgess, A. Rasmussen, R.P. Grewal, K. Watase, M. Khajavi, A.E. McCall, C.F. Davis, L. Zu, M. Achari, S.M. Pulst, E. Alonso, J.L. Noebels, D.L. Nelson, H.Y. Zoghbi, and T. Ashizawa. 2000. Large expansion of the ATTCT pentanucleotide repeat in spinocerebellar ataxia type 10. *Nature Genetics*. 26:191.

McCampbell, A., J.P. Taylor, A.A. Taye, J. Robitschek, M. Li, J. Walcott, D. Merry, Y. Chai, H. Paulson, G. Sobue, and K.H. Fischbeck. 2000. CREB-binding protein sequestration by expanded polyglutamine. *Hum. Mol. Genet.* 9:2197-2202.

McGrail, M., J. Gepner, A. Silvanovich, S. Ludmann, M. Serr, and T.S. Hays. 1995. Regulation of cytoplasmic dynein function in vivo by the Drosophila Glued complex. *J. Cell Biol.* 131:411-425.

McGrail, M., and T.S. Hays. 1997. The microtubule motor cytoplasmic dynein is required for spindle orientation during germline cell divisions and oocyte differentiation in Drosophila. *Development*. 124:2409-2419.

Medina, P., R. Worthen, L. Forsberg, and J. Brenman. 2008. The actin-binding protein capulet genetically interacts with the microtubule motor kinesin to maintain

neuronal dendrite homeostasis. *PLoS One*. 3:e3054.

Mische, S., M. Li, M. Serr, and T.S. Hays. 2007. Direct Observation of Regulated Ribonucleoprotein Transport Across the Nurse Cell/Oocyte Boundary. *Mol. Biol. Cell*. 18:2254-2263.

Moseley, M., K. Benzow, L. Schut, C.B. Gomez, PE, K. Blindauer, M. Labuda, M. Pandolfo, M. Koob, and L. Ranum. 1998. Incidence of dominant spinocerebellar and Friedreich triplet repeats among 361 ataxia families. *Neurology*. 51:1666-1671.

Moseley, M.L., Z. Tao, Y. Ikeda, G. Wangcai, A.K. Mosemiller, R.S. Daughters, C. Gang, M.R. Weatherspoon, H.B. Clark, T.J. Ebner, J.W. Day, and L.P.W. Ranum. 2006. Bidirectional expression of CUG and CAG expansion transcripts and intranuclear polyglutamine inclusions in spinocerebellar ataxia type 8. *Nature Genetics*. 38:758-769.

Muresan, V., M.C. Stankewich, W. Steffen, J.S. Morrow, E.L.F. Holzbaur, and B.J. Schnapp. 2001. Dynactin-Dependent, Dynein-Driven Vesicle Transport in the Absence of Membrane Proteins: A Role for Spectrin and Acidic Phospholipids. *Molecular Cell*. 7:173-183.

Ohara, O., R. Ohara, H. Yamakawa, D. Nakajima, and M. Nakayama. 1998. Characterization of a new beta-spectrin gene which is predominantly expressed in brain. *Brain Res. Mol. Brain Res.* 57:181-192.

Orita, M., Y. Suzuki, T. Sekiya, K. Hayashi, G. 5:874–879., and . 1989. Rapid and sensitive detection of point mutations and DNA polymorphisms using the polymerase chain reaction. . *Genomics*. 5:874-879.

Ortiz-Lopez, R., H. Li, J. Su, V. Goytia, and J.A. Towbin. 1997. Evidence for a Dystrophin Missense Mutation as a Cause of X-Linked Dilated Cardiomyopathy. *Circulation*. 95:2434-2440.

Osborne, R.J., and C.A. Thornton. 2006. RNA-dominant diseases. *Hum. Mol. Genet.* 15:R162-169.

Paik, J.E., N. Kim, S.S. Yea, W.H. Jang, J.Y. Chung, S.K. Lee, Y.H. Park, J. Han, and D. Seog. 2004. Kinesin Superfamily KIF5 Proteins Bind to beta-III Spectrin. *Korean J Physiol Pharmacol*. 8:167-172.

Park, E.C., and H.R. Horvitz. 1986. Mutations with dominant effects on the behavior and morphology of the nematode Caenorhabditis elegans. *Genetics*. 113:821-852.

Parkinson, N.J. 2001. Mutant beta-spectrin 4 causes auditory and motor neuropathies in quivering mice. *Nat. Genet.* 29:61-65.

Parks, A.L., K.R. Cook, M. Belvin, N.A. Dompe, R. Fawcett, K. Huppert, L.R. Tan, C.G. Winter, K.P. Bogart, J.E. Deal, M.E. Deal-Herr, D. Grant, M. Marcinko, W.Y. Miyazaki, S. Robertson, K.J. Shaw, M. Tabios, V. Vysotskaia, L. Zhao, R.S. Andrade, K.A. Edgar, E. Howie, K. Killpack, B. Milash, A. Norton, D. Thao, K. Whittaker, M.A. Winner, L. Friedman, J. Margolis, M.A. Singer, C. Kopczynski, D. Curtis, T.C. Kaufman, G.D. Plowman, G. Duyk, and H.L. Francis-Lang. 2004. Systematic generation of high-resolution deletion coverage of the Drosophila melanogaster genome. *Nature Genetics*. 36:288-292.

Pielage, J., L. Cheng, R.D. Fetter, P.M. Carlton, J.W. Sedat, and G.W. Davis. 2008. A Presynaptic Giant Ankyrin Stabilizes the NMJ through Regulation of Presynaptic

Microtubules and Transsynaptic Cell Adhesion. *Neuron*. 58:195-209.
Pielage, J., R.D. Fetter, and G.W. Davis. 2005. Presynaptic Spectrin Is Essential for Synapse Stabilization. *Current Biology*. 15:918-928.
Pielage, J., R.D. Fetter, and G.W. Davis. 2006. A postsynaptic Spectrin scaffold defines active zone size, spacing, and efficacy at the Drosophila neuromuscular junction. *J. Cell Biol.* 175:491-503.
Pilling, A.D., D. Horiuchi, C.M. Lively, and W.M. Saxton. 2006. Kinesin-1 and Dynein Are the Primary Motors for Fast Transport of Mitochondria in Drosophila Motor Axons. *Mol. Biol. Cell*. 17:2057-2068.
Preseley, J.F., and N.B. Cole. 1997. ER-to-Golgi transport visualized in living cells. *Nature*. 389:81.
Ranum, L.P.W., and T.A. Cooper. 2006. RNA-MEDIATED NEUROMUSCULAR DISORDERS. *Annual Review of Neuroscience*. 29:259-277.
Ranum, L.P.W., L.J. Schut, J.K. Lundgren, H.T. Orr, and D.M. Livingston. 1994. Spinocerebellar ataxia gene type 5 in a family descended from the paternal grandparents of President Lincoln maps to chromosome 11. *Nat. Genet.* 8:280-284.
Reiter, L.T., L. Potocki, S. Chien, M. Gribskov, and E. Bier. 2001. A Systematic Analysis of Human Disease-Associated Gene Sequences In Drosophila melanogaster. *Genome Research*. 11:1114-1125.
Rorth, P. 1996. A modular misexpression screen in Drosophila detecting tissue-specific phenotypes. *Proceedings of the National Academy of Sciences of the United States of America*. 93:12418-12422.
Rorth, P. 1998. Gal4 in the Drosophila female germline. *Mechanisms of Development*. 78:113-118.
Rusu, P., A. Jansen, P. Soba, J. Kirsch, A. LÃ¶wer, G. Merdes, K. Yung-Hui, A. Jung, K. Beyreuther, O. Kjaerulff, and S. Kins. 2007. Axonal accumulation of synaptic markers in APP transgenic Drosophila depends on the NPTY motif and is paralleled by defects in synaptic plasticity. *European Journal of Neuroscience*. 25:1079-1086.
Ryder, E., F. Blows, M. Ashburner, R. Bautista-Llacer, D. Coulson, J. Drummond, J. Webster, D. Gubb, N. Gunton, G. Johnson, C.J. O'Kane, D. Huen, P. Sharma, Z. Asztalos, H. Baisch, J. Schulze, M. Kube, K. Kittlaus, G. Reuter, P. Maroy, J. Szidonya, A. Rasmuson-Lestander, K. Ekstrom, B. Dickson, C. Hugentobler, H. Stocker, E. Hafen, J.A. Lepesant, G. Pflugfelder, M. Heisenberg, B. Mechler, F. Serras, M. Corominas, S. Schneuwly, T. Preat, J. Roote, and S. Russell. 2004. The DrosDel Collection: A Set of P-Element Insertions for Generating Custom Chromosomal Aberrations in Drosophila melanogaster. *Genetics*. 167:797-813.
Sakaguchi, G., S. Orita, A. Naito, M. Maeda, H. Igarashi, T. Sasaki, and Y. Takai. 1998. A Novel Brain-Specific Isoform of [beta] Spectrin: Isolation and Its Interaction with Munc13. *Biochemical and Biophysical Research Communications*. 248:846-851.
Sasaki, H., I. Yabe, and K. Tashiro. 2003. The hereditary spinocerebellar ataxias in Japan. *Cytogenetic & Genome Research*. 100:198-205.
Schroer, T.A., B.J. Schnapp, T.S. Reese, and M.P. Sheetz. 1988. The role of kinesin and

other soluble factors in organelle movement along microtubules. *J. Cell Biol.* 107:1785-1792.

Schuster, C.M., G.W. Davis, R.D. Fetter, and C.S. Goodman. 1996. Genetic Dissection of Structural and Functional Components of Synaptic Plasticity. II. Fasciclin II Controls Presynaptic Structural Plasticity. *Neuron*. 17:655-667.

Schut, L.J., J.W. Day, H.B. Clark, M.D. Koob, and L.P. Ranum. 2000. Spinocerebellar ataxia type 5. *In* Handbook of Ataxia Disorders. T. Klockgether, editor. Marcel Dekker, New York. 435-445.

Schuyler, S.C., and D. Pellman. 2001. Search, capture and signal: games microtubules and centrosomes play. *J Cell Sci*. 114:247-255.

Soong, B.-W., and H.L. Paulson. 2007. Spinocerebellar ataxias: an update.
. *Curr Opin Neurol*
20:438-446.

Speicher, D., and V. Marchesi. 1984. Erythrocyte spectrin is comprised of many homologous triple helical segments. *Nature*. 311:177-180.

Stabach, P.R., I. Simonovic, M.A. Ranieri, M.S. Aboodi, T.A. Steitz, M. Simonovic, and J.S. Morrow. 2009. The structure of the ankyrin-binding site of {beta}-spectrin reveals how tandem spectrin-repeats generate unique ligand-binding properties. *Blood*. 113:5377-5384.

Stankewich, M.C. 1998. A widely expressed betaIII spectrin associated with Golgi and cytoplasmic vesicles. *Proc. Natl. Acad. Sci. USA*. 95:14158-14163.

Stevanin, G. 2004. Spinocerebellar ataxia with sensory neuropathy (SCA25) maps to chromosome 2p. *Ann. Neurol.* 55:97-104.

Stevanin, G., A. Herman, A. Brice, and A. Durr. 1999. Clinical and MRI findings in spinocerebellar ataxia type 5. *Neurology*. 53:1355-1357.

Storey, E., M. Bahlo, M. Fahey, O. Sisson, C.J. Lueck, and R.J.M. Gardner. 2009. A new dominantly inherited pure cerebellar ataxia, SCA 30. *J Neurol Neurosurg Psychiatry*. 80:408-411.

Takeda, S., H. Yamazaki, D.-H. Seog, Y. Kanai, S. Terada, and N. Hirokawa. 2000. Kinesin Superfamily Protein 3 (KIF3) Motor Transports Fodrin-associating Vesicles Important for Neurite Building. *J. Cell Biol.* 148:1255-1266.

Tse, W.T., S.E. Lux, and Tse. 1999. Red blood cell membrane disorders. *British Journal of Haematology*. 104:2-13.

Ursitti, J.A., L. Kotula, T.M. DeSilva, P.J. Curtis, and D.W. Speicher. 1996. Mapping the Human Erythrocyte beta-Spectrin Dimer Initiation Site Using Recombinant Peptides and Correlation of Its Phasing with the alpha-Actinin Dimer Site. *J. Biol. Chem.* 271:6636-6644.

Van de Leemput, J., J. Chandran, M.A. Knight, L.A. Holtzclaw, S. Scholz, M.R. Cookson, H. Houlden, K. Gwinn-Hardy, F. Hon-Chung, L. Xian, D. Hernandez, J. Simon-Sanchez, N.W. Wood, P. Giunti, I. Rafferty, J. Hardy, E. Storey, R.J.M. Gardner, S.M. Forrest, and E.M.C. Fisher. 2007. Deletion at ITPR1 Underlies Ataxia in Mice and Spinocerebellar Ataxia 15 in Humans. *PLoS Genetics*. 3:e108-1082.

van de Warrenburg, B.P.C., R.J. Sinke, C.C. Verschuuren-Bemelmans, H. Scheffer, E.R. Brunt, P.F. Ippel, J.A. Maat-Kievit, D. Dooijes, N.C. Notermans, D. Lindhout,

N.V.A.M. Knoers, and H.P.H. Kremer. 2002. Spinocerebellar ataxias in the Netherlands: Prevalence and age at onset variance analysis. *Neurology*. 58:702-708.

van Swieten, J.C., E. Brusse, B.M. de Graaf, E. Krieger, R. van de Graaf, I. de Koning, A. Maat-Kievit, P. Leegwater, D. Dooijes, B.A. Oostra, and P. Heutink. 2003. A Mutation in the Fibroblast Growth Factor 14 Gene Is Associated with Autosomal Dominant Cerebral Ataxia. *The American Journal of Human Genetics*. 72:191-199.

Verbeek, D., J. Schelhaas, E. Ippel, F. Beemer, P. Pearson, and R. Sinke. 2002. Identification of a novel SCA locus (SCA19) in a Dutch autosomal dominant cerebellar ataxia family on chromosome region 1p21-q21. *Human Genetics*. 111:388-393.

Verbeek, D.S., B.P. van de Warrenburg, P. Wesseling, P.L. Pearson, H.P. Kremer, and R.J. Sinke. 2004. Mapping of the SCA23 locus involved in autosomal dominant cerebellar ataxia to chromosome region 20p13-12.3. *Brain*. 127:2551-2557.

Vuillaume, I., D. Devos, S. Schraen-Maschke, C. Dina, A. Lemainque, F. Vasseur, G. Bocquillon, P. Devos, C. Kocinski, C. Marzys, A. Destée, and B. Sablonnière. 2002. A new locus for spinocerebellar ataxia (SCA21) maps to chromosome 7p21.3-p15.1. *Annals of Neurology*. 52:666-670.

Waterman-Storer, C.M., S.B. Karki, S.A. Kuznetsov, J.S. Tabb, D.G. Weiss, G.M. Langford, and E.L.F. Holzbaur. 1997. The interaction between cytoplasmic dynein and dynactin is required for fast axonalâ€‰transport. *Proceedings of the National Academy of Sciences of the United States of America*. 94:12180-12185.

Waters, M.F., N.A. Minassian, G. Stevanin, K.P. Figueroa, J.P.A. Bannister, D. Nolte, A.F. Mock, V.G.H. Evidente, D.B. Fee, U. Muller, A. Durr, A. Brice, D.M. Papazian, and S.M. Pulst. 2006. Mutations in voltage-gated potassium channel KCNC3 cause degenerative and developmental central nervous system phenotypes. *Nature Genetics*. 38:447-451.

Williams, A.J., T.M. Knutson, V.F. Colomer Gould, and H.L. Paulson. 2009. In vivo suppression of polyglutamine neurotoxicity by C-terminus of Hsp70-interacting protein (CHIP) supports an aggregation model of pathogenesis. *Neurobiology of Disease*. 33:342-353.

Yan, Y., E. Winograd, A. Viel, T. Cronin, S.C. Harrison, and D. Branton. 1993. Crystal Structure of the Repetitive Segments of Spectrin. *Science*. 262:2027-2030.

Yanfei, F., A. Ueda, and W. Chun-Fang. 2004. A Modified Minimal Hemolymph-Like Solution, HL3.1, for Physiological Recordings at the Neuromuscular Junctions of Normal and Mutant Drosophila Larvae. *Journal of Neurogenetics*. 18:377-402.

Yang, J., J. Bai, and T. Lee. 2008. Dynein-dynactin complex is essential for dendritic restriction of TM1-containing Drosophila Dscam. *PLoS One*. 3::e3504.